# MODELLING BIOLOGICAL SULPHATE REDUCTION IN ANAEROBIC DIGESTION USING WEST®

**Shailendra Rajkumar**

***BScEng (Chem) Natal***

*Submitted in fulfilment of the academic requirements for the degree of*

***MScEng***

*in the*

*School of Chemical Engineering*

*University of KwaZulu-Natal, Durban*

**June 2009**

As the candidate's supervisor I agree/do not agree to the submission of this thesis

Name: _____

Signed: _____

Date: _____

# ABSTRACT

Researchers at Rhodes University conducted investigations into the anaerobic co-disposal of primary sewage sludge (PSS) and high sulphate acid mine drainage (AMD) resulting in the development of the Rhodes BioSURE Process® which forms the basis for the operation of a pilot recycling sludge bed reactor (RSBR). Further research has been conducted by researchers at the University of Cape Town (UCT), with the principle aim of determining the rate of hydrolysis of PSS under methanogenic, acidogenic and sulphate reducing conditions in laboratory-scale anaerobic digesters.

The University of Cape Town's Anaerobic Digestion Model No.1 (UCTADM1) which integrates various biological anaerobic processes for the production of methane was extended with the development of a mathematical model incorporating the processes of biosulphidogenic reduction and the biology of sulphate reducing bacteria (SRB). Kinetic parameters used in the model were obtained from Sötemann et al. (2005b) and Kalyuzhnyi et al. (1998).

The WEST® software was used as a platform in translation of the basic UCTADM1 from AQUASIM, and subsequently applied to data sets from UCT laboratory experiments. Incomplete closure of mass balances was attributed to incorrect reaction stoichiometry inherited through translation of the AQUASIM model into WEST®. The WEST® implementation of the model to the experimental methanogenic systems gave fairly close correlations between predicted and measured data for a single set of stoichiometric and kinetic constants, with regressed hydrolysis rate constants. Application of the extended UCTADM1 to experimental sulphidogenic systems demonstrated simulation results reasonably close to measured data, with the exception of effluent soluble COD and sulphate concentrations. Except for a single system with a high COD:$SO_4$ ratio, sulphidogens are out competed for substrate by methanogens within the model. Therefore the model does not properly represent the competition between methanogenic and sulphidogenic organism groups.

Trends observed in application of the model to available pilot plant RSBR data were similar to those observed in sulphidogenic systems, resulting in methanogens out-competing sulphidogens. The model was used as a tool to explore various scenarios regarding operation of the pilot plant. Based on the work conducted in this study, various areas for further information and research were highlighted and recommended.

| | |
|---|---|
| **treatment** | chemical oxygen demand (COD), pH, ammonia, etc., to enable it to meet discharge/reuse standards. |
| **Chemical oxygen demand** | The amount of oxygen required organic compounds present in wastewater |
| **Dissociation** | Dissociation in chemistry and biochemistry is a general process in which ionic compounds separate or split into smaller molecules, ions, or radicals, usually in a reversible manner. |
| **Effluent** | An outflow from a system, sewage system or discharge of liquid waste from an industry. |
| **Experiment** | Research method for testing different hypotheses under conditions constructed and controlled by the researcher. During the experiment, one or more conditions are allowed to change in an organized manner and the effects of these changes on associated conditions is measured, recorded, validated, and analysed for arriving at a conclusion. |
| **Hydrogenotrophic methanogenic bacteria** | Organisms that use hydrogen and carbon dioxide to produce methane and water. |
| **Hydrogenotrophic sulphate reducing bacteria** | Organisms using hydrogen and sulphate as substrates to form hydrogen sulphide and water. |
| **Hydrolysis** | The first step in the anaerobic degradation of complex polymeric organics required for microbial utilisation whereby fermentative bacteria colonise the surface of particles, secreting hydrolytic enzymes, which are responsible for the extracellular breakdown of complex organic materials. |

| | |
|---|---|
| **Stoichiometry** | Determination of the proportions (by weight or number of molecules) in which elements or compounds react with one another. |
| **Wastewater** | Spent or used water containing contaminants that is discharged from an industry, farm, commercial establishment or a household. |

## SYMBOLS

| Symbol | Description | Unit |
|---|---|---|
| $\mu max_a$ | Acidogenic biomass maximum specific growth rate constant | $d^{-1}$ |
| $\mu max_{ae}$ | Acetogenic biomass maximum specific growth rate constant | $d^{-1}$ |
| $\mu max_{am}$ | Acetoclastic methanogen biomass maximum specific growth rate constant | $d^{-1}$ |
| $\mu max_{as}$ | Acetoclastic sulphidogen biomass maximum specific growth rate constant | $d^{-1}$ |
| $\mu max_{hm}$ | Hydrogenotrophic methanogen biomass maximum specific growth rate constant | $d^{-1}$ |
| $\mu max_{hs}$ | Hydrogenotrophic sulphidogen biomass maximum specific growth rate constant | $d^{-1}$ |
| $\mu max_{ps}$ | Acetogenic sulphidogen biomass maximum specific growth rate constant | $d^{-1}$ |
| $AW_C$ | Atomic weight of carbon | g/mol |
| $AW_H$ | Atomic weight of hydrogen | g/mol |
| $AW_N$ | Atomic weight of nitrogen | g/mol |
| $AW_O$ | Atomic weight of oxygen | g/mol |
| $AW_P$ | Atomic weight of phosphorous | g/mol |
| $AW_S$ | Atomic weight of sulphur | g/mol |
| $b_a$ | Acidogenic biomass decay constant | $d^{-1}$ |
| $b_{ae}$ | Acetogenic biomass decay constant | $d^{-1}$ |
| $b_{am}$ | Acetoclastic methanogen biomass decay constant | $d^{-1}$ |
| $b_{as}$ | Acetoclastic sulphidogen biomass decay constant | $d^{-1}$ |

| | | |
|---|---|---|
| $K_{c2}$ | Equilibrium constant for $HCO_3/CO_3$ system | - |
| $k_{CO2}$ | Henry's law coefficient for $CO_2$ | - |
| $Kf_a$ | Forward dissociation constant for $HAc \leftrightarrow Ac^- + H^+$ | - |
| $Kf_{c1}$ | Forward dissociation constant for $H_2CO_3 \leftrightarrow HCO_3^- + H^+$ | - |
| $Kf_{c2}$ | Forward dissociation constant for $HCO_3^- \leftrightarrow CO_3^{2-} + H^+$ | - |
| $Kf_{HS}$ | Forward dissociation constant for $H_2S \leftrightarrow HS^- + H^+$ | - |
| $Kf_n$ | Forward dissociation constant for $NH_4^+ \leftrightarrow NH_3 + H^+$ | - |
| $Kf_{p1}$ | Forward dissociation constant for $H_3PO_4 \leftrightarrow H_2PO_4^- + H^+$ | - |
| $Kf_{p2}$ | Forward dissociation constant for $H_2PO_4^- \leftrightarrow HPO_4^{2-} + H^+$ | - |
| $Kf_{p3}$ | Forward dissociation constant for $HPO_4^{2-} \leftrightarrow PO_4^{3-} + H^+$ | - |
| $Kf_{Pr}$ | Forward dissociation constant for $HPr \leftrightarrow Pr^- + H^+$ | - |
| $Kf_S$ | Forward dissociation constant for $HS^- \leftrightarrow S^{2-} + H^+$ | - |
| $Kf_W$ | Forward dissociation constant for $H_2O \leftrightarrow OH^- + H^+$ | - |
| $K_{H2}$ | Hydrogen inhibition coefficient for high $pH_2$ | mol $H_2/\ell$ |
| $k_{H2S}$ | Henry's law coefficient for $H_2S$ | - |

| | | |
|---|---|---|
| $Kr_a$ | Reverse dissociation constant for $HAc \leftrightarrow Ac^- + H^+$ | - |
| $Kr_{c1}$ | Reverse dissociation constant for $H_2CO_3 \leftrightarrow HCO_3^- + H^+$ | - |
| $Kr_{c2}$ | Reverse dissociation constant for $HCO_3^- \leftrightarrow CO_3^{2-} + H^+$ | - |
| $Kr_{CO2}$ | Reverse dissociation constant for CO2 expulsion | - |
| $Kr_{H2S}$ | Reverse dissociation constant for H2S expulsion | - |
| $Kr_{HS}$ | Reverse dissociation constant for $H_2S \leftrightarrow HS^- + H^+$ | - |
| $Kr_n$ | Reverse dissociation constant for $NH_4^+ \leftrightarrow NH_3 + H^+$ | - |
| $Kr_{p1}$ | Reverse dissociation constant for $H_3PO_4 \leftrightarrow H_2PO_4^- + H^+$ | - |
| $Kr_{p2}$ | Reverse dissociation constant for $H_2PO_4\text{-} \leftrightarrow HPO_4^{2-} + H^+$ | - |
| $Kr_{p3}$ | Reverse dissociation constant for $HPO_4^{2-} \leftrightarrow PO_4^{3-} + H^+$ | - |
| $Kr_{Pr}$ | Reverse dissociation constant for $HPr \leftrightarrow Pr^- + H^+$ | - |
| $Kr_S$ | Reverse dissociation constant for $HS^- \leftrightarrow S^{2-} + H^+$ | - |
| $Kr_W$ | Reverse dissociation constant for $H_2O \leftrightarrow OH^- + H^+$ | - |
| $Ks_a$ | Acidogenic biomass half saturation constant | mol/ℓ |
| $Ks_{ac}$ | Acetogenic biomass half saturation constant | mol/ℓ |

| | | |
|---|---|---|
| $MW_{HCO3}$ | Molecular weight of $HCO_3^-$ | g/mol |
| $MW_{HPO4}$ | Molecular weight of $HPO_4^{2-}$ | g/mol |
| $MW_{HPr}$ | Molecular weight of HPr | g/mol |
| $MW_{HS}$ | Molecular weight of $HS^-$ | g/mol |
| $MW_{NH3}$ | Molecular weight of $NH_3$ | g/mol |
| $MW_{NH4}$ | Molecular weight of $NH_4$ | g/mol |
| $MW_{OH}$ | Molecular weight of $OH^-$ | g/mol |
| $MW_{PO4}$ | Molecular weight of $PO_4^{3-}$ | g/mol |
| $MW_{Pr}$ | Molecular weight of $Pr^-$ | g/mol |
| $MW_S$ | Molecular weight of $S^{2-}$ | g/mol |
| $MW_{SO4}$ | Molecular weight of $SO_4^{2-}$ | g/mol |
| Patm | Atmospheric pressure | atm |
| $pCH_4$ | Partial pressure of $CH_4$ gas | - |
| $pCO_2$ | Partial pressure of $CO_2$ gas | - |
| $pH_2S$ | Partial pressure of $H_2S$ gas | - |
| $pK_a$ | pK constant for $HAc \leftrightarrow Ac^- + H^+$ | - |
| $pK_{c1}$ | pK constant for $H_2CO_3 \leftrightarrow HCO_3^- + H^+$ | - |
| $pK_{c2}$ | pK constant for $HCO_3^- \leftrightarrow CO_3^{2-} + H^+$ | - |
| $pKH_{CO2}$ | pK constant for the dissolution of $CO_2$ | - |
| $pKH_{H2S}$ | pK constant for the dissolution of $H_2S$ | - |
| $pKH_{HS}$ | pK constant for $H_2S \leftrightarrow HS^- + H^+$ | - |
| $pKH_{Pr}$ | pK constant for $HPr \leftrightarrow Pr^- + H^+$ | - |
| $pK_n$ | pK constant for $NH_4^+ \leftrightarrow NH_3 + H^+$ | - |
| $pK_{p1}$ | pK constant for $H_3PO_4 \leftrightarrow H_2PO_4^- + H^+$ | - |
| $pK_{p2}$ | pK constant for $H_2PO_4^- \leftrightarrow HPO_4^{2-} + H^+$ | - |
| $pK_{p3}$ | pK constant for $HPO_4^{2-} \leftrightarrow PO_4^{3-} + H^+$ | - |

| | | |
|---|---|---|
| $Y_{hm}$ | Hydrogenotrophic methanogen biomass yield coefficient | mol VSS/mol COD |
| $Y_{hs}$ | Hydrogenotrophic sulphidogen biomass yield coefficient | mol VSS/mol COD |
| $Y_{ps}$ | Acetogenic sulphidogen biomass yield coefficient | mol VSS/mol COD |
| $Z_{ae}$ | Acetogenic organism concentration | $g/m^3$ |
| $Z_{ai}$ | Acidogen active biomass concentration | $g/m^3$ |
| $Z_{am}$ | Acetoclastic methanogen organism concentration | $g/m^3$ |
| $Z_{as}$ | Acetoclastic sulphidogen organism concentration | $g/m^3$ |
| $Z_{hm}$ | Hydrogenotrophic methanogen organism concentration | $g/m^3$ |
| $Z_{hs}$ | Hydrogenotrophic sulphidogen organism concentration | $g/m^3$ |
| $Z_{ps}$ | Acetogenic sulphidogen organism concentration | $g/m^3$ |

# LIST OF TABLES

# CHAPTER 1

# INTRODUCTION

## 1.1 Background

The South African mining industry has been one of the primary contributors to the economic upliftment and development of the country for more than a century (Pulles, 2003, WRC, 2005). Exploitation of the national mineral resource has resulted in employment, foreign currency earnings, national tax revenues and national infrastructure development (Pulles, 2003). However, these benefits have come with a consequence of environmental risk associated with obsolete and abandoned mines, current operational mines and the future closure of mines. Post-mining wastes emanating from sulphidic mine activities undergoes chemical and biological oxidation processes when exposed to water and air resulting in a highly acidic leachate characterised by low pH and high concentrations of sulphate and heavy metal ions (Christensen, et al., 1996, Gibert, et al., 2004). These effluents are known as acid mine drainage (AMD).

Anaerobic waste treatment is one of the major biological waste treatment processes in use today. It has been employed for many years in the stabilisation of municipal sewage sludges (primary and waste activated), and more recently, in the treatment of high and medium strength industrial wastes. Over the past two decades anaerobic biological sulphate reduction has received increasing attention as an accepted technology suited to the treatment of sulphate-rich waste streams such as AMD (Knobel and Lewis, 2002). During this process sulphate reducing bacteria (SRB) use the sulphate as an electron acceptor directly reducing salinity and protons, generating alkalinity and sulphide which results in an increase in the pH and the precipitation of many heavy metals as sulphides, carbonates or hydroxides (Knobel and Lewis, 2002, Ristow, et al., 2002). Sources of carbon or simple electron donors, including methanol and ethanol, are fairly expensive and are therefore not suitable for use in developing countries such as South Africa (Molwantwa, et al., 2004). The use of primary sewage sludge (PSS) has been identified as a practically feasible carbon source or electron donor and an attractive economic alternative for the treatment of AMD (Ristow, et al., 2004). Primary sludge originates from the solid component of raw sewage settled prior to any biological treatment (Hansford, 2004). The complex particulate sewage sludge would need to be degraded anaerobically to produce simple soluble organic substrates for SRB in order to achieve successful sulphate reduction (Hansford, 2004, Ristow, et al., 2005).

methanogenic bacteria. However the UCTADM1 does not account for the processes of biological sulphate reduction and does not apply to the anaerobic degradation processes that take place in the treatment of sulphate-rich wastewaters such as AMD. The UCTADM1 needed to be extended to incorporate the processes of biosulphidogenic reduction and the biology of SRB.

This dissertation details the implementation, extension (to incorporate biosulphidogenic reduction), calibration and application of the UCTADM1 to a range of operating scenarios using the WEST® (**W**astewater Treatment Plant **E**ngine for **S**imulation and **T**raining) modelling platform. WEST® is a modelling and simulation environment and can, together with a model base, be used in the design, operation and optimisation of a wastewater treatment system.

## 1.2 Research Objectives

The principal aim of this research is to model biological sulphate reduction in anaerobic digestion using WEST®. The experimental results of researchers together with a new mathematical representation of anaerobic digestion developed at UCT and previously modelled in AQUASIM (simulation software of aquatic systems) will be used to model the combined process including the RSBR in WEST®. The main objectives of this study were:

i. Translation and coding of the basic UCTADM1 (without sulphate reduction) from AQUASIM to WEST®.

ii. Extension of the model to include reactions for sulphate reducing processes.

iii. Calibration of the model using data sets from the UCT laboratory experiments carried out in completely mixed reactors.

iv. Adaptation of the model to represent the Rhodes BioSURE pilot plant's RSBR configuration and its calibration using available operating data.

v. Highlight requirements for further information and research.

a typical composition of an AMD waste stream from a coal mine.

**Table 2-1:** Typical composition of an AMD wastewater from a coal mine (Burgess and Stuetz, 2002)

| Constituent | Concentration | Unit |
|---|---|---|
| pH | 3.0-5.5 | - |
| $Mg^{2+}$ | 80 | mg/ℓ |
| $Ca^{2+}$ | 200 | mg/ℓ |
| $Al_{total}$ | 50 | mg/ℓ |
| $Fe_{total}$ | 50-300 | mg/ℓ |
| $Mn^{2+}$ | 20-300 | mg/ℓ |
| $SO4^{2-}$ | 20-2000 | mg/ℓ |

Other than sulphuric acid (formed as a result of pyrite oxidation), AMD contains high concentrations of heavy metals, as is evident from Table 2-1, which are released due to direct solubilisation of metal sulphides by acidic extraction of metals adsorbed on mineral surfaces (Burgess and Stuetz, 2002).

It is clearly evident from Table 2-1 that sulphate is the most significant constituent having the highest concentration. According to Toerien and Maree (1987), sulphate is directly responsible for the salination or mineralisation of receiving waters in excessive amounts but constitutes greater indirect problems including corrosion, imparting of tastes to drinking water, scaling of pipes, boilers and heat exchangers, and facilitating biocorrosion.

### 2.1.1 Formation and Chemistry of Acid Mine Drainage

The Pennsylvania Department of Environmental Protection (DEP, 1999), states that the formation of AMD is primarily a function of the geology, hydrology and mining technology employed for the mine site and is formed by a series of complex geochemical and microbial reactions that occur when water comes in contact with pyrite in coal or overburden of a mining operation. The result is a wastewater typically high in acidity and dissolved metals that remain dissolved in solution until the pH is raised to a level where precipitation occurs.

### 2.1.2 Impacts of Acid Mine Drainage

Murphy, et al. (1999) describe the negative impacts of AMD on the ecology of streams, affecting the beneficial use of waterways downstream of mining activities as the following:

- Leaching of high levels of heavy metals into groundwater that become harmful to aquatic ecosystems and human health.
- Limiting of downstream beneficial uses of receiving waters to stock, recreation, fishing, aquaculture and irrigation.
- Altering important life supporting balances in water chemistry such as the bicarbonate buffering system.
- Result in the development of harmful chemical precipitates such as ferric hydroxide and aluminium hydroxide that smother the aquatic habitat and reduce light penetration.
- Impact groundwater quality.
- Lead to installation of expensive control, treatment and rehabilitation processes.
- Limitation of mine water reuse and aggravation of corrosion to site infrastructure and equipment.
- The creation of long-term environmental liabilities.

### 2.1.3 Treatment and Remediation of Acid Mine Drainage

AMD control and treatment techniques can be broadly classified into chemical, biological, and those using a combination of the two. AMD remediation is aimed at increasing the pH of the wastewater as well as the reduction of heavy metals and salts to acceptable concentration levels.

#### 2.1.3.1 Chemical Treatment

The chemical remediation of AMD may involve the use of active or passive treatment technologies. Active treatment involves the addition of alkaline reagents, like CaO, $Ca(OH)_2$, $CaCO_3$, NaOH, $NH_3$ and $Na_2CO_3$, resulting in acid water neutralisation and the precipitation of heavy metals (Ledin and Pedersen, 1996, Petrik, et al., 2005). Reagents are relatively cost

The $H_2S$ and $HCO_3^-$ formed during sulphate reduction equilibrate into a mixture of $H_2S$, $HS^-$, $S^{2-}$ $CO_2$, $HCO_3^-$, and $CO_3^{2-}$, which will buffer the solution pH to a value typically in the range of 6-7 provided sufficient sulphate reduction takes place and the specific quantities and types of end-products are formed.

Sources of carbon or simple electron donors, including methanol and ethanol, are fairly expensive and are therefore not suitable for use in developing countries such as South Africa (Molwantwa, et al., 2004). Alternative relatively inexpensive soluble carbon sources that have been evaluated for active bacterial sulphate reduction include producer gas (Du Preez, et al., 1992), molasses (Maree and Hill, 1989), lactate and cheese whey (Oleszkiewicz and Hilton, 1986), cattle waste (Ueki, et al., 1988) and sewage sludge (Burgess and Wood, 1961).

The use of sewage sludge as an organic electron donor for the bioremediation of AMD in developing countries such as South Africa is possibly the most cost-effective option as costs associated with chemical reagents, labour and sludge removal are negligible (Molwantwa, et al., 2004). The additional advantage of treating AMD in conjunction with sewage sludge is that there is no longer a need to treat sewage sludge independently (Ristow, 1999).

## 2.2 Mechanisms and Kinetics of Anaerobic Digestion and Sulphate Reduction with regard to the UCTADM1

### 2.2.1 Overview of Anaerobic Digestion

Anaerobic digestion is a natural biological process in which an interdependent community of bacteria work together to form a stable, autonomous fermentation that converts organic material into a mixture of inorganic end-products including methane, carbon dioxide and sulphide, in the absence of oxygen.

Biological treatment of sewage and industrial wastewaters such as aerobic treatment generates additional sludge which must be disposed of in a method which is deemed to be acceptable to any community owing to environmental concern (Roberts, et al., 1999). The synthesis of biological cells during anaerobic treatment is significantly lower than with aerobic processes, tending to minimise waste sludge disposal problems and nutrient requirements (McCarty, 1974). Due to anaerobic treatment not requiring oxygen, treatment rates are not limited by oxygen transfer and the non-requirement for oxygen reduces power requirements (Sacks and Buckley, 2004). An additional advantage of anaerobic digestion is the production

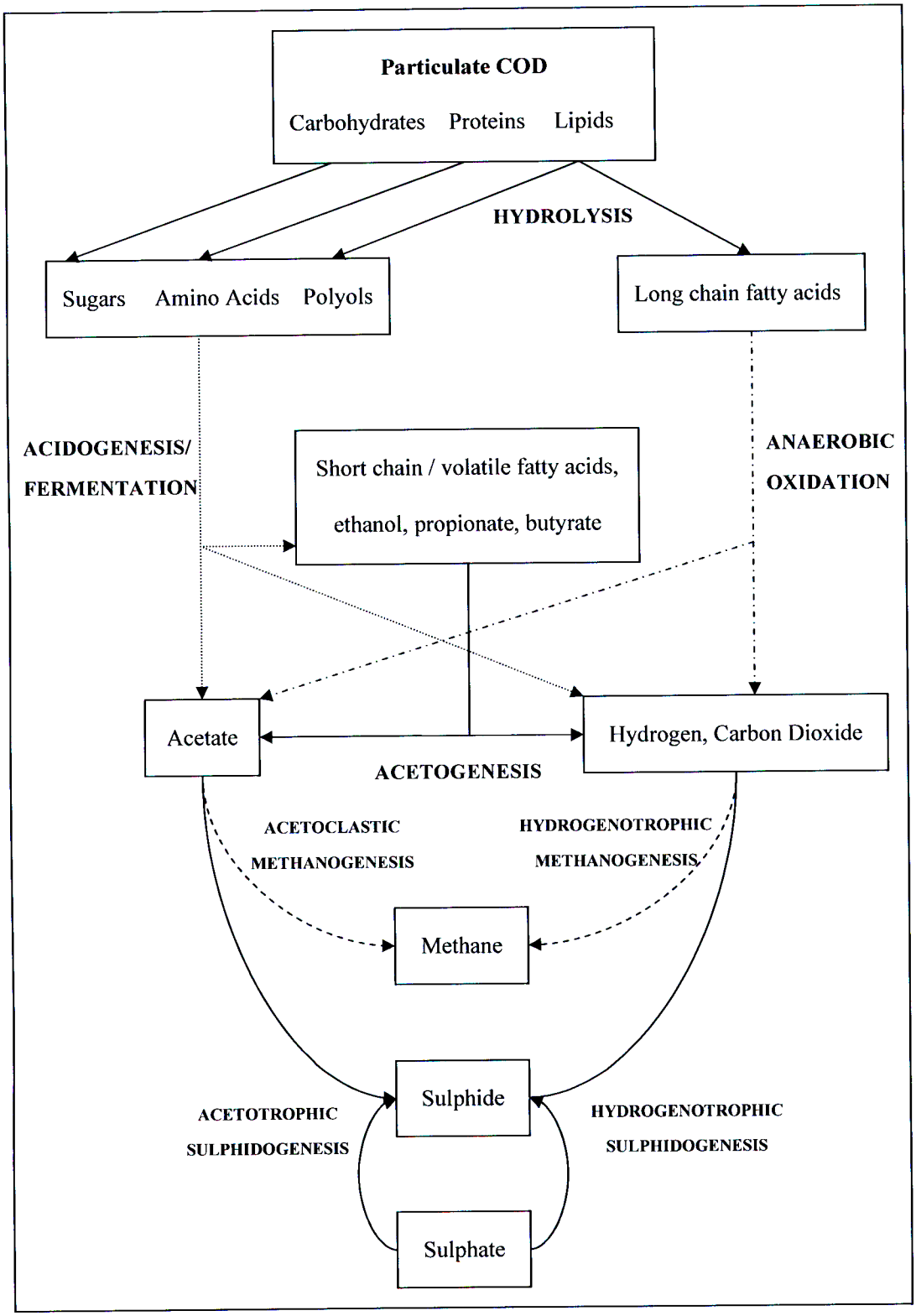


**Figure 2-1:** Reaction scheme showing the interacting flows of substrates between each biological process of anaerobic digestion including sulphate reduction. (From Hansford (2004) and Ristow (1999) who modified the original reaction scheme proposed by Gujer and Zehnder (1983))

processes of anaerobic digestion into the two phase (aqueous-gas) mixed weak acid/base chemistry model of Musvoto et al. (2000a), viz. $CO_2$, $CH_4$, $H_2$ and $NH_3$. Only the physical processes for carbon dioxide gas exchange with the atmosphere were included (i = 27, j = 29-30). $CO_2$ was modelled with both expulsion and dissolution due to its significantly soluble nature.

Sötemann et al. (2005b) obtained the rate equations for the ten biological processes (Table 2-2) in the UCTADM1 from various literature sources and modified them, where possible to best describe the reactions as realistically and accurately as possible. The kinetic model was extended to include to the condition of digester failure due to hydrogen ion activity (pH) and hydrogen partial pressure ($pH_2$), to which certain organisms are most sensitive to. The experimental data set of Izzett et al. (1992) was used for the successful calibration and validation of the UCTADM1 in the AQUASIM modelling and simulation platform. It must be noted that the basic UCTADM1 does not include the processes of biological sulphate reduction and would therefore need to be extended to incorporate this. The kinetic rate equations chosen for the biological processes in the anaerobic digestion model are described below:

### 2.2.2 Hydrolysis

Bacteria are unable to take up polymeric material unless it is broken down to soluble compounds such as soluble polymers, monomers or dimers, and therefore hydrolysis is the first step in the anaerobic degradation of complex polymeric organics required for microbial utilisation (Gujer and Zehnder, 1983, Pavlostathis and Giraldo-Gomez, 1991). During hydrolysis fermentative bacteria colonise the surface of particles, secreting hydrolytic enzymes, which are responsible for the extracellular hydrolysis of complex organic materials such as PSS. According to Hansford (2004), the following reactions are expected to occur:

- Hydrolysis of amide bonds of proteins to yield amino acids;
- Hydrolysis of ester bonds of lipids to yield LCFAs, glycerol (and other polyols) and alcohols;
- Hydrolysis of glucoside bonds of polysaccharides to yield dimeric and monomeric sugars.

Further, the rate of hydrolysis has been shown to be dependent on a large number of factors and is generally the rate-limiting step in the anaerobic digestion of particulate matter.

- In model application accumulation of glucose will not occur, even under digester failure conditions.

- Glucose acts merely as an intermediate compound, which is acidified to SCFAs as soon as it is produced.

- Irrespective of the hydrolysis formulation used, no acidogen biomass growth takes place and 1 g COD biodegradable sewage sludge forms 1 g COD glucose intermediate.

Various kinetic formulations for the hydrolysis process were investigated:

#### 2.2.2.1 First Order Kinetics

Although the rate of hydrolysis is affected by all of the above-mentioned factors, the most common rate equation with respect to the total biodegradable particulate COD ($S_p$) concentration (Eastman and Ferguson, 1981, Gujer and Zehnder, 1983, Henze and Harremöes, 1983, Pavlostathis and Giraldo-Gomez, 1991):

$$r_{HYD} = K_h \left[ S_p \right] \tag{2-9}$$

where:

$r_{HYD}$ = hydrolysis rate (mol $S_{bp}$/ℓ.d)

$K_h$ = first order hydrolysis rate constant ($d^{-1}$)

$[S_p]$ = sum of biodegradable ($S_{bp}$) and unbiodegradable ($S_{up}$) particulate fractions (mol/ℓ)

The hydrolysis rate constant is a function of the conditions used, with substrates used ranging from primary domestic sludge (Eastman and Ferguson, 1981), to organic solids (Gujer and Zehnder, 1983), to wastewater (Henze and Harremöes, 1983).

Ristow, et al. (2005) and Ristow (1999) stated that in all applications of the first order rate equation above, the hydrolysis rate was formulated with respect to the total particulate COD ($S_p$) and no differentiation was made between the biodegradable ($S_{bp}$) and unbiodegradable ($S_{up}$) fractions. Further, for pure substrates this omission is reasonable as the substrate is known and defined, but for waste sludges such as PSS, the $S_{up}$ fraction would need to be considered, since

#### 2.2.2.3 Surface mediated reaction (or Contois) kinetics

Sötemann, et al., (2005b) investigated the use of surface mediated reaction kinetics for their anaerobic digestion model and implemented the approach of Levenspiel (1972), used by Dold et al. (1980) to model the hydrolysis of particulate slowly biodegradable COD in activated sludge systems. Using a single set of constants, these kinetics gave reasonable predictions over a wide range of activated sludge system conditions and is therefore feasible to use this approach as the hydrolysis processes in activated sludge and anaerobic digestion can be regarded as similar and operate on the same organics present in raw sludge (Sötemann, et al., 2005b):

$$r_{HYD} = \left[ \frac{k_{\max,HYD} \frac{[S_{bp}]}{[Z_{ai}]}}{K_{SS,HYD} + \frac{[S_{bp}]}{[Z_{ai}]}} \right] [Z_{ai}] \qquad (2\text{-}13)$$

where:

$k_{max,HYD}$ = maximum specific hydrolysis rate constant (mol $S_{bp}$/mol $Z_{ai}$.d)

$K_{SS,HYD}$ = Half saturation constant for hydrolysis (mol $S_{bp}$/mol $Z_{AD}$)

The data set of Izzett et al. (1992) was used to calibrate the constants for the four variations in hydrolysis kinetics. It was difficult to decide which rate expression was best and each yielded a slightly different unbiodegradable particulate COD fraction on the sewage sludge between 0.33 and 0.36. It was decided by Sötemann et al. (2005b) that since this process is mediated by the acidogens, the surface reaction mediated kinetics which includes this organism group would naturally be more reasonable, and was therefore accepted for incorporation with the UCTADM1.

### 2.2.3 Acidogenesis

Acidogenesis refers to the use of the model intermediate, glucose ($S_{bs}$), by acidogenic or fermentative organisms, producing propionic acid, acetic acid, hydrogen, carbon dioxide and protons.

Acidogenic organisms produce acetic acid, propionic acid, hydrogen and carbon dioxide according to the following reactions (Hansford, 2004, Mosey, 1983):

from 1.

### 2.2.4 Acetogenesis

Acetogenesis is the process whereby under low hydrogen partial pressure acetogenic organisms convert propionic acid generated by acidogenesis under high hydrogen partial pressure to acetic acid. McCarty and Mosey (1991) describe the anaerobic oxidation of propionate:

$$CH_3CH_2COOH + 2H_2O \rightarrow CH_3COOH + CO_2 + 3H_2 \qquad (2\text{-}18)$$

The rate of acetogenesis was modelled in terms of acetogen growth rate ($r_{Zae}$) and with a Monod equation for the specific growth rate:

$$r_{Z_{ae}} = \frac{\mu_{\max,ae}[H\,\mathrm{Pr}]}{K_{S,ae} + [H\,\mathrm{Pr}]}\left\{1 - \frac{[H_2]}{k_{H_2} + [H_2]}\right\}[Z_{ae}] \qquad (2\text{-}19)$$

where:

$\mu_{max,ae}$ = maximum specific growth rate constant for acetogens ($d^{-1}$)

$K_{S,ae}$ = half saturation concentration for acetogens growth on propionic acid (mol/ℓ)

[HPr] = undissociated propionic acid concentration (mol/ℓ)

$[Z_{ae}]$ = acetogenic organism concentration (mol/ℓ)

The non-competitive inhibition function in the { } brackets is also present as in Equation 2-16 due to the acetogenesis process being sensitive to $pH_2$, the rate decreases as $pH_2$ increases. As $pH_2$ increases, acidogens begin to produce propionic acid and the rate of propionic acid utilisation by acetogens decreases resulting in a build-up of propionic acid which contributes to a drop in the pH.

### 2.2.5 Acetoclastic Methanogenesis

Acetoclastic methanogenesis, or acetate cleavage, is the process whereby acetic acid is converted to methane and carbon dioxide. The overall reaction for the biological production of methane from acetic acid is given by:

$$CH_3COOH \rightarrow CH_4 + CO_2 \qquad (2\text{-}20)$$

$$r_{Z_{hm}} = \frac{\mu_{\max,hm}[H_2]}{K_{S,hm} + [H_2]\left\{1 + \frac{[H^+]}{K_{i,hm}}\right\}}[Z_{hm}] \qquad (2\text{-}23)$$

where:

$\mu_{max,hm}$ = maximum specific growth rate constant for hydrogenotrophic methanogens ($d^{-1}$)

$K_{S,hm}$ = half saturation concentration of hydrogenotrophic methanogens growth on hydrogen (mol/ℓ)

$Ki_{,hm}$ = inhibition constant (mol/ℓ) i.e. the hydrogen ion concentration at which the growth of hydrogenotrophic methanogens is half the maximum rate

$[H_2]$ = molecular hydrogen concentration (mol/ℓ)

$[Z_{hm}]$ = hydrogenotrophic methanogen organism concentration (mol/ℓ)

The effect of hydrogenotrophic methanogens is to keep the hydrogen partial pressure low and like acetoclastic methanogens, they are sensitive to a pH decrease within in anaerobic digesters. A first order inhibition term for hydrogen ion or pH inhibition was again included in the growth rate equation.

### 2.2.7 Sulphate Reduction

SRB are capable of growing on more varied substrates than methane producing bacteria (Oude Elferink, et al., 1994). Both sulphate reduction and methanogenesis can be the final step in the degradation process of sulphate fed anaerobic reactors, due to SRB being capable of utilising many of the intermediates formed during methanogenesis (Kalyuzhnyi, et al., 1998). This is illustrated in Figure 2-2.

Competition for substrate in such systems is possible on two levels: competition between SRB and acetogenic bacteria for VFA and a carbon source, and competition between SRB and methanogenic bacteria for acetate and hydrogen.

During the process of biological sulphate reduction, sulphate is reduced to the main product of this process viz. sulphide, which is a strong toxicant for most anaerobic organisms including acetogens, methanogens and SRB. Sulphide inhibition is related with the undissociated form which can permeate the cell membrane, affecting the activity of the organism. Small variations in pH can also result in significant changes in the degree of inhibition.

The model proposed by Vavilin et al. (1994) did not address the competition between sulphate reduction and methanogenesis. All the above-mentioned models, including that of Kalyuzhnyi and Fedorovich (1997 and 1998), were developed mainly for continuously stirred tank reactors (CSTR's).

Kalyuzhnyi et al. (1998) developed a new integrated mathematical model of the functioning of a sulphate fed granular sludge reactor which takes into account concentration gradients on substrates, intermediates, products and organisms inside the digester. The proposed model was developed for the degradation of a mixture of sucrose, propionate, acetate and sulphate. Multiple-reaction stoichiometry and kinetics have also been developed and verified for this dispersed plug-flow model of upflow anaerobic sludge blanket (UASB) reactors.

#### 2.2.7.1 Acetogenic Sulphidogenesis

Acetogenic sulphidogenesis is the process whereby propionate degrading SRB convert propionic acid and sulphate to acetic acid, sulphide, carbon dioxide and water. Kalyuzhnyi et al. (1998) presented the reaction sequence for substrate utilisation of propionate to produce acetate as follows:

$$CH_3CH_2COOH + \frac{3}{4}SO_4^{2-} + \frac{3}{2}H^+ \rightarrow CH_3COOH + \frac{3}{4}H_2S + CO_2 + H_2O \qquad (2\text{-}24)$$

This process was formulated in terms of the acetogenic sulphidogen growth rate ($r_{Zps}$), which is modelled with a Monod equation including a sulphide inhibition term in { }:

$$r_{Z_{ps}} = \frac{\mu_{\max,ps}[H\,\mathrm{Pr}]}{K_{S,ps} + [H\,\mathrm{Pr}]}\left\{1 - \frac{[H_2S]}{Ki_{ps}}\right\}\left(\frac{[SO_4^{2-}]}{Kn_{ps} + [SO_4^{2-}]}\right)[Z_{ps}] \qquad (2\text{-}25)$$

where:

$\mu_{max,ps}$ = maximum specific growth rate constant for acetogenic sulphidogens ($d^{-1}$)

$K_{S,ps}$ = half saturation concentration for acetogenic sulphidogen growth on propionic acid (g COD/ℓ)

$Ki_{,ps}$ = inhibition constant i.e. the hydrogen sulphide concentration at which the growth of acetogenic sulphidogens is half the maximum rate (g S/ℓ)

$Kn_{,ps}$ = half saturation concentration for acetogenic sulphidogen growth on sulphate (g/ℓ)

[HPr] = total propionic acid concentration (g COD/ℓ)

This process is also modelled in terms of the growth rate of hydrogenotrophic methanogens ($r_{Zhm}$), using a Monod equation with a sulphide inhibition term in { }:

$$r_{Z_{hs}} = \frac{\mu_{max,hs}[H_2]}{K_{S,hs}+[H_2]}\left\{1-\frac{[H_2S]}{Ki_{hs}}\right\}\left(\frac{[SO_4^{2-}]}{Kn_{hs}+[SO_4^{2-}]}\right)[Z_{hs}] \qquad (2\text{-}29)$$

where:

$\mu_{max,hs}$ = maximum specific growth rate constant for hydrogenotrophic sulphidogens ($d^{-1}$)

$K_{S,hs}$ = half saturation concentration for hydrogenotrophic sulphidogen growth on hydrogen (g COD/ℓ)

$Ki_{,hs}$ = inhibition constant i.e. the hydrogen sulphide concentration at which the growth of hydrogenotrophic sulphidogens is half the maximum rate (g S/ℓ)

$Kn_{,hs}$ = half saturation concentration for hydrogenotrophic sulphidogen growth on sulphate (g/ℓ)

$[H_2]$ = total hydrogen concentration (g COD/ℓ)

$[Z_{hs}]$ = hydrogenotrophic sulphidogen organism concentration (g/ℓ)

### 2.2.8 Death/Endogenous Respiration of organisms

Organism death in anaerobic digestion is associated with endogenous respiration only, as predation apparently does not occur. The organism death rate for each organism group was modelled with first order kinetics:

$$-r_Z = b_Z[Z] \qquad (2\text{-}30)$$

where:

$b_Z$ = death/endogenous respiration rate for a specific organism group ($d^{-1}$)

$[Z]$ = specific organism group concentration (mol/ℓ)

### 2.2.9 Kinetic and Stoichiometric Parameters

The kinetic and stoichiometric parameters shown in Table 2-3 were used by Sötemann et al. (2005b) in the calibration and verification of the UCTADM1 and were obtained from Sam-Soon et al. (1991) at 37 °C. The data set of Izzett et al. (1992) was used to calibrate constants for hydrolysis kinetics i.e. $K_{max,HYD}$ and $K_{s,HYD}$.

**Table 2-4:** Kinetic parameters used in the sulphate reduction model (From Kalyuzhnyi et al., 1998)

| Organism Group | $\mu_{max}$ ($d^{-1}$) | $K_s$ (g COD/ℓ) | $K_n$ (g/ℓ) | $K_i$ (g S/ℓ) | Y (g VSS/g COD) | b ($d^{-1}$) |
|---|---|---|---|---|---|---|
| Acidogens | 4 | 0.028 | - | 0.55 | 0.034 | 0.09 |
| Acetogens | 0.16 | 0.247 | - | 0.19 | 0.016 | 0.014 |
| Acetogenic sulphidogens | 0.583 | 0.295 | 0.0074 | 0.185 | 0.027 | 0.0185 |
| Acetoclastic methanogens | 0.264 | 0.12 | - | 0.185 | 0.0215 | 0.02 |
| Acetoclastic sulphidogens | 0.612 | 0.024 | 0.0192 | 0.164 | 0.033 | 0.0275 |
| Hydrogenotrophic methanogens | 1 | 1.2E-04 | - | 0.165 | 0.015 | 0.04 |
| Hydrogenotrophic sulphidogens | 2.8 | 7E-05 | 0.0192 | 0.55 | 0.05 | 0.06 |

## 2.3 The Rhodes BioSURE Process®

Researchers in the Environmental Biotechnology Research Unit and Department of Biochemistry, Microbiology and Biotechnology at Rhodes University studied the use of PSS for sulphate reduction. This research resulted in the development of the Rhodes BioSURE Process® which links AMD bioremediation and sewage sludge disposal. The Rhodes BioSURE Process® has been developed as a low-cost active treatment method for AMD wastewaters, where the process development was based on prior studies in the microbial ecology of sulphidogenic ponding environments (Rose, et al., 2002, Whittington-Jones, et al., 2002).

The Rhodes BioSURE Process® was claimed to be more economic than any other biological treatment option presently available, reducing costs from approximately R5/kℓ to R1/kℓ in operating expenditure (WISA, 2005).

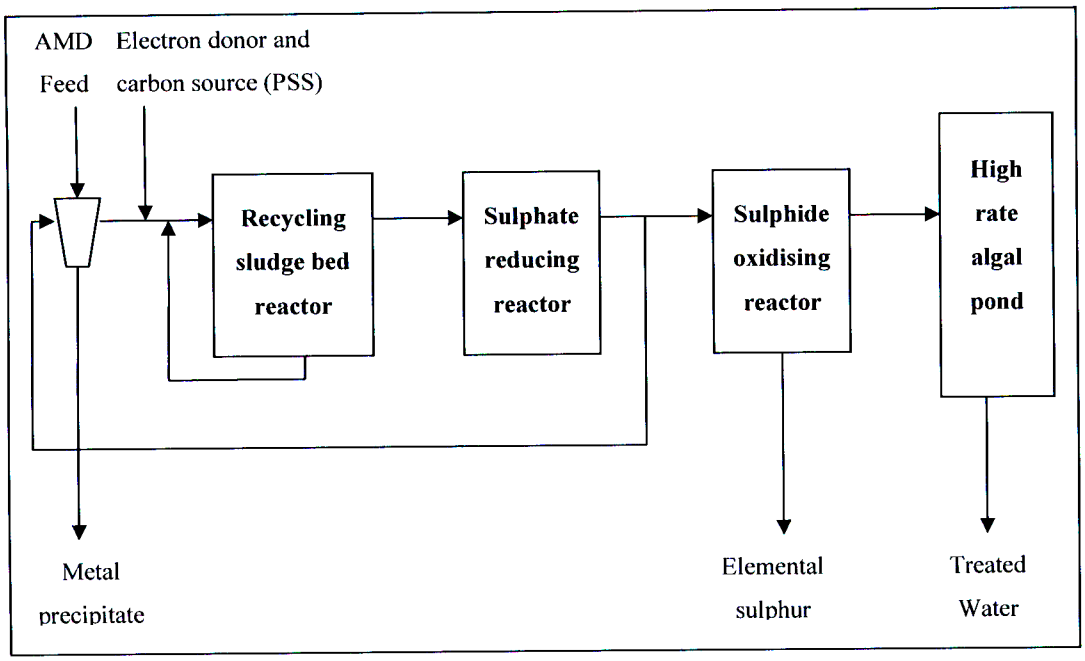


**Figure 2-3:** Process flow diagram of the Rhodes BioSURE Process ® applied to the treatment of acid mine drainage (From Rose et al., 2002)

The products from the RSBR are then used by SRB in the sulphate reducing digester. The configuration selected for the sulphate reducing digester is that of an anaerobic baffled reactor (ABR). Sulphate reduction is optimised further by the recycling of sulphide and carbonate alkalinity which comes into contact with the feed AMD, neutralising the pH and precipitating the feed heavy metals as metal sulphides, carbonates and hydroxides (Ristow, et al., 2005). The fraction of the sulphide-rich stream that is not recycled is passed to a sulphide oxidising reactor where it is reduced to elemental sulphur and removed from the process. The final unit operation in the process is a high rate algal pond, where the neutralised stream from the sulphide oxidising reactor is polished and disinfected prior to discharge of treated water.

## 2.4 Closure

In summary, Sötemann et al., (2005b) developed the UCTADM1 which integrates various biological anaerobic processes for the production of methane. This methanogenic model forms the basis to be extended with the development of a mathematical model incorporating the processes of biosulphidogenic reduction and the biology of SRB. Kinetic parameters of Sötemann et al. (2005b) and Kalyuzhnyi et al. (1998) will be further investigated in this work for application within the model.

# CHAPTER 3

# EXPERIMENTAL AND PILOT PLANT STUDIES

## 3.1 The UCT Experimental Investigation

The main reaction in the Rhodes BioSURE Process® is biosulphidogenic reduction of AMD with PSS, and therefore the design, operation and control of this process is dependent on the rate at which PSS is used (Ristow, et al., 2005). The Water Research Group at the University of Cape Town (UCT) have conducted an experimental investigation into, as well as the mathematical modelling of the rate of PSS hydrolysis under methanogenic, acidogenic and sulphate reducing conditions.

According to Ristow et al., (2005), the principle aim of this research was to determine the rate of hydrolysis of PSS under methanogenic, acidogenic and sulphate reducing conditions, and the influence of the system physical constraints on the rate which will enable a direct comparison of the rate under each of the three conditions and possible influences thereof. The experimental investigation undertaken by Ristow and co-workers (2005) is summarised as follows:

### 3.1.1 Feed collection and storage

PSS was collected from the Athlone Wastewater Treatment Works in Cape Town and stored in a cold room at a temperature of 4 °C for the duration of a digester steady state. The PSS was passed through a mesh sieve to remove large particles such as rags, cigarette butts, seeds and other debris, but without changing the nature of the feed by removing a significant fraction of the feed.

### 3.1.2 Feed preparation

The feed was prepared by weighing a mass of PSS and then adding warm or hot water to a temperature of 35 °C, until a desired final mass of diluted sludge was obtained. This would minimise the temperature shock load to the system as the digester operating temperature is 35 °C before feeding the headspace of the digester was purged with nitrogen to remove any oxygen from the system and capture any $H_2S$ formed in and $FeCl_3$ solution and after feeding was resealed. After sealing it was again purged with $N_2$. This enabled a completely anaerobic environment to be maintained.

mentioned above.

**Table 3-1:** Steady states measured for varying hydraulic retention times and feed COD concentrations, where numbers indicate steady state period number for methanogenic systems (From Ristow et al., 2005)

| Feed COD Concentration | Hydraulic Retention Time (d) | | | | | | | |
|---|---|---|---|---|---|---|---|---|
| (g COD/ℓ) | 60 | 20 | 15 | 10 | 8 | 6.67 | 5.71 | 5 |
| 40 | | | 10, 11 | 12 | 21 | 23 | 28 | |
| 25 | | 3 | 4 | 1 | 2 | 7 | 8 | 9 |
| 13 | | | 5 | 13 | 14 | 24 | 31 | |
| 9 | 17 | | | | | | | |
| 2 | | | | 25 | 18, 19, 26, 27 | | | |

### 3.1.6 Acidogenic Systems

Steady state acidogenic digesters were operated under hydraulic retention times from 3.33-10 days and feed COD concentrations 2-40 g COD/ℓ at a constant temperature of 35 °C (Table 3-2).

**Table 3-2:** Steady states measured for varying hydraulic retention times and feed COD concentrations, where numbers indicate steady state period numbers for acidogenic systems (From Ristow et al., 2005)

| Feed COD Concentration | Hydraulic Retention Time (d) | | |
|---|---|---|---|
| (g COD/ℓ) | 10 | 5 | 3.33 |
| 40 | | 30 | 29 |
| 13 | 38 | 33 | 32 |
| 2 | 39 | 35 | 34 |

As mentioned above, the reduction in hydraulic retention times for each feed concentration in methanogenic systems resulted in the methanogenic biomass becoming unstable and

## 3.2 The Pilot Plant

One of the areas in South Africa where AMD and decanting mine water is becoming a significant issue is the Witwatersrand Basin. According to WRC (2005), the gold mines in the basin contribute as much as 35 % of the salt load entering the Vaal Barrage by way of their point source discharges. Mines are required to pump water from underground to dewater areas for development or to prevent flooding of existing works. The closure of mines through the years has resulted in the Grootvlei Mine taking on the responsibility of pumping most of the water from the Eastern Basin (WRC, 2005).

The Environmental Biotechnology Research Unit was invited toward the end of 1997 to participate in the Grootvlei desalination technology evaluation exercise and since 1998 have proceeded to design, construct and implement the Rhodes BioSURE® pilot plant on-site at the East Rand Watercare Company's (ERWAT) Ancor Works at the Grootvlei Mine. Hydrolysis of PSS, a by-product from ERWAT, together with AMD provides the primary reaction in the Rhodes BioSURE Process® and takes place in the pilot RSBR.

The existing design and configuration of the pilot RSBR, illustrated in Figure 3-2, has been revised to that of an upflow anaerobic sludge blanket (UASB) with recycle of the clarified liquid and wasting of the sludge. The most significant characteristic of this configuration is the improved separation of particulates from the overflow effluent and their retention time in the reactor. The UASB vessel has three outlets viz. overflow, recycle and gas streams.

At the time of this study, the pilot plant had only been in operation for a short period due to equipment teething problems and therefore the available operating data is minimal. Figure 3-1 contains all the information available at the time (Ristow, 2005), including estimated values and qualitative statements. The recycle stream was removed from 1 m below the liquid level at a flowrate of 5 $m^3/h$. The sludge bed was maintained at ± 0.5 m below the liquid level by a sludge withdrawal rate of ± 1 $m^3/h$. The overflow was practically free of suspended solids.

# CHAPTER 4

# WEST®: A PLATFORM FOR MODELLING AND SIMULATION

## 4.1 Introduction to Modelling

Modelling is an important tool and forms an inherent part in the comprehensive study of microbial ecology, process design and the determination of optimal operating conditions in biological wastewater treatment plants. It allows the evaluation of key hypotheses and predicting the effects of a perturbation on the system without actually disturbing it. Attention is drawn to deficiencies in the conceptual structure by the comparison of simulated and experimental responses which allows potentially feasible solutions to be explored without pilot-scale or experimental studies, thereby aiding the selection of more promising ones for testing (Kalyuzhnyi, et al., 1998).

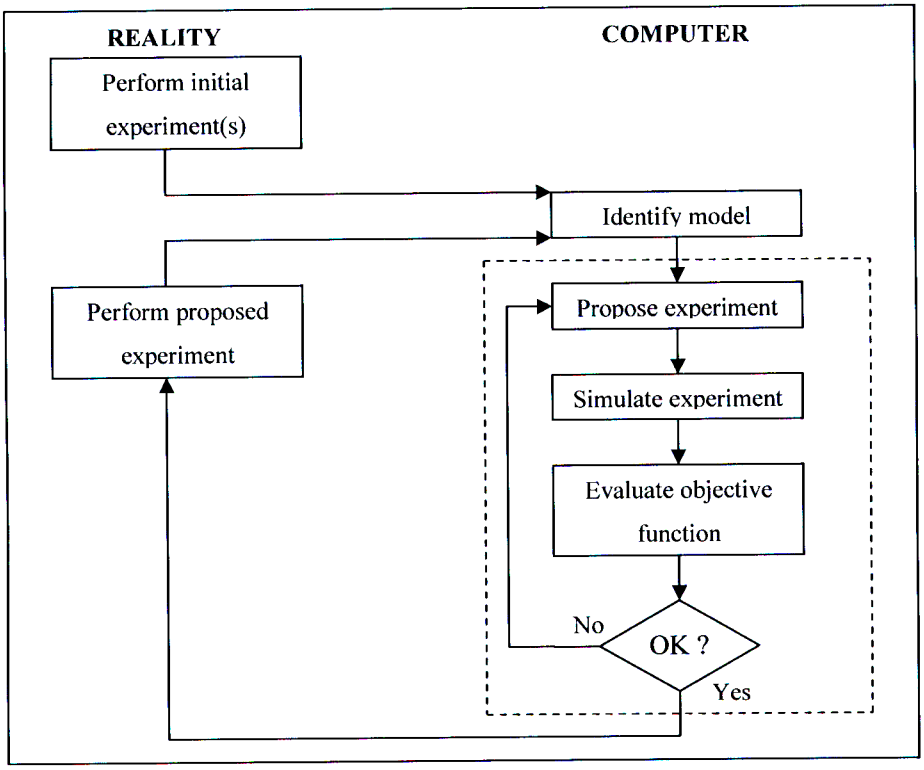


**Figure 4-1:** General procedure for optimal experimental design (From Dochain and Vanrolleghem, 2001)

### 4.2.2 WEST® Software Architecture

The functional architecture of WEST® and the different steps that need to be followed to build a model and perform experiments with it, as explained by Vanhooren and co-workers (2003), is graphically represented in Figure 4-2.

The model base is the core of WEST® whereby models are described in MSL-USER (MSL stands for model specification language), a high level object-oriented declarative language specifically developed to incorporate models. Figure 4-3 represents a model base in the WEST® MSL Editor. The purpose of the model base is to maximise the reuse of existing knowledge such as mass balances, physical units, default parameter values and applicable ranges, and is therefore structured hierarchically.

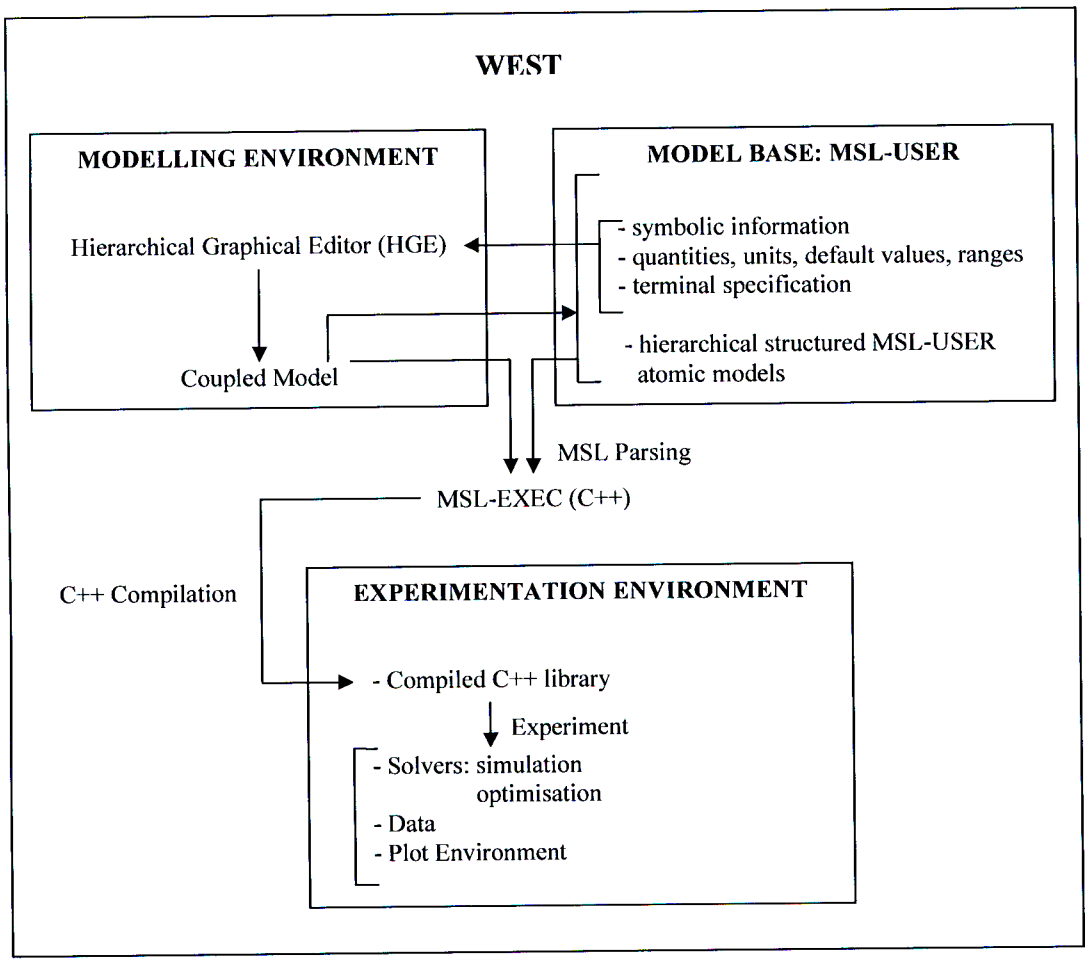


**Figure 4-2:** Functional architecture of WEST® (From Vanhooren et al., 2003)

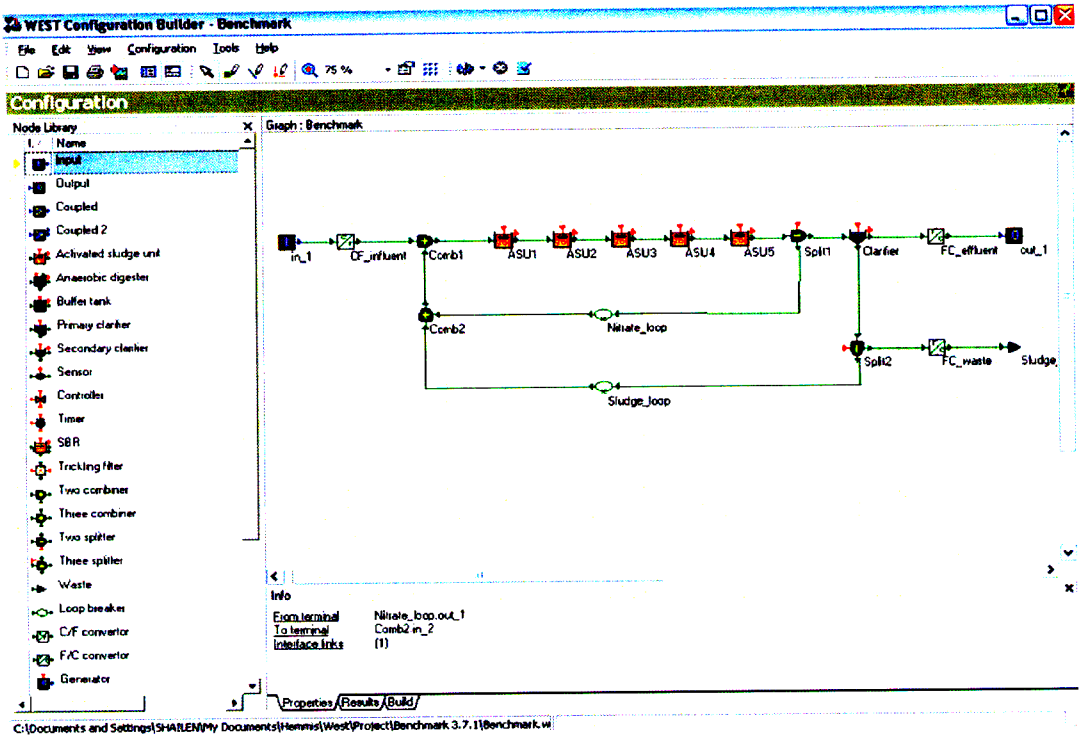


**Figure 4-4:** Depiction of a wastewater treatment plant model in the Hierarchical Graphical Editor (HGE) of the configuration builder


**Figure 4-5:** The WEST® experimentation environment, showing a plot and a variable listing

**Table 4-1:** Petersen matrix representation of biochemical rate coefficients $\upsilon_{i,j}$ and kinetic process rate equations $\rho_j$ for components (i = 1-m, j = 1-n)

| **Component** | $C_1$ | $C_2$ | | | $C_i$ | | | $C_m$ | **Rates** |
|---|---|---|---|---|---|---|---|---|---|
| **Process 1** | $\upsilon_{1,1}$ | $\upsilon_{2,1}$ | | | $\upsilon_{i,1}$ | | | | $\rho_1$ |
| | | | | | | | | | |
| | | | | | | | | | |
| **Process j** | | | | | $\upsilon_{i,j}$ | | | | $\rho_j$ |
| | | | | | | | | | |
| | | | | | | | | | |
| **Process n** | | | | | | | | $\upsilon_{mn}$ | $\rho_n$ |

Once biological processes, model components, biochemical rate coefficients and kinetic process rates are implemented in the WEST® Petersen matrix of the model editor, the MSL-USER compiler generates the simulation code.

The matrix representation is not only limited to already built-in models such as ASM1 or ADM1, but allows the modeller to implement mass balance models himself using only the component vector, the reaction vector and the stoichiometric and kinetic coefficients that need to be specified, as in the case of the UCTADM1. The Petersen matrix or table format offers the best opportunity for overcoming the difficulty of tracing all the interactions of the system components, while conveying the maximum amount of information.

Multiplying Equation 5-2 by the anabolic yield ($Y'_{ps}$) of acetogenic bacteria and adding the associated Equation 5-1 to it:

$$\begin{aligned}&\left(1+3Y'_{ps}\right)CH_3CH_2COOH+\frac{3}{4}SO_4^{2-}+Y'_{ps}\,CO_2+2Y'_{ps}\,NH_4^{+}+\frac{3}{2}H^{+}\\&\rightarrow 2Y'_{ps}\,C_5H_7O_2N+CH_3COOH+\frac{3}{4}H_2S+CO_2+Y'_{ps}\,H_2+2Y'_{ps}\,H^{+}\\&+\left(1+4Y'_{ps}\right)H_2O\end{aligned}\qquad (5\text{-}3)$$

Dividing Equation 5-3 by $2Y'_{ps}$ for 1 mole biomass generation and simplifying:

$$\begin{aligned}&\left(\frac{1+3Y'_{ps}}{2Y'_{ps}}\right)CH_3CH_2COOH+\frac{3}{8Y'_{ps}}SO_4^{2-}+NH_4^{+}\rightarrow C_5H_7O_2N+\frac{1}{2Y'_{ps}}CH_3COOH\\&+\frac{3}{8Y'_{ps}}H_2S+\left(\frac{1}{2Y'_{ps}}-\frac{1}{2}\right)CO_2+\frac{1}{2}H_2+\left(1-\frac{3}{4Y'_{ps}}\right)H^{+}+\left(\frac{1+4Y'_{ps}}{2Y'_{ps}}\right)H_2O\end{aligned}\qquad (5\text{-}4)$$

The stoichiometry in terms of the anabolic organism yield $Y'_{ps}$ for the growth process of acetogenic SRB is taken directly from Equation 5-4 and listed in Table 5-1. It must be noted that the anabolic organism yield $Y'_{ps}$ is not the true yield as it excludes the catabolic propionate requirement of the organisms. The metabolic (anabolic + catabolic) yield is a true yield in terms of propionate utilisation and since it is more conventional to express yields as true yields, this approach is also adopted here. The metabolic yield is obtained from Equation 5-4.

Let $Y_{ps}$ = metabolic yield.

1 mol biomass (160 g COD) grows from $\frac{1+3Y'_{ps}}{2Y'_{ps}}$ mol propionate. The true yield $Y_{ps}$ (mol/mol) is expressed as:

$$Y_{ps}=\frac{2Y'_{ps}}{1+3Y'_{ps}} \qquad (5\text{-}5)$$

Making $Y'_{ps}$ the subject of Equation 5-5:

terms of the true metabolic organism yield, shown in Table 5-2.

**Table 5-2:** Stoichiometry for acetogenic SRB in terms of the true organism yield

| Component | Unit | Stoichiometric coefficient |
|---|---|---|
| HPr | mol | $-\left(\frac{1}{Y_{ps}}\right)$ |
| $SO_4^{2-}$ | mol | $-\left(\frac{3}{4Y_{ps}}-\frac{9}{8}\right)$ |
| $H_2CO_3$ | mol | $\frac{1}{Y_{ps}}-2$ |
| $NH_4^+$ | mol | $-1$ |
| $Z_{ps}$ | mol | 1 |
| HAc | mol | $\frac{1}{Y_{ps}}-\frac{3}{2}$ |
| $H_2S$ | mol | $\frac{3}{4Y_{ps}}-\frac{9}{8}$ |
| $H_2$ | mol | $\frac{1}{2}$ |
| $H^+$ | mol | $\frac{13}{4}-\frac{3}{2Y_{ps}}$ |
| $H_2O$ | mol | $\frac{1}{Y_{ps}}+\frac{1}{2}$ |

### 5.1.2 Acetoclastic Sulphidogenesis

The same methodology applied for acetogenic sulphidogenesis was used for the growth of acetoclastic SRB. The reaction sequence (Kalyuzhnyi, et al., 1998) for use of acetate as a substrate is as follows:

**Table 5-3:** Stoichiometry for acetoclastic SRB in terms of the anabolic organism yield

| Component | Unit | Stoichiometric coefficient |
|---|---|---|
| HAc | mol | $-\left(\frac{1+5Y'_{as}}{2Y'_{as}}\right)$ |
| $SO_4^{2-}$ | mol | $-\left(\frac{1}{2Y'_{as}}\right)$ |
| $NH_4^+$ | mol | $-1$ |
| $Z_{as}$ | mol | 1 |
| $H_2S$ | mol | $\frac{1}{2Y'_{as}}$ |
| $H_2CO_3$ | mol | $\frac{1}{Y'_{as}}$ |
| $H^+$ | mol | $1-\frac{1}{Y'_{as}}$ |
| $H_2O$ | mol | $\frac{1+3Y'_{as}}{Y'_{as}}$ |

Substituting Equation 5-12 into the stoichiometry shown in Table 5-3 provides the stoichiometry for acetoclastic SRB in terms of the true (metabolic) yield, shown in Table 5-4.

Multiplying Equation 5-14 by the anabolic organism yield ($Y'_{hs}$) and adding Equation 5-13 to Equation 5-14:

$$5Y'_{hs}\,CO_2 + \left(4+10Y'_{hs}\right)H_2 + SO_4^{2-} + Y'_{hs}\,NH_4^{+} + 2H^{+} \rightarrow Y'_{hs}\,C_5H_7O_2N + H_2S + Y'_{hs}\,H^{+} + \left(4+8Y'_{hs}\right)H_2O \tag{5-15}$$

Dividing Equation 5-15 by $2Y'_{hs}$ and simplifying:

$$5CO_2 + \left(\frac{4+10Y'_{hs}}{Y'_{hs}}\right)H_2 + \frac{1}{Y'_{hs}}SO_4^{2-} + NH_4^{+} \rightarrow C_5H_7O_2N + \frac{1}{Y'_{hs}}H_2S + \left(1-\frac{2}{Y'_{hs}}\right)H^{+} + \left(\frac{4+8Y'_{hs}}{Y'_{hs}}\right)H_2O \tag{5-16}$$

The stoichiometry in terms of anabolic organism yield for the growth process of hydrogenotrophic SRB is taken directly from Equation 5-16 and listed in Table 5-5:

**Table 5-5:** Stoichiometry for hydrogenotrophic SRB in terms of anabolic yield

| Component | Unit | Stoichiometric coefficient |
|---|---|---|
| $H_2CO_3$ | mol | $-5$ |
| $H_2$ | mol | $-\left(\frac{4+10Y'_{hs}}{Y'_{hs}}\right)$ |
| $SO_4^{2-}$ | mol | $-\left(\frac{1}{Y'_{hs}}\right)$ |
| $NH_4^{+}$ | mol | $-1$ |
| $Z_{hs}$ | mol | 1 |
| $H_2S$ | mol | $\frac{1}{Y'_{hs}}$ |
| $H^{+}$ | mol | $1-\frac{2}{Y'_{hs}}$ |
| $H_2O$ | mol | $\frac{4+8Y'_{hs}}{Y'_{hs}}$ |

## 5.2 Kinetic Process Rates

### 5.2.1 Growth

Bacterial growths of each sulphidogenic organism group were modelled using Monod kinetics with simultaneous inhibition by pH and undissociated sulphide. The undissociated sulphide inhibition was reported as first order for all bacterial groups. The principles of the kinetic description are taken from Kalyuzhnyi et al. (1998). Thus, a specific growth rate equation for SRB was expressed as:

$$\mu_j = \mu_{max,j} \frac{[S_i]F(pH)}{K_{s,j}+[S_i]}\left[1-\frac{H_2S_f}{Ki_j}\right]\left[\frac{[SO_4^{2-}]}{Kn+[SO_4^{2-}]}\right] \quad (5\text{-}19)$$

The method of approach used by Kalyuzhnyi et al. (1998) in defining the kinetic rates was the same as that used in the UCTADM1 (Sötemann, et al., 2005b). A decision was made to include total substrate concentrations with respect to propionate and acetate for the respective organism growth processes in the model. This decision was based on the fact that Sötemann et al. (2005b) obtained kinetic parameters from Sam-Soon et al. (1991) which were based on total substrate concentrations in mg COD/ℓ. The kinetic principles of the Kalyuzhnyi et al. (1998) model were adapted from the model of Kalyuzhnyi and Fedorovich (1998), which were also based on total substrate concentrations in g COD/ℓ, and therefore kinetic parameters were selected based on this. Total substrate concentrations for propionate and acetate, represented by the addition of the undissociated and dissociated forms, were included in the respective Monod growth process terms of acetogenesis, acetoclastic methanogenesis, acetogenic sulphidogenesis and acetoclastic sulphidogenesis in the UCTADM1.

A major mismatch between the two reaction schemes of Sötemann et al. (2005b) and Kalyuzhnyi et al. (1998) concerned the representation of pH and $H_2S$ inhibition. The UCTADM1 did not consider $H_2S$ inhibition, since $H_2S$ is not present in the absence of sulphate reduction. The model proposed by Kalyuzhnyi et al. (1998) did not explicitly consider pH inhibition because it is difficult to distinguish between the effects of pH and $H_2S$ inhibition experimentally. Sulphide is present in solution as $H_2S$ and $HS^-$, and only the undissociated form appears to be toxic to the organisms. As the pH drops, $HS^-$ is progressively converted to $H_2S$, and this occurs chiefly in the pH range where pH inhibition becomes significant. Hence the $H_2S$ inhibition coefficients in the Kalyuzhnyi et al. (1998) model effectively contain the pH inhibition effect also. Hence it was decided to adopt a consistent set of inhibition terms

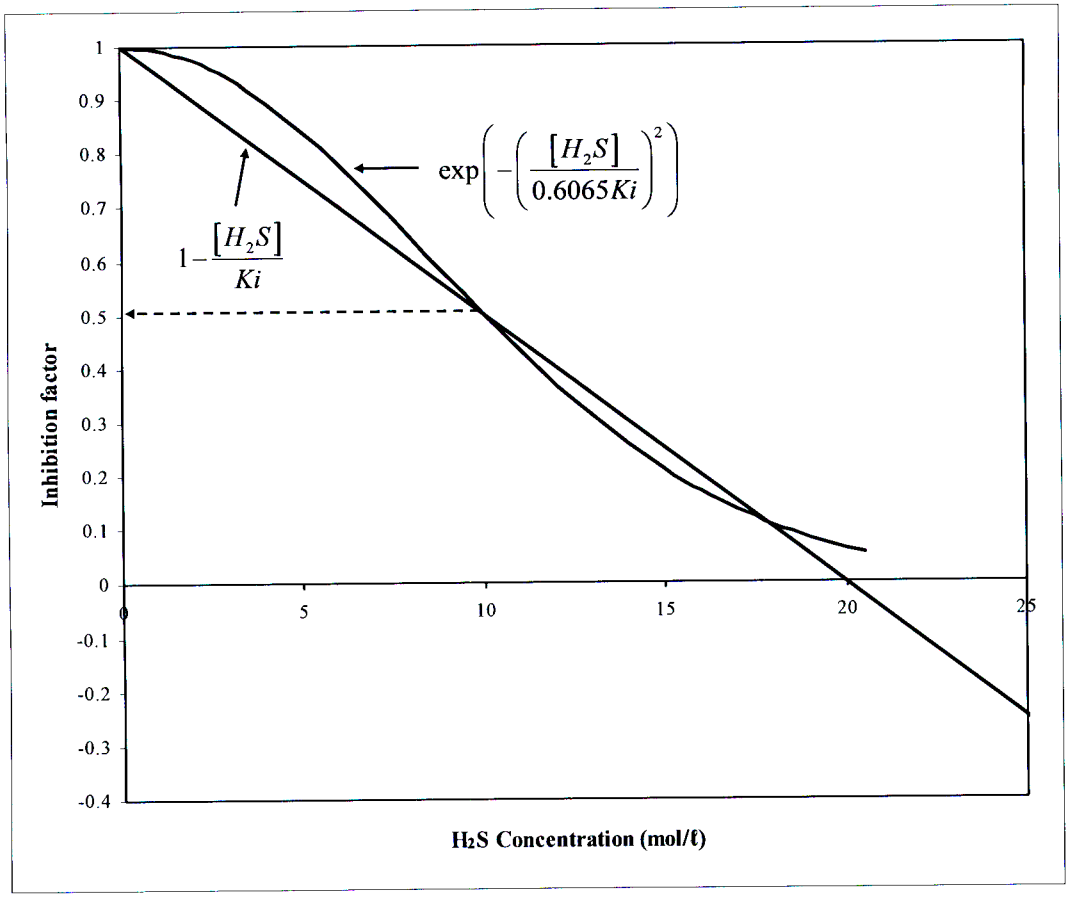


**Figure 5-1:** Comparison of inhibition factor forms

5.2.1.1 Acetogenic SRB

The specific growth rate of the acetogenic sulphidogenic organisms, including the revised form of the sulphide inhibition term in { } is given as follows:

$$r_{Z_{ps}} = \frac{\mu_{\max,ps}\left([H\,\mathrm{Pr}]+[\mathrm{Pr}^-]\right)}{K_{S,ps}+\left([H\,\mathrm{Pr}]+[\mathrm{Pr}^-]\right)}\left\{\exp\left(-\left(\frac{[H_2S]}{0.6065Ki_{ps}}\right)^2\right)\right\}\left(\frac{[SO_4^{2-}]}{Kn_{ps}+[SO_4^{2-}]}\right)[Z_{ps}] \quad (5\text{-}22)$$

where:

$\mu_{max,ps}$ = maximum specific growth rate constant for acetogenic sulphidogens ($d^{-1}$)

$K_{S,ps}$ = half saturation concentration for acetogenic sulphidogen growth on propionic acid (mol/ℓ)

$Ki_{,ps}$ = inhibition constant i.e. the hydrogen sulphide concentration at which the growth of acetogenic sulphidogens is half the maximum rate (mol/ℓ)

where:

$\mu_{max,hs}$ = maximum specific growth rate constant for hydrogenotrophic sulphidogens ($d^{-1}$)

$K_{S,hs}$ = half saturation concentration for hydrogenotrophic sulphidogen growth on acetic acid (mol/ℓ)

$Ki_{,hs}$ = inhibition constant i.e. the hydrogen sulphide concentration at which the growth of hydrogenotrophic sulphidogens is half the maximum rate (mol/ℓ)

$Kn_{,hs}$ = half saturation concentration for hydrogenotrophic sulphidogen growth on sulphate (mol/ℓ)

$[H_2]$ = hydrogen concentration (mol/ℓ)

$[Z_{hs}]$ = hydrogenotrophic sulphidogen organism concentration (mol/ℓ)

### 5.2.2 Endogenous Decay

The endogenous decay or death of organisms is described in Kalyuzhnyi et al. (1998) by first order kinetics. Bacterial decay in the UCTADM1 is also described by first order kinetics, hence this approach is used here.

#### 5.2.2.1 Acetogenic SRB

The specific rate equation for the decay of acetogenic SRB is expressed by first order kinetics according to:

$$r_{Z_{ps}} = b_{ps}\left[Z_{ps}\right] \tag{5-25}$$

where:

$b_{ps}$ = specific decay constant for acetogenic sulphidogens ($d^{-1}$)

$[Z_{ps}]$ = acetogenic sulphidogen organism concentration (mol/ℓ)

#### 5.2.2.2 Acetoclastic SRB

The endogenous decay of acetoclastic sulphidogens is represented with the following specific rate equation:

$$r_{Z_{as}} = b_{as}\left[Z_{as}\right] \tag{5-26}$$

and the reverse dissociation reaction is expressed as:

$$\text{Reverse dissociation}\left(H_2S\right) = Kr_{HS}\left[HS^-\right]\left[H^+\right] \tag{5-30}$$

with

$$Kf_{HS} = Kr_{HS}\frac{10^{-pK_{HS}}}{f_m^{\,2}} \tag{5-31}$$

where:

$Kf_{HS}$ = forward dissociation constant for $H_2S$ (mol/ℓ)

$Kr_{HS}$ = reverse dissociation constant for $H_2S$ (mol/ℓ)

$[H_2S]$ = undissociated hydrogen sulphide concentration (mol/ℓ)

$[HS^-]$ = dissociated hydrogen sulphide concentration (mol/ℓ)

$[H^+]$ = hydrogen ion concentration (mol/ℓ)

$pK_{HS}$ = pK constant for the dissociation of $H_2S$

$f_m$ = monovalent activity coefficient

The standard enthalpy equation for the effect of temperature on the equilibrium constant is given by Smith et al. (1996), as follows:

$$\frac{d\ln K}{dT} = \frac{\Delta H^o}{RT^2} \tag{5-32}$$

T = temperature in Kelvin (K)

K = equilibrium constant at 298.15 K

$\Delta H^o$ = heat of reaction at 298.15 K

R = universal gas constant (kJ/mol.K)

Thermodynamic data:

Heats of formation (at a temperature of 298.15 K):

$H_2S$ = -39.75 kJ/mol

$H^+$ = 0

$HS^-$ = -17.6 kJ/mol

with

$$Kf_S = Kr_S \frac{10^{-pK_S}}{f_d} \tag{5-38}$$

where:

$Kf_S$ = forward dissociation constant for $HS^-$ (mol/ℓ)

$Kr_S$ = reverse dissociation constant for $HS^-$ (mol/ℓ)

$[HS^-]$ = dissociated hydrogen sulphide concentration (mol/ℓ)

$[S^{2-}]$ = elemental sulphur concentration (mol/ℓ)

$[H^+]$ = hydrogen ion concentration (mol/ℓ)

$pK_S$ = pK constant for the dissociation of $HS^-$

$f_d$ = divalent activity coefficient

Thermodynamic data:

Heats of formation (at a temperature of 298.15 K):

$HS^-$ = -17.6 kJ/mol

$H^+$ = 0

$S^{2-}$ = 33 kJ/mol

Universal gas constant

R = 8.314 E-03 kJ/mol.K

Equilibrium constant (at a temperature of 298.15 K)

K = 1 E-19

The standard enthalpy equation (Smith, et al., 1996) was again used, and by integrating Equation 5-32 and including the above thermodynamic data with a conversion factor from ln K to $\log_{10}$K:

$$\log_{10} K = \frac{-2.6427E+03}{T} - 10.1363 \tag{5-39}$$

Thermodynamic data:

Heats of formation (at a temperature of 298.15 K):

$H_2S_{(aq)}$ = -39.75 kJ/mol

$H_2S_{(g)}$ = -20.63 kJ/mol

Universal gas constant

R = 8.314 E-03 kJ/mol.K

Equilibrium constant (at a temperature of 298.15 K)

K = 1.05 E-01

Integrating Equation 5-32 and including the above thermodynamic data with a conversion factor from ln K to $\log_{10}$K:

$$\log_{10} K = \frac{-9.9858E+02}{T} + 2.3705 \tag{5-45}$$

From the definition of pK = - $\log_{10}$K, therefore:

$$pK_S = \frac{9.9858E+02}{T} - 2.3705 \tag{5-46}$$

## 5.3 Model Kinetic Parameters

Sötemann et al. (2005b) obtained kinetic constants (on a molar basis at 37 °C) from Sam-Soon et al. (1991) for the calibration and validation of the UCTADM1 excluding sulphate reduction. The hydrolysis kinetic parameters were obtained by calibration (refer Table 2-3, Chapter 2). Kalyuzhnyi et al. (1998) proposed a complete set of kinetic parameters (on a mass basis at 30 °C) for the anaerobic digestion of soluble organic wastewater containing sulphate (refer Table 2-4, Chapter 2). Both sets of kinetic parameters by Sam-Soon et al. (1991) and Kalyuzhnyi et al. (1998) were based on mathematical models developed for upflow anaerobic sludge blanket (UASB) type bioreactors. The above-mentioned kinetic parameter sets needed to be converted to a common set of units.

**Table 5-7:** Kinetic and stoichiometric constants of Sötemann et al. (2005b) at 35 °C and 23 °C

| Organism Group | $\mu_{max}$ 35 °C ($d^{-1}$) | $\mu_{max}$ 23 °C ($d^{-1}$) | $K_s$ (mol/ℓ) | Y (mol org/mol substrate) | b 35 °C ($d^{-1}$) | b 23 °C ($d^{-1}$) |
|---|---|---|---|---|---|---|
| $Z_{ai}$ | 0.700 | 0.314 | 7.80E-04 | 0.107 | 0.036 | 0.016 |
| $Z_{ae}$ | 1.006 | 0.452 | 8.90E-05 | 0.028 | 0.013 | 0.006 |
| $Z_{am}$ | 3.842 | 1.726 | 1.30E-05 | 0.016 | 0.032 | 0.015 |
| $Z_{hm}$ | 1.050 | 0.472 | 1.56E-04 | 0.004 | 0.009 | 0.004 |
| Hydrogen inhibition coefficient for high $pH_2$ (mol $H_2$/ℓ): | | | | | 6.25E-4 | |
| Surface mediated reaction (Contois): $k_{max,HYD}$ (g COD $S_{bp}$/mol $Z_{ai}$.d) | | | | | 769 | |
| | | | | $K_{SS,HYD}$ (g COD $S_{bp}$/mol $Z_{ai}$) | 1225 | |

The kinetic parameters used in the mathematical model developed by Kalyuzhnyi et al. (1998) were specified on a mass basis. The units of these constants need to be converted from mass units to mole units prior to the processes of sulphate reduction being integrated with the UCTADM1. Conversion factors (Table 5-8) together with molecular weights were used in obtaining kinetic constants on a molar basis.

**Table 5-8:** Conversion factors used in the model

| Component | Conversion factor | Unit |
|---|---|---|
| Glucose ($C_6H_{12}O_6$) | 192 | g COD/mol |
| Propionate ($CH_3CH_2COOH$) | 112 | g COD/mol |
| Acetate ($CH_3COOH$) | 64 | g COD/mol |
| Hydrogen ($H_2$) | 16 | g COD/mol |
| Sulphur ($S^{2-}$) | 32 | g S/mol |
| Sulphate ($SO_4^{2-}$) | 96 | g/mol |

phosphorous content of PSS.

### 6.1.1 COD

The PSS total influent COD ($S_{ti}$) consists of a biodegradable particulate fraction ($S_{bpi}$), unbiodegradable particulate fraction ($S_{upi}$), biodegradable soluble fraction in the form of glucose ($S_{bsi}$), unbiodegradable soluble fraction ($S_{usi}$), and volatile fatty acids ($S_{VFAi}$). The total COD balance for the feed is given in units of mg COD/ℓ by:

$$S_{ti} = S_{bpi} + S_{upi} + S_{bsi} + S_{usi} + S_{VFAi} \tag{6-1}$$

and the total soluble influent COD ($S_{si}$) in mg COD/ℓ is given by:

$$S_{si} = S_{bsi} + S_{usi} + S_{VFAi} \tag{6-2}$$

Ristow et al. (2005) made the assumption that the unbiodegradable particulate COD fraction forms 33.45 % of the total COD. Furthermore, an assumption was made that the biodegradable soluble COD fraction is equivalent to that of volatile fatty acids. The unbiodegradable COD fractions remain the same through the system i.e. effluent concentration is same as the influent concentration. Using Equation 6-1 and Equation 6-2 as well as taking into consideration the above-mentioned assumptions, the various COD fractions can be determined by the following equations:

$$S_{upi} = 0.3345 \times S_{ti} \tag{6-3}$$

$$S_{usi} = S_{us}\left(Effluent\right) \tag{6-4}$$

$$S_{bsi} = S_{VFAi} = \frac{\left(S_{si} - S_{usi}\right)}{2} \tag{6-5}$$

$$S_{bpi} = S_{ti} - S_{bsi} - S_{VFAi} - S_{usi} - S_{upi} \tag{6-6}$$

Multiplying by the flowrate in the reactor, all COD fractions were converted from concentration units of mg COD/ℓ to flux units of g COD/d, with the exception of $S_{bsi}$, which was converted to

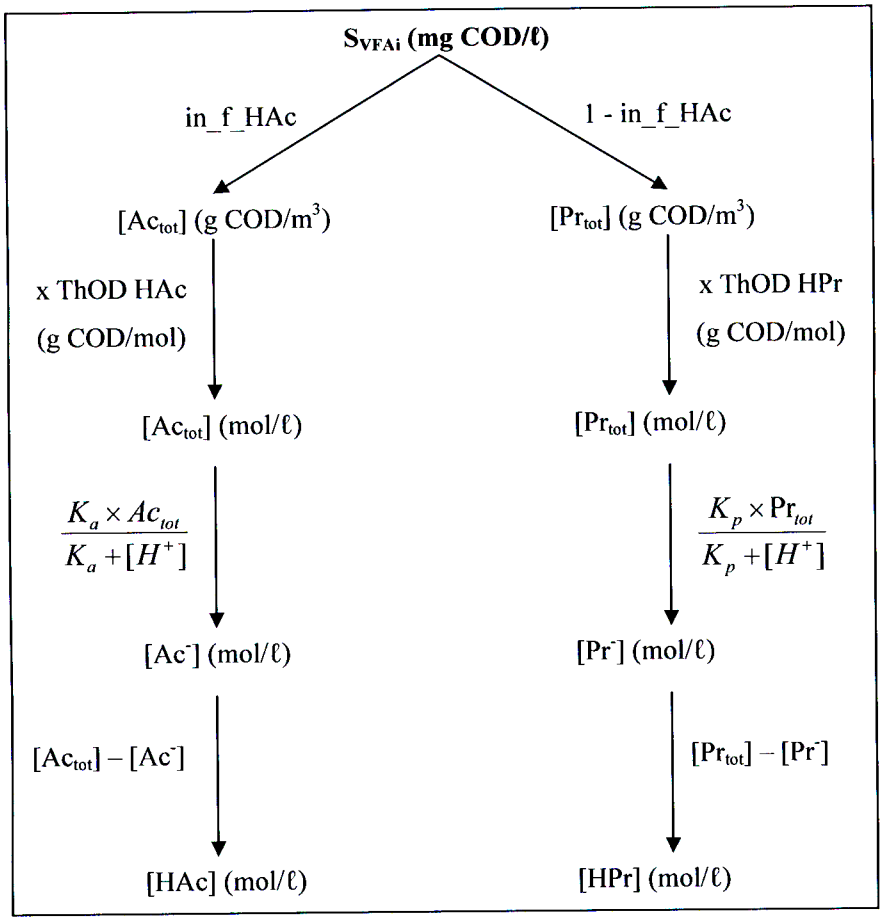


**Figure 6-1:** Method of approach in fractioning the VFA component of the influent COD into the undissociated and dissociated forms of acetate and propionate

The molar concentrations of the undissociated and dissociated forms of acetate and propionate were converted to flux units by multiplying with the reactor flowrate and their respective molecular weights.

### 6.1.4 Free and Saline Ammonia

The calculation of ammonia and the ammonium ion influx was based on the influent FSA concentration (mg N/ℓ) together with the ammonium ion equilibrium constant. The calculation of the influent ammonia and ammonium ion concentrations on a molar basis are given by the following equations respectively:

where:

| | | |
|---|---|---|
| Alkalinity | = | influent alkalinity expressed in mg/ℓ as $CaCO_3$ |
| $MW_{CaCO3}$ | = | molecular weight of calcium carbonate (g/mol) |
| $[H^+]$ | = | influent hydrogen ion molar concentration (mol/ℓ) (from above) |
| $[OH^-]$ | = | influent hydroxyl ion molar concentration (mol/ℓ) (from above) |
| $K_{c1}$ | = | equilibrium constant for dissociation of carbonic acid at 25 °C |
| $K_{c2}$ | = | equilibrium constant for dissociation of bicarbonate at 25 °C |

The molar concentrations of $CO_3^{2-}$, $HCO_3^-$ and $H_2CO_3$ were converted to flux units by multiplying with the reactor flowrate and their respective molecular weights.

### 6.1.6 Sulphate

The available influent sulphate concentration in mass units of mg/ℓ did not require much manipulation in determining its influx value. This concentration was simply multiplied with the reactor flowrate in ℓ/d to obtain the influent flux in g/d.

### 6.1.7 Influent Data

The characterisation structure developed here was used in the manipulation of available influent data from Ristow et al. (2005) and Ristow (2005) to specify input fluxes for subsequent simulation of UCT laboratory experiments and the pilot plant RSBR respectively in WEST®. The equilibrium constants used the characterisation methodology were obtained from Stumm and Morgan (1996) and are listed in Table 6-1.

**Table 6-1:** Equilibrium constants at 25 °C at infinite dilution used to characterise the influent of various systems

(Stumm and Morgan, 1996)

| Symbol | Value | Description |
|---|---|---|
| $K_a$ | 1.75E-05 | equilibrium constant for dissociation acetic acid |
| $K_p$ | 1.32E-05 | equilibrium constant for dissociation of propionic acid |
| $K_n$ | 5.60E-10 | equilibrium constant for dissociation ammonium ion |
| $K_{c1}$ | 4.35E-07 | equilibrium constant for dissociation of carbonic acid |
| $K_{c2}$ | 4.69E-11 | equilibrium constant for dissociation of bicarbonate |

of the characterised influent used as input for simulation in WEST® for each steady state experiment is shown in Table B-2 to Table B-4, Appendix B.

The experimental setup was modelled in WEST® using the UCTADM1 which is symbolically represented by an anaerobic digester icon together with an input and output node representing the interface of the model and contain the characteristics of the feed and of the treated water respectively (refer to Figure 6-1).

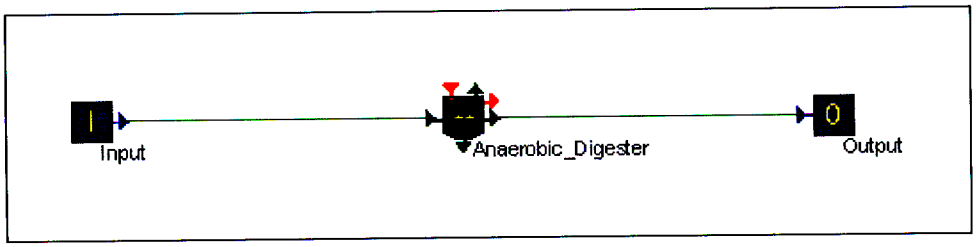


**Figure 6-1:** Configuration of the UCT experimental system in WEST®

The kinetic parameters used in the model were not derived from the UCT laboratory experiments, but were independent and obtained from Sötemann et al. (2005b) and Kalyuzhnyi et al. (1998), refer to Section 2.2.9, Chapter 2. It is therefore imperative to select a set of kinetic constants accurately predict the behaviour of these experimental systems. The single, complete set of kinetic parameters from Kalyuzhnyi et al. (1998) was initially selected for the simulation of experimental data sets. Hydrolysis kinetic parameters were obtained from Sötemann et al. (2005b). However, upon preliminary simulations, it was observed that simulation of experimental systems showed a negative response to these kinetic parameters i.e. death of organisms and no degradation of influent COD even if hydrolysis kinetic constants were manipulated. It was subsequently decided to use a combination of kinetic parameters from Sötemann et al. (2005b) and Kalyuzhnyi et al. (1998). In addition to hydrolysis kinetic parameters, kinetic and stoichiometric constants for the four anaerobic digestion organism groups of acidogens, acetogens, acetoclastic methanogens and hydrogenotrophic methanogens were obtained from Sötemann et al. (2005b) as per Table 5-7, Chapter 5. The remaining kinetic parameters for acetogenic, acetoclastic and hydrogenotrophic SRB were acquired from Kalyuzhnyi et al. (1998) according to Table 5-9, Chapter 5. Merging these two sets of kinetic parameters proved positive and considering that no kinetic parameters, other than that of hydrolysis (refer to Section 7.3, Chapter 7) were calibrated, the simulation results (discussed in Sections 7.1 and 7.2, Chapter 7) of methanogenic and sulphidogenic systems, with exception of desired sulphate removal efficiencies, fitted well to the experimental data. The complete set of kinetic parameters, except for those of hydrolysis, used in application of the model to

## 6.3 WEST® Implementation of the Pilot Plant RSBR

Available pilot plant data that was obtained from Ristow (2005), and presented in Figure 3-1, Chapter 3, was used to simulate the configuration of the RSBR in WEST®. Other than temperatures and flowrates, only the total COD for the PSS stream; and the pH, alkalinity and sulphate concentration of the mine water stream are known. The total COD of 30 g/ℓ was fractionated into its various components by using steady state experimental data as a guideline in terms of the average fraction that each component forms of the total COD. The remainder of the feed characteristics had to be constructed from judicious assumptions.

Insufficient feed data was available to predict the fraction of VFA in the feed COD using the steady state model of Sötemann et al. (2005a). It was therefore decided to revert to the assumption made by Ristow et al. (2005) that the $S_{VFAi}$ fraction is equivalent to the $S_{bsi}$ fraction of influent COD. All $S_{VFAi}$ was again assumed as being acetate only. PSS was obtained directly from ERWAT without being stored prior to feeding, and therefore a pH value of 7 was estimated for PSS in its pristine state. An FSA value of 39 mg N/ℓ was taken from the measured data of steady state number 1 above, which has a feed COD of PSS closest to that of the pilot plant. Influent alkalinity of this stream was assumed to be 300 mg/ℓ as $CaCO_3$ to correspond to some extent to an influent pH of 7 for PSS. The mine water feed stream to the pilot plant would only represent the concentration of sulphate, together with pH and alkalinity. Influent sulphate concentration of 1300 mg/ℓ, a pH value of 7 and an alkalinity of 350 mg/ℓ as $CaCO_3$ were obtained from available influent data in Figure 3-1, Chapter 3. The characterisation method was again performed externally to the simulation software according to the method outlined in Section 6.1. Refer to Table B-5, Appendix B, for the summarised influent characterisation of the PSS and mine water feed streams to the RSBR that was used as input for simulation in WEST®.

The pilot plant configuration of the RSBR was modelled and represented by using various symbolic icons (refer to Figure 6-2). The core of the model configuration is an anaerobic digester which includes the UCTADM1. Two input nodes contain the characteristics of the PSS and mine water feed, and three outlets of gas, overflow and recycle streams represent the reactor effluent. Two additional parameters were created to represent the fraction of the feed flow that is recycled and the ratio of particulate concentration in the overflow to particulate concentration in the reactor. The recycle ratio was set to 50 % and the latter concentration ratio was set to a very low value of 0.0001 to allow the overflow effluent stream to be practically free of solids. The RSBR was modelled such that only the gaseous components of methane, carbon dioxide and hydrogen sulphide exit only through the gas stream. The recycle stream is mediated by

**Table 6-3:** Kinetic parameters used in modelling the pilot plant RSBR at 23 °C

| Organism Group | $\mu_{max}$ ($d^{-1}$) | $K_s$ (mol/ℓ) | $K_n$ (mol/ℓ) | $K_i$ (mol/ℓ) | Y (mol org/mol substrate) | b ($d^{-1}$) |
|---|---|---|---|---|---|---|
| $Z_{ai}$ | 0.314 | 7.80E-04 | - | 1.72E-02 | 0.107 | 0.016 |
| $Z_{ae}$ | 0.452 | 8.90E-05 | - | 5.94E-03 | 0.028 | 0.006 |
| $Z_{ps}$ | 0.366 | 2.63E-03 | 7.71E-05 | 5.78E-03 | 0.027 | 0.012 |
| $Z_{am}$ | 1.726 | 1.30E-05 | - | 5.78E-03 | 0.016 | 0.015 |
| $Z_{as}$ | 0.384 | 3.75E-04 | 2.00E-04 | 5.13E-03 | 0.019 | 0.017 |
| $Z_{hm}$ | 0.472 | 1.56E-04 | - | 5.16E-03 | 0.004 | 0.004 |
| $Z_{hs}$ | 1.755 | 4.38E-06 | 2.00E-04 | 1.72E-02 | 0.0071 | 0.038 |

## 6.4 Model Verification

An important asset in modelling is model verification which proves that the model conforms to 100% COD, C, H, O, N and S mass balances. Performing a continuity check through calculation of a series of continuity equations is a valuable tool for model verification. These equations are the mathematical equivalent of the principle that in chemical reactions, elements, theoretical oxygen demand and net electrical charges may neither be formed nor destroyed. The continuity check determines whether the result of the equation is equal to zero or not. If the result is different from zero the element is either formed or destroyed in the biological system.

A continuity check was performed on model influent and effluent flux data. A single methanogenic system (Steady State Number 1) and a sulphidogenic system (Steady State Number 6) were used to perform a continuity check on and hence verify the model. With the exception of COD, the Ristow et al., (2005) influent and effluent experimental data proved insufficient in performing a continuity check as per to the method adopted in the model. The results of the continuity check in flux (g/d) and percentage error between influent and effluent data for both model systems are tabulated in Table 6-4.

producing inadequate amounts of methane, carbon dioxide and biomass. Further, the N:C balance discrepancy is approximately the same as N:C balance in biodegradable particulate COD. This again could be attributed to inaccurate reaction stoichiometry in the production of methane, carbon dioxide and biomass.

Upon further manipulation of the model to allow stoichiometric coefficients to be visible which were previously hidden by default in the simulation output, it was discovered that WEST® incorrectly computed a single stoichiometric coefficient viz. 'EndogenousProt'. This term was programmed as a variable within the software to simplify the stoichiometry of certain reactions. The 'EndogenousProt' coefficient was calculated from 'HydrolysisProt' which was also programmed into the model as a variable. The software accepts the computation of 'HydrolysisProt', but incorrectly calculates that of 'EndogenousProt' and carries the error through the simulation. Both coefficients were subsequently re-programmed as parameters within Petersen Matrix, MSL code re-generated, model re-configured and a new model experimentation environment created. Considering that the model baseline data was the same as the previous one, the continuity check with respective input and output fluxes resulted in a margin of error that was 5 % when compared to the previous WEST® and AQUASIM models for which mass balances did not close.

In summary, it can be concluded that the major portion of mass balance errors can be attributed to incorrect reaction stoichiometry that was inherited via the translation of the AQUASIM model into WEST® with a minor portion due to inconsistencies in computation of reaction stoichiometry within the WEST® software.

**Table 7-1:** Summary of results from the simulation of each steady state methanogenic system

| | | INFLUENT | | | EFFLUENT | | | | | | | | |
|---|---|---|---|---|---|---|---|---|---|---|---|---|---|
| Steady State Number | Reactor Volume (ℓ) | Retention Time (d) | Total COD ($S_{ti}$) (mg COD/ℓ) | Soluble COD ($S_{si}$) (mg COD/ℓ) | Total COD ($S_t$) (mg COD/ℓ) | Soluble COD ($S_s$) (mg COD/ℓ) | pH | VFA (mg HAc/ℓ) | Alkalinity (mg/ℓ as $CaCO_3$) | Methane Production (ℓ/d) | Methane Composition (% vol) | FSA (mg N/ℓ) | TKN (mg N/ℓ) |
| 1 | 16 | 10 | 28876 | 5254 | 11079.48 | 215.73 | 6.83 | 1.01 | 2475.25 | 12.23 | 59.86 | 205.02 | 488.13 |
| 2 | 16 | 8 | 26439 | 3161 | 11223.93 | 215.60 | 6.57 | 1.62 | 1407.98 | 13.19 | 58.62 | 196.21 | 480.68 |
| 3 | 20 | 20 | 26654 | 3027 | 10402.06 | 200.76 | 6.62 | 0.60 | 1576.84 | 7.05 | 58.70 | 240.00 | 516.39 |
| 4 | 20 | 15 | 26608 | 3302 | 10370.99 | 189.51 | 6.61 | 0.99 | 1561.55 | 9.38 | 58.71 | 218.18 | 494.35 |
| 5 | 20 | 15 | 14011 | 1825 | 5711.95 | 129.93 | 6.34 | 1.38 | 854.83 | 4.83 | 57.01 | 111.53 | 259.35 |
| 7 | 16 | 6.67 | 25228 | 2374 | 12549.55 | 257.55 | 6.63 | 1.90 | 1518.46 | 13.19 | 61.52 | 239.92 | 529.95 |
| 8 | 16 | 5.71 | 25061 | 2604 | 12713.84 | 273.94 | 6.62 | 2.38 | 1470.85 | 15.01 | 61.37 | 246.47 | 538.51 |
| 9 | 16 | 5 | 24880 | 2693 | 12847.97 | 382.47 | 6.60 | 2.96 | 1412.22 | 16.71 | 61.34 | 247.66 | 539.42 |
| 10 | 20 | 15 | 39984 | 3715 | 17033.63 | 276.86 | 6.83 | 0.67 | 2442.00 | 13.30 | 61.11 | 459.10 | 893.84 |
| 11 | 20 | 15 | 39965 | 4165 | 17214.72 | 325.84 | 6.85 | 0.66 | 2535.34 | 13.17 | 61.14 | 466.54 | 902.59 |
| 12 | 20 | 10 | 39810 | 4436 | 18629.35 | 293.88 | 6.83 | 1.01 | 2425.72 | 18.38 | 61.17 | 437.82 | 888.51 |
| 13 | 20 | 10 | 13270 | 1174 | 6147.25 | 147.03 | 6.35 | 1.63 | 820.53 | 6.19 | 60.56 | 141.18 | 290.30 |
| 14 | 20 | 8 | 13269 | 1524 | 6384.39 | 152.34 | 6.40 | 2.01 | 903.30 | 7.47 | 60.76 | 143.00 | 295.88 |
| 17 | 20 | 60 | 9810 | 1204 | 3657.88 | 100.84 | 6.18 | 0.44 | 619.27 | 0.90 | 55.38 | 104.38 | 205.97 |
| 18 | 16 | 8 | 1949 | 283 | 864.43 | 97.48 | 7.50 | 1.00 | 1536.15 | 0.94 | 94.72 | 18.67 | 39.44 |
| 19 | 16 | 8 | 1949 | 283 | 864.69 | 97.76 | 7.02 | 1.15 | 1328.49 | 0.94 | 86.40 | 19.69 | 40.46 |
| 21 | 20 | 8 | 34819 | 3829 | 15490.07 | 252.20 | 6.73 | 1.39 | 1952.11 | 20.97 | 60.45 | 245.52 | 631.80 |
| 23 | 20 | 6.67 | 34819 | 4399 | 15405.23 | 264.17 | 6.76 | 1.69 | 2081.30 | 25.24 | 60.56 | 257.31 | 642.65 |
| 24 | 20 | 6.67 | 13580 | 1846 | 6094.14 | 154.92 | 6.38 | 2.65 | 893.28 | 9.73 | 59.48 | 107.58 | 258.20 |
| 25 | 20 | 10 | 1950 | 254 | 935.25 | 85.15 | 5.65 | 9.36 | 193.85 | 0.88 | 52.20 | 16.36 | 37.95 |
| 26 | 20 | 8 | 1949 | 283 | 921.82 | 117.40 | 5.65 | 11.89 | 194.80 | 1.11 | 52.32 | 18.24 | 39.38 |
| 27 | 16 | 8 | 2017 | 224 | 920.30 | 63.58 | 6.58 | 1.60 | 949.28 | 0.95 | 72.85 | 20.31 | 42.43 |
| 28 | 20 | 5.71 | 41442 | 2583 | 20388.97 | 363.72 | 6.66 | 2.27 | 1671.18 | 32.13 | 60.63 | 280.51 | 759.16 |
| 31 | 20 | 5.71 | 13186 | 956 | 7007.94 | 193.50 | 6.20 | 4.88 | 595.68 | 9.42 | 59.16 | 86.68 | 243.37 |

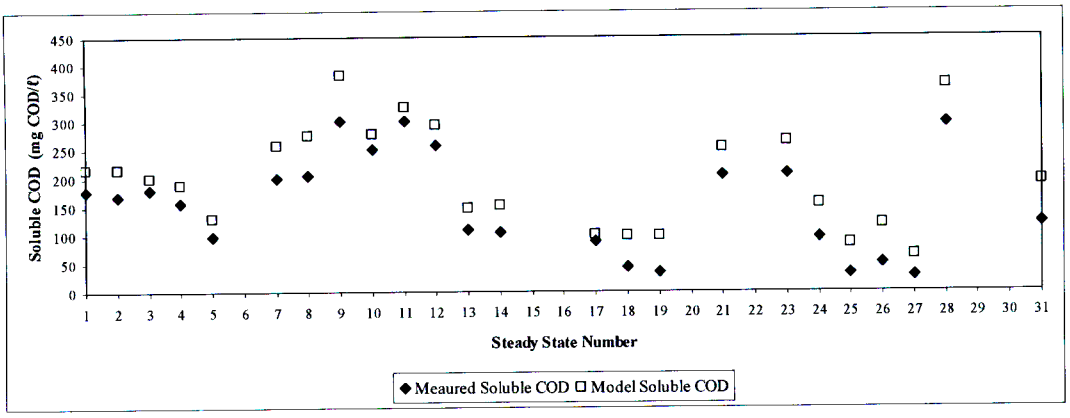


**Figure 7-2:** Measured and predicted effluent soluble COD concentrations for respective steady state methanogenic systems

### 7.1.2 pH and Alkalinity

The predicted steady state model operating pH and effluent alkalinity values for each methanogenic system are compared to the measured values in Figure 7-3. The pH for steady states 18, 19 and 27 were controlled to 7.5, 7, and 6.5 respectively. This was done in the model by adding either hydrogen or hydroxyl ion to the influent to maintain a given pH.

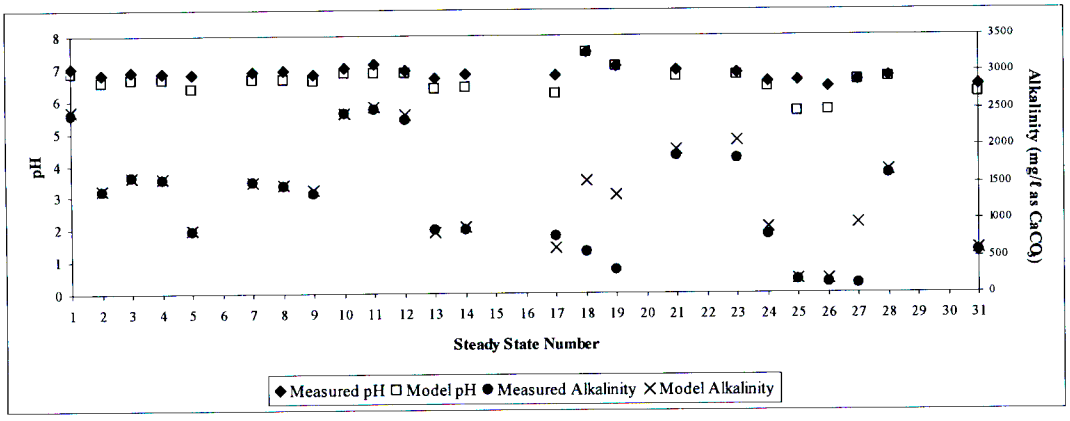


**Figure 7-3:** Measured and predicted operating pH and effluent alkalinity concentrations for respective steady state methanogenic systems

However this method as well as alternate pH correction techniques in model application must be investigated further. The model pH and alkalinity compare remarkably well to the experimental data for most steady states indicating that bioprocesses and mixed weak acid base chemistry has been correctly integrated and accurately modelled.

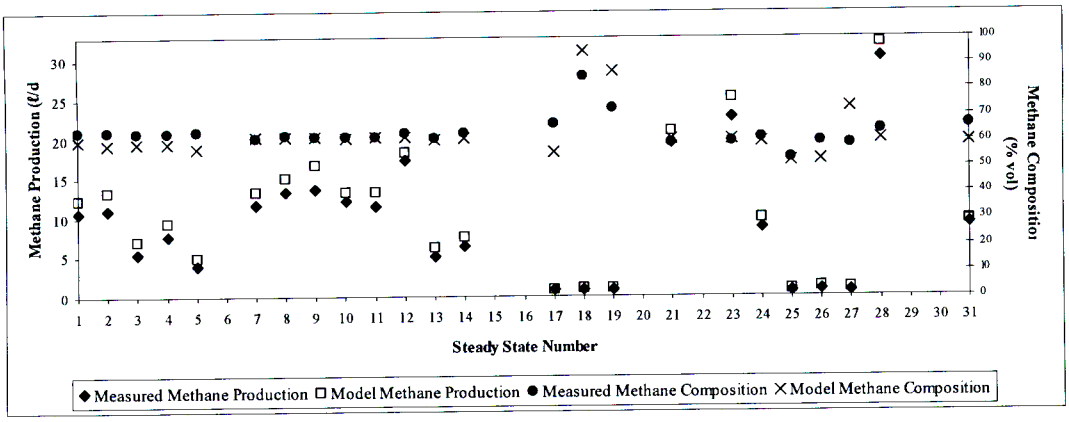


**Figure 7-5:** Measured and predicted methane production and methane composition for respective steady state methanogenic systems

### 7.1.5 FSA and TKN

Figures 7-6 and 7-7 illustrate the comparison of predicted effluent TKN and FSA concentrations to measured data for each steady state system respectively. Model predictions of FSA compare fairly well with the exception of a steady states 7 – 12 and 28 which predict a greater effluent value than that measured.

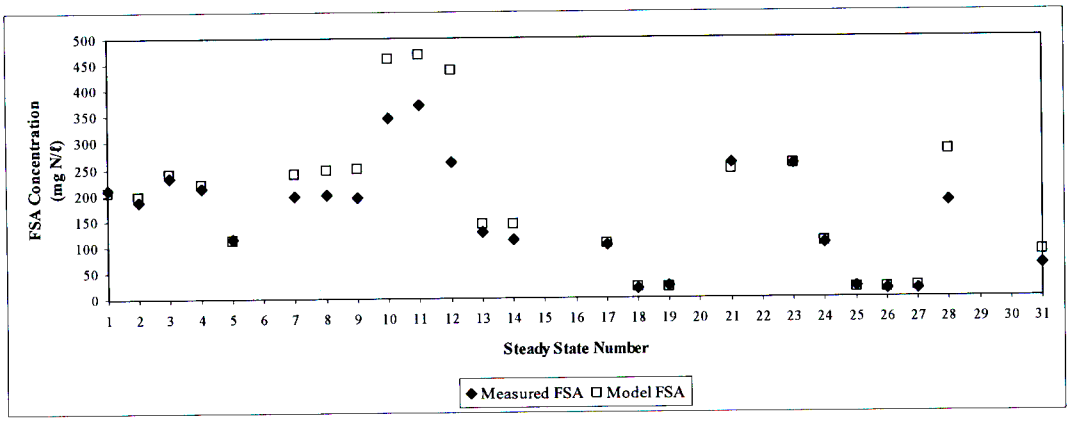


**Figure 7-6:** Measured and predicted effluent FSA concentrations for respective steady state methanogenic systems

As in the case of FSA concentrations, the predicted TKN values in Figure 7-7 compare reasonably well to measured effluent data, with the exception of same steady state systems as shown in Figure 7-6 in which higher values are predicted. Again the difference is due to the data not conforming to the 100% N mass balance.

**Table 7-2:** Summary of results from the simulation of each steady state sulphidogenic system

| | | | INFLUENT | | | EFFLUENT | | | | | | | |
|---|---|---|---|---|---|---|---|---|---|---|---|---|---|
| Steady State Number | Reactor Volume (ℓ) | Retention Time (d) | Total COD ($S_o$) (mg COD/ℓ) | Soluble COD ($S_{si}$) (mg COD/ℓ) | Sulphate (mg $SO_4$/ℓ) | Total COD ($S_t$) (mg COD/ℓ) | Soluble COD ($S_s$) (mg COD/ℓ) | Sulphate (mg $SO_4$/ℓ) | pH | VFA (mg HAc/ℓ) | Alkalinity (mg/ℓ as $CaCO_3$) | FSA (mg N/ℓ) | TKN (mg N/ℓ) |
| 6 | 16 | 10 | 28876 | 5254 | 1000 | 11109.43 | 221.95 | 1.19 | 6.99 | 0.92 | 3492.40 | 203.05 | 486.41 |
| 15 | 16 | 8 | 13269 | 1524 | 9600 | 5969.54 | 192.45 | 5952.53 | 6.87 | 0.98 | 2483.95 | 141.72 | 288.68 |
| 20 | 16 | 8 | 1949 | 283 | 2000 | 1117.75 | 247.63 | 1522.68 | 7.52 | 0.16 | 1812.58 | 17.41 | 39.21 |
| 22 | 16 | 8 | 1949 | 283 | 2000 | 994.07 | 123.95 | 1522.68 | 6.41 | 0.17 | 873.92 | 19.43 | 41.23 |
| 36 | 16 | 8 | 1949 | 283 | 2000 | 996.00 | 125.87 | 1522.68 | 6.46 | 0.17 | 937.84 | 22.42 | 44.22 |
| 41 | 20 | 16 | 2012 | 212 | 2000 | 898.94 | 66.44 | 1424.99 | 6.32 | 0.13 | 789.57 | 19.55 | 41.46 |
| 42 | 20 | 13.3 | 2017 | 224 | 2000 | 918.44 | 69.90 | 1438.52 | 6.31 | 0.14 | 776.91 | 22.54 | 44.59 |
| 46 | 20 | 10 | 989 | 102 | 1000 | 477.42 | 71.89 | 734.09 | 5.98 | 0.14 | 414.56 | 13.06 | 23.76 |
| 47 | 16 | 8 | 1900 | 203 | 2000 | 1206.19 | 392.69 | 1487.19 | 8.27 | 0.17 | 2104.80 | 14.76 | 35.67 |

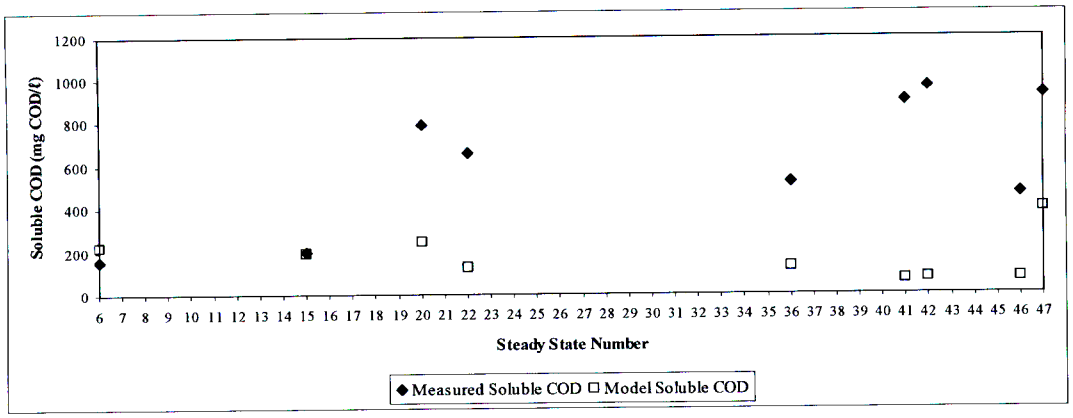


**Figure 7-9:** Measured and predicted effluent soluble COD concentrations for respective steady state sulphidogenic systems

### 7.2.2 pH and Alkalinity

The predicted model operating pH and effluent alkalinity values for each sulphidogenic system are compared to the measured values in Figure 7-10. The pH for all steady state systems, excluding steady state numbers 41, 42 and 46, were controlled by manually adding either hydrogen or hydroxyl ion to the influent to maintain a given pH. As pointed out for methanogenic systems, this method as well as alternate pH correction techniques in model application must be investigated further. The model predicts a lower pH for systems where pH was observed from steady state operation.

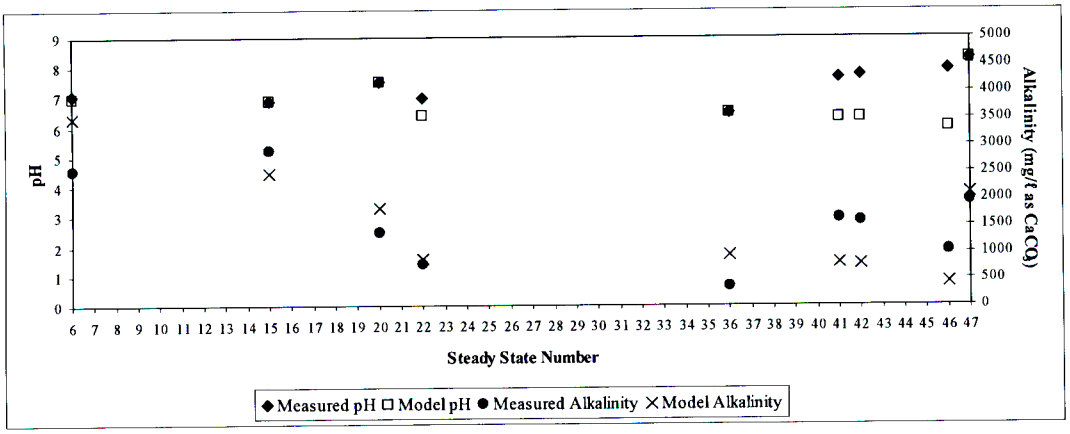


**Figure 7-10:** Measured and predicted operating pH and effluent alkalinity concentrations for respective steady state sulphidogenic systems

For steady state experiments where pH was not controlled, and steady state operation allowed to prevail, the model yielded alkalinity values lower than that measured. However in the case

### 7.2.4 Sulphate

The predicted model values of effluent sulphate concentration are compared to the experimental values as illustrated in Figure 7-12. It can be seen that the model predicts reasonable sulphate reduction for steady states 6 only when compared to the measured values. The model is able to reduce sulphate by 99.88 % for steady state 6 and according to Ristow et al. (2005) complete sulphate reduction was probable for this steady state. This is due to using a very high influent COD:$SO_4$ ratio of 28.88, which can result in the complete reduction of sulphate. For the remaining steady state systems predicted effluent sulphate concentrations are significantly higher than the respective measured values with an average sulphate removal efficiency of 27.33 %. It is clearly evident that high model sulphate removal efficiencies are obtained at high COD:$SO_4$ ratios as in the case of steady state 6. COD:$SO_4$ ratios for the remaining steady states range from 0.95 to 1.38 for steady states 47 (25.64 % sulphate removal) and 15 (37.99 % sulphate removal) respectively, hence substantiating the deduction made above. With the exception of steady state 6, the model does not properly represent competition between methanogenic and sulphidogenic organisms as discussed in literature (refer to Chapter 2) and as occurs in reality. Other than steady state 6, sulphidogens are clearly out-competed for substrate by methanogens, resulting in methane production within the model; whereas negligible methane data was recorded for the remaining steady state experiments (refer to Appendix C for detailed steady state data). However it must be noted that the laboratory experiments were not designed to investigate competition between methanogenic and sulphidogenic organisms but rather to determine the rate of hydrolysis of PSS under methanogenic, acidogenic and sulphate-reducing conditions and the influences thereof, to which independent sets of kinetic parameters were applied.

Undissociated aqueous sulphide concentrations range from 0.96 mg/ℓ to 8.86 mg/ℓ for steady states 6 and 20 respectively, therefore maintaining sulphide inhibition to a minimum. No experimental measurement for effluent sulphate was made for steady state number 41. Considering that the sulphur mass balance in the model conforms to 100% closure, one can be sure that the derivation of the model stoichiometry is correct.

could be due to the data not conforming to the 100% N mass balance.

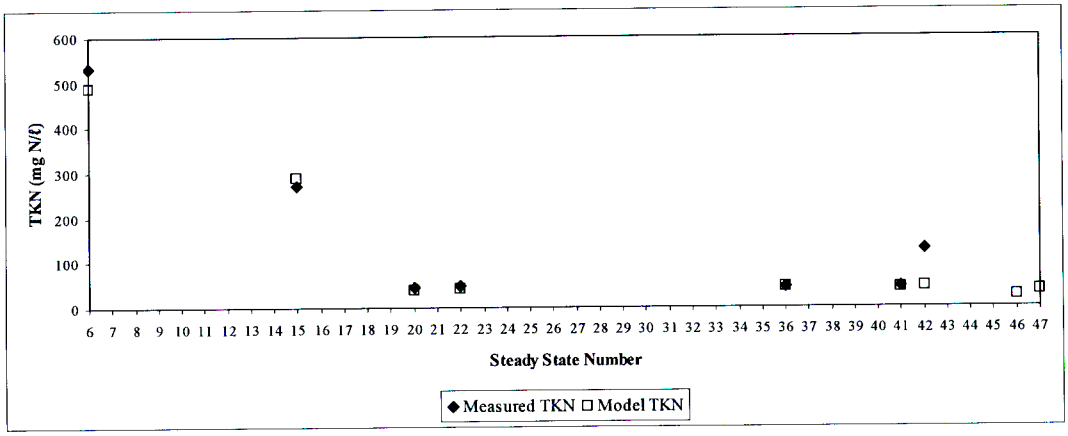


**Figure 7-14:** Measured and predicted effluent TKN for respective steady state sulphidogenic systems

## 7.3 Parameter Calibration

### 7.3.1 Sensitivity Analysis

Sensitivity of a given variable due to a perturbation of a given parameter will indicate which parameters need to be calibrated, in order to get accurate simulation outputs. Sensitivity analysis was performed on the model for each steady state simulation in WEST® to identify and determine the model parameters that influence simulated outputs. The absolute and relative sensitivity of a given variable due to a change in the given parameter was calculated by using the sensitivity function in WEST®. In application of the model and analysing all the steady state sensitivity output data from sensitivity analyses, it was clearly evident and therefore determined that the hydrolysis maximum specific rate constant ($k_{max,HYD}$) and half saturation constant ($K_{SS,HYD}$) were most sensitive and influenced simulation results significantly. This result was not unexpected and is in agreement with the literature in Chapter 2, showing that hydrolysis is the rate-limiting step in the anaerobic digestion process treating PSS. Accordingly, for each system simulated, these two constants were calibrated using the optimiser function in WEST®.

### 7.3.2 Parameter Regression

The values of the hydrolysis kinetic constants were expected to vary from one simulation to another depending on the operating conditions and the amount of particulate organic matter fed into a given system. Initial values of 769 g COD $S_{bp}$/mol $Z_{ai}$.d and 1225 g COD $S_{bp}$/mol $Z_{ai}$

predicted results with respect the average hydrolysis constants need to be assessed when applied to new methanogenic and sulphate-reducing systems.

**Table 7-4:** Regressed average hydrolysis kinetic parameters for methanogenic and sulphidogenic systems

| System Type | Average $k_{max,HYD}$ (g COD $S_{bp}$/mol $Z_{ai}$.d) | Average $k_{SS,HYD}$ (g COD $S_{bp}$/mol $Z_{ai}$.d) |
|---|---|---|
| Methanogenic | 839 | 379 |
| Sulphidogenic | 814 | 359 |

**Table 8-1:** Summary of results from the simulation of the pilot plant RSBR

| Variable | Value |
|---|---|
| Reactor Volume (ℓ) | 250 000 |
| Retention Time (d) | 1 |
| Feed Total COD (mg COD/ℓ) | 30 000 |
| Feed Soluble COD (mg COD/ℓ) | 2694 |
| Feed Sulphate (mg $SO_4$/ℓ) | 1300 |
| Effluent Total COD (mg COD/ℓ) | 8681.34 |
| Effluent Soluble COD (mg COD/ℓ) | 37.92 |
| Effluent Sulphate (mg $SO_4$/ℓ) | 702.07 |
| Reactor pH | 7.18 |
| Effluent VFA (mg HAc/ℓ) | 0.07 |
| Effluent Alkalinity (mg/ℓ as $CaCO_3$) | 1001.45 |
| Methane Production (ℓ/d) | 72.77 |
| Gas composition (% $CH_4$) | 15.58 |
| Total Gas production (ℓ/d) | 130.43 |
| Effluent FSA (mg N/ℓ) | 19.02 |
| Effluent TKN (mg N/ℓ) | 119.90 |

**Table 8-2:** Comparison between pilot plant measurements and model predictions

| | Measured | Model |
|---|---|---|
| **Effluent Sulphate (mg $SO_4$/ℓ)** | < 200 | 702.07 |
| **Effluent pH** | ~ 7.7 (not confirmed) | 7.18 |
| **Effluent Alkalinity (mg/ℓ as $CaCO_3$)** | 1500 | 1001.45 |
| **Effluent VFA (mg HAc/ℓ)** | < 50 | 0.07 |

provides an extremely useful tool to explore various scenarios, to select the more promising for experimental evaluation. Accordingly, the model was used to explore the effects of changing the ratio between PSS and AMD fed to the reactor. This work follows that of Ristow et al. (2006), however updated in the form of sludge and mine water flowrate ranges applied to the current model.

As mentioned above, the preliminary nature of the model application using available pilot plant operating data, indicates that the reliability of results of this section of the investigation is unknown, and should therefore only be taken as indicating qualitative trends. Nevertheless, Ristow (2005) confirmed that the pilot plant reflects certain important features of the model that have emerged while simulating various scenarios:

- The process seems to be quite resilient in the face of upsets. In particular, it does not seem to suffer from the pH related instabilities typical of methanogenic anaerobic digestion.
- Production of methane is negligible under the current operating conditions.
- $H_2S$ inhibition is not an important factor under the current operating conditions.

### 8.2.1 Qualitative Characteristics of the Model

A simplified conceptual view of the model is useful for qualitative understanding of its behaviour. The rate limiting process is the first step of hydrolysing the particulate COD, and thus the dominant factor determining the model's characteristics. Once the substrate has been solubilised, the methanogenic and sulphate reducing populations of organisms compete for it, and the outcome of this competition determines the second level of characteristics, i.e. how much COD goes into sulphate reduction, and how much into methane production. Issues such as sulphide inhibition fall into a third level, and do not seem to be significant under the conditions experienced by the pilot plant.

### 8.2.2 Investigation of the COD:$SO_4$ feed ratio

It is assumed here that the sulphate rich mine water is in excess, so that obtaining the maximum sulphate reduction for the COD used is desirable. Under this assumption there is still a compromise to be made between the effluent quality of the treated water and the load of sulphate removed. If the treated water is to be discharged to a receiving body, the load is the important criterion, whereas if it is to be reused, the quality is relevant. In considering the latter option, there is a follow-up unit operation to remove the sulphide generated, so that the water

and a range of mine water flow rates from 23 to 690 $m^3/d$ (the current nominal feed rate to the pilot plant is 230 $m^3/d$). This gives a similar system response, as shown in Figure 8-2.

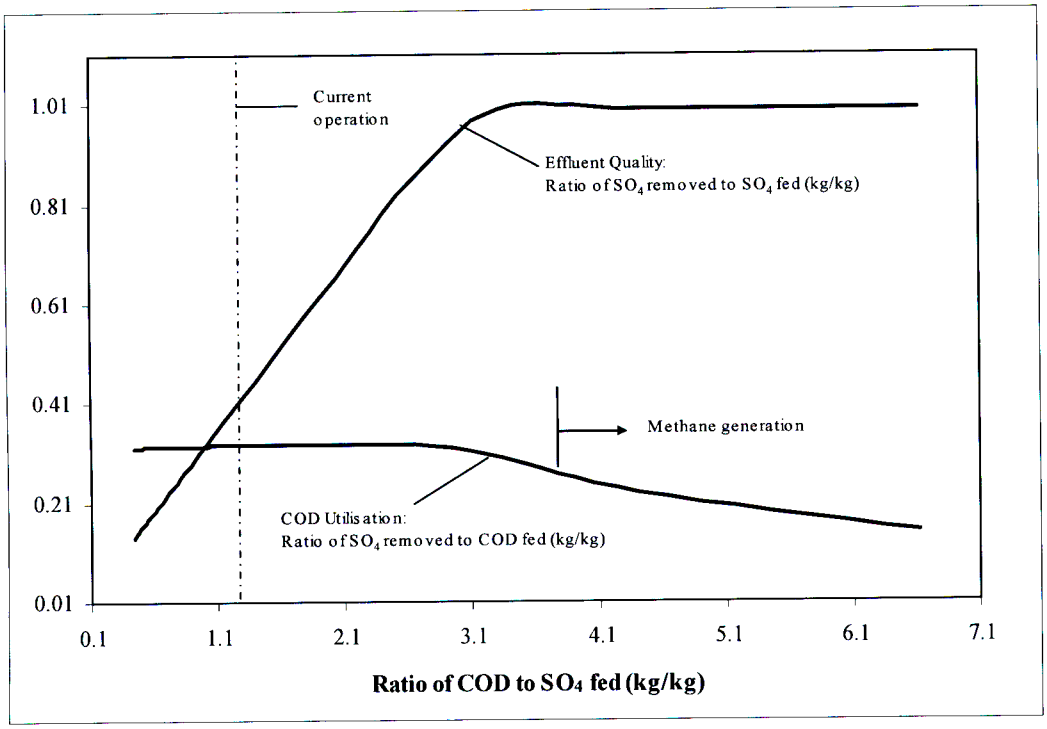


**Figure 8-2:** Simulated $SO_4$ removal and COD utilisation ratios for a varying mine water feed rate

In this case the effluent quality responds very much as before. The COD utilisation remains effectively constant until complete sulphate removal is approached. This is again a consequence of the limiting hydrolysis rate, since the sludge residence time is held constant, the reaction rate remains constant.

Figures 8-1 and 8-2 tend to obscure the effect of the limitation of reactor volume, although it is implied in the results. When designing a system, the reactor size would be a variable, which adds a degree of freedom to the system response. The above diagrams should be seen as examples of how the model could be used, rather than as definitive characteristics of the process, particularly in view of the uncertainties in the kinetic parameter values.

resulted in a margin of error that was 5 % when compared to the previous WEST® and AQUASIM models for which mass balances did not close. It can therefore be concluded that the major portion of mass balance errors can be attributed to incorrect reaction stoichiometry that was inherited via the translation of the AQUASIM model into WEST® with the remainder due to inconsistencies in computation of reaction stoichiometry within the WEST® software.

4. WEST® was subsequently used in application of the extended UCTADM1 to data sets from the UCT laboratory experiments carried out in completely mixed reactors. Application of the WEST® implementation of the model to the experimental methanogenic anaerobic digestion systems (described in Section 3.1.5, Chapter 3) gave reasonably close correlations (refer to Section 7.1, Chapter 7) between predicted and measured data for a single set of stoichiometric and kinetic constants, with the exception of the hydrolysis rate constants, which were regressed (refer to Section 7.3, Chapter 7) using the optimiser function in WEST®. The regressed hydrolysis maximum specific rate constants and half saturation kinetic rates were then averaged for methanogenic and sulphidogenic systems to check if the values differed from each other as well as to that of experimental data. The results did not differ significantly for respective systems with a 3 % deviation in hydrolysis maximum specific rate constant and 5 % for the half saturation kinetic rate which is in accordance with conclusions of Ristow et al., (2005). Calibrated kinetic constants calculated from methanogenic experimental data by Ristow et al., (2005) when compared to averaged regressed methanogenic data resulted in errors of 51 % and 288 % for $k_{max,HYD}$ and $K_{SS,HYD}$ respectively.

5. Application of the extended UCTADM1 to experimental sulphidogenic anaerobic systems demonstrated simulation results (refer to Section 7.2, Chapter 7) fairly close to measured data with the exception of effluent soluble COD and sulphate concentrations. The probability of soluble COD concentration being influenced by the contribution of COD due to total dissolved sulphides in addition to other potential factors must be investigated further. Model sulphate removal efficiencies for steady state sulphidogenic systems range from 25.64 % to 99.88 %. This characteristic of the model is due to varying influent COD:$SO_4$ ratios ranging from 0.95 to 28.88 with maximum model sulphate removal efficiencies being achieved at the highest ratio. As a result sulphidogens, with the exception of a single simulated system (steady state 6 with the highest COD:$SO_4$ ratio), are out competed for substrate by methanogens within the model, hence the model does not

be in the conversion of biodegradable particulate COD into methane, carbon dioxide and biomass. The inconsistency in computation regarding variations of reaction stoichiometry as programmed within WEST® need to be presented to the developers (HEMMIS) of the software to allow for rectification in subsequent versions.

2. The most obvious needs for further research are to reduce the uncertainties in the kinetic parameters values that are appropriate for the operating conditions of laboratory experiments and the pilot plant. The most important aspect of the operating conditions seem to be:

   - *Operating temperatures at 35 °C and 23 °C for laboratory experiments and pilot plant respectively.*

     Temperature dependences are unavailable for methanogenic and sulphidogenic anaerobic digestion reaction rates, nor the pilot plant. Kinetic parameters obtained from literature had to be temperature corrected to operating temperatures of experimental and pilot systems for model application. However, the approximate and interactive nature of the model makes it probable that the entire set of reaction parameters needs to be determined together, rather than attributing an independent reality to any subset.

   - *Experiment design*

     The conventional way of addressing the need for a single set of kinetic parameters would be to embark on a comprehensive programme of experiments similar to the ones carried out in the UCT laboratory. This exercise should focus on demonstrating the competition between methanogenic and sulphidogenic organisms with the ultimate objective of deriving a single set of kinetic parameters that is representative of the systems under investigation. Although the efficacy of this approach is proven, the requirements in terms of time, expense and experimental effort are known to be high.

2. A cooperative project should be established between the modelling and pilot plant teams to take advantage of the opportunity to maximise the benefits of the combined modelling and experimental effort. Thus the model could be used to explore gaps in the understanding of the process and suggest experiments to be tried on the pilot plant. The data from the pilot plant can then be fed back to improve the model. This is the basic strategy of 'optimal experimental design' as outlined by Dochain and Vanrolleghem (2001). What is novel here is the opportunity to apply the technique to such a large scale reactor, and it may represent a significant advance in the practice of piloting biological treatment processes, which frequently only confirm the operability of a process and add little to the scientific

the model simulations presented in this study, the sludge withdrawal flow rate was set at 1 $m^3/d$, the value estimated by the operators for current operation. It is quite likely that this rate would need to be adjusted to maintain the sludge separation when varying the feed rates to the reactor.

GUJER W and ZEHNDER AJB (1983) Conversion processes in anaerobic digestion. *Water Science and Technology* **15** 127-167.

HANSFORD GS (2004) The mechanisms and kinetics of biological treatment of metal-containing effluent. WRC Report No. 1080/1/04, Water Research Commission, PO Box 824, Pretoria 0001, South Africa.

HENZE M, GRADY CPL, GUJER W, MARAIS G and MATSUO T (1987) *Activated Sludge Model No. 1.* IAWPRC Scientific and Technical Reports No. 1, International Association on Water Pollution Research and Control, IAWPRC, London.

HENZE M and HARREMÖES P (1983) Anaerobic treatment of wastewater in fixed film reactors-A literature review. *Water Science and Technology* **15** 1-101.

KALYUZHNYI SV, FEDOROVICH VV, LENS P, POL LH and LETTINGA G (1998) Mathematical modelling as a tool to study population dynamics between sulfate reducing and methanogenic bacteria. *Biodegradation* **9** 187-199.

KNOBEL AN and LEWIS AE (2002) A mathematical model of a high sulphate wastewater anaerobic treatment system. *Water Research* **36** 257-265.

LEDIN M and PEDERSEN K (1996) The environmental impact of mine wastes-Roles of microorganisms and their significance in treatment of mine wastes. *Earth-Science Reviews* **41** 67-108.

MAREE JP and HILL E (1989) Biological removal of sulphate from industrial effluents and concomitant production of sulphur. *Water Science and Technology* **21** 265-276.

MCCARTY PL (1974) Anaerobic processes. *Proc. Birmingham Short Course on Design Aspects of Biological Treatment, International Association of Water Pollution Research, September 18*, Birmingham, England.

MOLWANTWA JB, WHITTINGTON-JONES KJ and ROSE PD (2004) An investigation into the mechanism underlying enhanced hydrolysis of complex carbon in a biosulphidogenic recycling sludge bed reactor (RSBR). *Water SA* **30** (5) 150-154.

MOSEY FE (1983) Mathematical modelling of the anaerobic digestion process: Regulatory mechanisms for the formation of short-chain volatile fatty acids from glucose. *Water Science and Technology* **15** 209-232.

RISTOW NE, WHITTINGTON-JONES KJ, CORBETT CJ, ROSE PD and HANSFORD GS (2002) Modelling of a recycling sludge bed reactor using AQUASIM. *Water SA* **28** (1) 111-120.

ROBERTS R, DAVIES WJ and FORSTER CF (1999) Two-stage, thermophilic-mesophilic anaerobic digestion of sewage sludge. *Trans IChemE* **77** (B) 93-97.

ROSE PD (2002) Salinity, sanitation, and sustainability - A study in environmental biotechnology and integrated wastewater beneficiation in South Africa. WRC Report No. TT 187/02, Water Research Commission, PO Box 824, Pretoria 0001, South Africa.

ROSE PD, CORBETT CJ, WHITTINGTON-JONES KJ and HART OO (2002) The Rhodes BioSURE Process ® - Part 1: Biodesalination of mine drainage wastewaters. WRC Report No. TT 195/02, Water Research Commission, PO Box 824, Pretoria 0001, South Africa.

SACKS J and BUCKLEY CA (2004) Anaerobic digestion of high-strength or toxic organic effluents in available digester capacity. WRC Report No. 762/1/04, Water Research Commission, PO Box 824, Pretoria 0001, South Africa.

SAM-SOON PALNS, WENTZEL MC, DOLD PL, LOEWENTHAL RE and MARAIS $G_VR$ (1991) Mathematical modelling of upflow anaerobic sludge bed (UASB) systems treating carbohydrate waste waters. *Water SA* **17** (2) 91-106.

SMITH JM, VAN HESS HC and ABBOTT MM (1996) *Introduction to Chemical Engineering Thermodynamics* (5th ed.). McGraw-Hill International Editions.

SÖTEMANN SW, RISTOW NE, WENTZEL MC and EKAMA GA (2005a) A steady state model for anaerobic digestion of sewage sludges. *Water SA* **31** (4) 511-527.

SÖTEMANN SW, VAN RENSBURG P, RISTOW NE, WENTZEL MC, LOEWENTHAL RE and EKAMA GA (2005b) Integrated chemical/physical and biological processes modelling Part 2-Anaerobic digestion of sewage sludges. *Water SA* **31** (4) 545-568.

STUMM W and MORGAN JJ (1996) *Aquatic Chemistry-Chemical Equilibria and Rates in Natural Waters* (3rd ed.). John Wiley & Sons, Inc.

UEKI K, KOTAKA K, ITOH K and UEKI A (1988) Potential availability of anaerobic treatment with digester slurry of animal waste for the reclamation of acid mine water containing sulphate and heavy metals. *J. Ferment. Technol.* **66** 43-50.

# APPENDIX A

## UCT ANAEROBIC DIGESTION MODEL NO. 1 (UCTADM1)

**Table A-1:** Petersen matrix representation of biochemical rate coefficients ($\upsilon_{i,j}$) and kinetic process rate equations ($\rho_j$) for components (i = 1-27, j = 1-30) in the UCTADM1 (excluding sulphate reduction)

| Component → | i | 1 | 2 | 3 | 4 | 5 | 6 | 7 | 8 | 9 | 10 | 11 | 12 | 13 | 14 | 15 | 16 | 17 | 18 | 19 | 20 | 21 | 22 | 23 | 24 | 25 | 26 | 27 | Process Rate ($\rho$) |
|---|---|---|---|---|---|---|---|---|---|---|---|---|---|---|---|---|---|---|---|---|---|---|---|---|---|---|---|---|---|
| j | Process ↓ | $H_2O$ | HPr | Pr | HAc | $Ac^-$ | $NH_4^+$ | $NH_3$ | $H_2$ | $H^+$ | $OH^-$ | $H_3PO_4$ | $H_2PO_4^-$ | $HPO_4^{2-}$ | $PO_4^{3-}$ | $H_2CO_3$ | $HCO_3^-$ | $CO_3^{2-}$ | $S_{ba}$ | $S_{ai}$ | $S_{up}$ | $S_{bp}$ | $S_{ap}$ | $Z_{ac}$ | $Z_{ae}$ | $Z_{am}$ | $Z_{hm}$ | $CH_4(g)$ | $CO_2(g)$ | |
| 1 | Hydrolysis | | | | | | | $\frac{PsN \times MW_{NH_3}}{\frac{Hydrolysis\ Prot}{2} \times AW_O}{MW_{NH_3}}$ | | | | | | | | $\frac{\left(\frac{6 \times Hydrolysis\ Prot}{24} - PsC\right) \times MW_{CO_2}}{\frac{Hydrolysis\ Prot}{2} \times AW_O}{MW_{CO_2}}$ | | | $\frac{Hydrolysis\ Prot \times MW_{C_6H_{12}O_6}}{\frac{24}{\frac{Hydrolysis\ Prot}{2} \times AW_O}{MW_{C_6H_{12}O_6}}}$ | | -1 | | | | | | | | | | $\rho_1$ |
| 2 | Acidogenesis (low and high $pH_2$) | | | | $\frac{2}{Y_{ac}}$ | | -1 | | $\frac{4}{Y_{ai}}$ | 1 | | | | | | $\frac{2}{Y_{ai}}$ | | | $-\frac{1+\frac{5}{6}Y_{ai}}{Y_{ai}}$ | | | | 1 | | | | | | | $\rho_2$ |
| 3 | Acidogenesis (high $pH_2$ only) | | $\frac{1}{Y_{ai}}$ | | $\frac{1}{Y_{ai}}$ | | -1 | | $\frac{1}{Y_{ai}}$ | 1 | | | | | | | | | $-\frac{1+\frac{5}{6}Y_{ai}}{Y_{ai}}$ | | | | 1 | | | | | | | $\rho_3$ |
| 4 | Acidogen Endogenous Decay | | | | | | | $(1 - Endogenous\ Prot \times PsN)$ | | | | | | | | $(5 - Endogenous\ Prot \times PsC)$ | | | | | 160 | | -1 | | | | | | | $\rho_4$ |
| 5 | Acetogenesis | | $-\frac{1+\frac{3}{2}Y_{ae}}{Y_{ae}}$ | | $\frac{1}{Y_{ae}}$ | | -1 | | $\frac{1}{2}+\frac{3}{Y_{ae}}$ | 1 | | | | | | $\left(\frac{1}{Y_{ae}}-\frac{1}{2}\right)$ | | | | | | | | 1 | | | | | $\rho_5$ |
| 6 | Acetogen Endogenous Decay | | | | | | | $(1 - Endogenous\ Prot \times PsN)$ | | | | | | | | $(5 - Endogenous\ Prot \times PsC)$ | | | | | 160 | | | -1 | | | | | | $\rho_6$ |
| 7 | Acetoclastic Methanogenesis | | | | $-\frac{1+\frac{5}{2}Y_{am}}{Y_{am}}$ | | -1 | | | 1 | | | | | | $\frac{1}{Y_{am}}$ | | | | | | | | | 1 | | $\frac{1}{Y_{am}}$ | | | $\rho_7$ |
| 8 | Acetoclastic Methanogen Endogenous Decay | | | | | | | $(1 - Endogenous\ Prot \times PsN)$ | | | | | | | | $(5 - Endogenous\ Prot \times PsC)$ | | | | | 160 | | | | -1 | | | | | $\rho_8$ |
| 9 | Hydrogenotrophic Methanogenesis | | | | | | -1 | | $-\frac{4+10Y_{hm}}{Y_{hm}}$ | 1 | | | | | | $-\frac{1+5Y_{hm}}{Y_{hm}}$ | | | | | | | | | | | 1 | $\frac{1}{Y_{hm}}$ | | $\rho_9$ |
| 10 | Hydrogenotrophic Methanogen Endogenous Decay | | | | | | | $(1 - Endogenous\ Prot \times PsN)$ | | | | | | | | $(5 - Endogenous\ Prot \times PsC)$ | | | | | 160 | | | | | -1 | | | | $\rho_{10}$ |
| 11 | Forward Dissociation of $H_3PO_4$ | | | | | | | | | 1 | | -1 | 1 | | | | | | | | | | | | | | | | $\rho_{11}$ |
| 12 | Reverse Dissociation of $H_3PO_4$ | | | | | | | | | -1 | | 1 | -1 | | | | | | | | | | | | | | | | $\rho_{12}$ |
| 13 | Forward Dissociation of $H_2PO_4^-$ | | | | | | | | | 1 | | | -1 | 1 | | | | | | | | | | | | | | | $\rho_{13}$ |
| 14 | Reverse Dissociation of $H_2PO_4^-$ | | | | | | | | | -1 | | | 1 | -1 | | | | | | | | | | | | | | | $\rho_{14}$ |
| 15 | Forward Dissociation of $HPO_4^{2-}$ | | | | | | | | | 1 | | | | -1 | 1 | | | | | | | | | | | | | | $\rho_{15}$ |
| 16 | Reverse Dissociation of $HPO_4^{2-}$ | | | | | | | | | -1 | | | | 1 | -1 | | | | | | | | | | | | | | $\rho_{16}$ |
| 17 | Forward Dissociation of $H_2CO_3$ | | | | | | | | | 1 | | | | | | -1 | 1 | | | | | | | | | | | | $\rho_{17}$ |
| 18 | Reverse Dissociation of $H_2CO_3$ | | | | | | | | | -1 | | | | | | 1 | -1 | | | | | | | | | | | | $\rho_{18}$ |
| 19 | Forward Dissociation of $HCO_3^-$ | | | | | | | | | 1 | | | | | | | -1 | 1 | | | | | | | | | | | $\rho_{19}$ |
| 20 | Reverse Dissociation of $HCO_3^-$ | | | | | | | | | -1 | | | | | | | 1 | -1 | | | | | | | | | | | $\rho_{20}$ |
| 21 | Forward Dissociation of $NH_4^+$ | | | | | | -1 | 1 | | 1 | | | | | | | | | | | | | | | | | | | $\rho_{21}$ |
| 22 | Reverse Dissociation of $NH_4^+$ | | | | | | 1 | -1 | | -1 | | | | | | | | | | | | | | | | | | | $\rho_{22}$ |
| 23 | Forward Dissociation of HPr | | -1 | 1 | | | | | | 1 | | | | | | | | | | | | | | | | | | | $\rho_{23}$ |
| 24 | Reverse Dissociation of HPr | | 1 | -1 | | | | | | -1 | | | | | | | | | | | | | | | | | | | $\rho_{24}$ |
| 25 | Forward Dissociation of HAc | | | | -1 | 1 | | | | 1 | | | | | | | | | | | | | | | | | | | $\rho_{25}$ |
| 26 | Reverse Dissociation of HAc | | | | 1 | -1 | | | | -1 | | | | | | | | | | | | | | | | | | | $\rho_{26}$ |
| 27 | Forward Dissociation of $H_2O$ | | | | | | | | | 1 | 1 | | | | | | | | | | | | | | | | | | $\rho_{27}$ |
| 28 | Reverse Dissociation of $H_2O$ | | | | | | | | | -1 | -1 | | | | | | | | | | | | | | | | | | $\rho_{28}$ |
| 29 | Dissolution of $CO_2(g)$ | | | | | | | | | | | | | | | 1 | | | | | | | | | | | | -1 | $\rho_{29}$ |
| 30 | Expulsion of $CO_2(g)$ | | | | | | | | | | | | | | | -1 | | | | | | | | | | | | 1 | $\rho_{30}$ |
| | Unit | | $mol/\ell$ | $mol/\ell$ | $mol/\ell$ | $mol/\ell$ | $mol/\ell$ | $mol/\ell$ | $mol/\ell$ | $mol/\ell$ | $mol/\ell$ | $mol/\ell$ | $mol/\ell$ | $mol/\ell$ | $mol/\ell$ | $mol/\ell$ | $mol/\ell$ | $mol/\ell$ | $mol/\ell$ | $mol/\ell$ | $gCOD/\ell$ | $gCOD/\ell$ | $gCOD/\ell$ | $mol/\ell$ | $mol/\ell$ | $mol/\ell$ | $mol/\ell$ | $mol/\ell$ | $mol/\ell$ | |

**Table A-2:** Key of process rates (ρ = 1-30) in Petersen matrix representation of the UCTADM1 (excluding sulphate reduction)

| Process Rate (ρ) |
|---|
| $\rho_1$ : $\left(\frac{HydK\max \times \frac{[S_{bp}]}{[Z_{ai}]}}{Ks_{Hyd}+\frac{[S_{bp}]}{[Z_{ai}]}}\right)\times[Z_{ai}]$ |
| $\rho_2$ : $\left(\frac{\mu\max_a \times [S_{bs}]}{Ks_a+[S_{bs}]}\right)\times\left(1-\frac{[H_2]}{K_{H_2}+[H_2]}\right)\times[Z_{ai}]$ |
| $\rho_3$ : $\left(\frac{\mu\max_a \times [S_{bs}]}{Ks_a+[S_{bs}]}\right)\times\left(\frac{[H_2]}{K_{H_2}+[H_2]}\right)\times[Z_{ai}]$ |
| $\rho_4$ : $b_a \times [Z_{ai}]$ |
| $\rho_5$ : $\left(\frac{\mu\max_{ae} \times [H\,\mathrm{Pr}]}{Ks_{ae}+[H\,\mathrm{Pr}]}\right)\times\left(1-\frac{[H_2]}{K_{H_2}+[H_2]}\right)\times[Z_{ae}]$ |
| $\rho_6$ : $b_{ae} \times [Z_{ae}]$ |
| $\rho_7$ : $\left(\frac{\mu\max_{am} \times [HAc]}{(Ks_{am}+[HAc])\times\left(1+\frac{[H]}{Ki_{am}}\right)}\right)\times[Z_{am}]$ |
| $\rho_8$ : $b_{am} \times [Z_{am}]$ |
| $\rho_9$ : $\left(\frac{\mu\max_{hm} \times [H_2]}{(Ks_{hm}+[H_2])\times\left(1+\frac{[H]}{Ki_{hm}}\right)}\right)\times[Z_{hm}]$ |
| $\rho_{10}$ : $b_{hm} \times [Z_{hm}]$ |
| $\rho_{11}$ : $Kf_{p1} \times [H_3PO_4]$ |

**Table A-2:** Key of process rates (ρ = 1-30) in Petersen matrix representation of the UCTADM1 (excluding sulphate reduction)

| Process Rate (ρ) |
|---|
| $\rho_1$ : $\left(\frac{HydK\max\times\frac{[S_{bp}]}{[Z_{ai}]}}{Ks_{Hyd}+\frac{[S_{bp}]}{[Z_{ai}]}}\right)\times[Z_{ai}]$ |
| $\rho_2$ : $\left(\frac{\mu\max_a\times[S_{bs}]}{Ks_a+[S_{bs}]}\right)\times\left(1-\frac{[H_2]}{K_{H_2}+[H_2]}\right)\times[Z_{ai}]$ |
| $\rho_3$ : $\left(\frac{\mu\max_a\times[S_{bs}]}{Ks_a+[S_{bs}]}\right)\times\left(\frac{[H_2]}{K_{H_2}+[H_2]}\right)\times[Z_{ai}]$ |
| $\rho_4$ : $b_a\times[Z_{ai}]$ |
| $\rho_5$ : $\left(\frac{\mu\max_{ae}\times[H\,\mathrm{Pr}]}{Ks_{ae}+[H\,\mathrm{Pr}]}\right)\times\left(1-\frac{[H_2]}{K_{H_2}+[H_2]}\right)\times[Z_{ae}]$ |
| $\rho_6$ : $b_{ae}\times[Z_{ae}]$ |
| $\rho_7$ : $\left(\frac{\mu\max_{am}\times[HAc]}{(Ks_{am}+[HAc])\times\left(1+\frac{[H]}{Ki_{am}}\right)}\right)\times[Z_{am}]$ |
| $\rho_8$ : $b_{am}\times[Z_{am}]$ |
| $\rho_9$ : $\left(\frac{\mu\max_{hm}\times[H_2]}{(Ks_{hm}+[H_2])\times\left(1+\frac{[H]}{Ki_{hm}}\right)}\right)\times[Z_{hm}]$ |
| $\rho_{10}$ : $b_{hm}\times[Z_{hm}]$ |
| $\rho_{11}$ : $Kf_{p1}\times[H_3PO_4]$ |

$\rho_{12}$ : $Kr_{p1} \times [H_2PO_4] \times [H]$

$\rho_{13}$ : $Kf_{p2} \times [H_2PO_4]$

$\rho_{14}$ : $Kr_{p2} \times [HPO_4] \times [H]$

$\rho_{15}$ : $Kf_{p3} \times [HPO_4]$

$\rho_{16}$ : $Kr_{p3} \times [PO_4] \times [H]$

$\rho_{17}$ : $Kf_{c1} \times [H_2CO_3]$

$\rho_{18}$ : $Kr_{c1} \times [HCO_3] \times [H]$

$\rho_{19}$ : $Kf_{c2} \times [HCO_3]$

$\rho_{20}$ : $Kr_{c2} \times [CO_3] \times [H]$

$\rho_{21}$ : $Kf_n \times [NH_4]$

$\rho_{22}$ : $Kr_n \times [NH_3] \times [H]$

$\rho_{23}$ : $Kf_{\mathrm{Pr}} \times [H\,\mathrm{Pr}]$

$\rho_{24}$ : $Kr_{\mathrm{Pr}} \times [\mathrm{Pr}] \times [H]$

$\rho_{25}$ : $Kf_a \times [HAc]$

$\rho_{26}$ : $Kr_a \times [Ac] \times [H]$

$\rho_{27}$ : $Kf_W$

$\rho_{28}$ : $Kr_W \times [OH] \times [H]$

$\rho_{29}$ : $Kr_{CO_2} \times p_{CO_2} \times KH_{CO_2}$

$\rho_{30}$ : $Kr_{CO_2} \times [H_2CO_3]$

**Table A-3:** Petersen matrix representation of biochemical rate coefficients ($\upsilon_{i,j}$) and kinetic process rate equations ($\rho_j$) for water (i = 1; j = 1-42) and soluble components (i = 2-13; j = 1-42) in the UCTADM1 (including sulphate reduction)

| Component → | | 1 | 2 | 3 | 4 | 5 | 6 | 7 | 8 | 9 | 10 | 11 | 12 | 13 | Process Rate (ρ) |
|---|---|---|---|---|---|---|---|---|---|---|---|---|---|---|---|
| j | Process ↓ | $H_2O$ | HPr | $Pr^-$ | HAc | $Ac^-$ | $NH_4^+$ | $NH_3$ | $H_2$ | $H^+$ | $OH^-$ | $H_3PO_4$ | $H_2PO_4^-$ | $HPO_4^{2-}$ | |
| 1 | Hydrolysis | | | | | | $-1\times MW_{NH_4}\times 1000$ | $\left(\frac{PsN\times MW_{NH_3}}{\frac{Hydrolysis\ Prot}{2}\times AW_O}{MW_{NH_3}}\right)\times MW_{NH_3}\times 1000$ | | | | | | | $\rho_1$ |
| 2 | Acidogenesis (low and high $pH_2$) | | | | $\frac{2}{Y_{ai}}\times MW_{HAc}\times 1000$ | | $-1\times MW_{NH_4}\times 1000$ | | $\frac{4}{Y_{ai}}\times MW_{H_2}\times 1000$ | $1\times MW_H\times 1000$ | | | | | $\rho_2$ |
| 3 | Acidogenesis (high $pH_2$ only) | | $\frac{1}{Y_{ai}}\times MW_{HPr}\times 1000$ | | $\frac{1}{Y_{ai}}\times MW_{HAc}\times 1000$ | | $-1\times MW_{NH_4}\times 1000$ | $(1-Endogenous\,Prot\times PsN)\times MW_{NH_3}\times 1000$ | $\frac{1}{Y_{ai}}\times MW_{H_2}\times 1000$ | $1\times MW_H\times 1000$ | | | | | $\rho_3$ |
| 4 | Acidogen Endogenous Decay | | | | $\frac{1}{Y_{ae}}\times MW_{HAc}\times 1000$ | | $-1\times MW_{NH_4}\times 1000$ | | $\left(\frac{1}{2}+\frac{3}{Y_{ae}}\right)\times MW_{H_2}\times 1000$ | $1\times MW_H\times 1000$ | | | | | $\rho_4$ |
| 5 | Acetogenesis | | $\left(\frac{1+\frac{3}{2}Y_{ae}}{-\frac{Y_{ae}}{Y_{ae}}}\right)\times MW_{HPr}\times 1000$ | | | | | $(1-Endogenous\,Prot\times PsN)\times MW_{NH_3}\times 1000$ | | | | | | | $\rho_5$ |
| 6 | Acetogen Endogenous Decay | | | | $\left(\frac{1+\frac{5}{2}Y_{am}}{-\frac{Y_{am}}{Y_{am}}}\right)\times MW_{HAc}\times 1000$ | | $-1\times MW_{NH_4}\times 1000$ | | | $1\times MW_H\times 1000$ | | | | | $\rho_6$ |
| 7 | Acetoclastic Methanogenesis | | | | | | | $(1-Endogenous\,Prot\times PsN)\times MW_{NH_3}\times 1000$ | | | | | | | $\rho_7$ |
| 8 | Acetoclastic Methanogen Endogenous Decay | | | | | | $-1\times MW_{NH_4}\times 1000$ | | | | | | | | $\rho_8$ |
| 9 | Hydrogenotrophic Methanogenesis | | | | | | | $(1-Endogenous\,Prot\times PsN)\times MW_{NH_3}\times 1000$ | $\left(-\frac{4+10Y_{hm}}{Y_{hm}}\right)\times MW_{H_2}\times 1000$ | $1\times MW_H\times 1000$ | | | | | $\rho_9$ |
| 10 | Hydrogenotrophic Methanogen Endogenous Decay | | | | | | $-1\times MW_{NH_4}\times 1000$ | $(1-Endogenous\,Prot\times PsN)\times MW_{NH_3}\times 1000$ | | | | | | | $\rho_{10}$ |
| 11 | Acetogenic Sulphidogenesis | | $-\frac{1}{Y_{pS}}\times MW_{HPr}\times 1000$ | | $\left(\frac{1}{Y_{pS}}-\frac{3}{2}\right)\times MW_{HAc}\times 1000$ | | $-1\times MW_{NH_4}\times 1000$ | $0.761\times MW_{NH_3}\times 1000$ | $\frac{1}{2}\times MW_{H_2}\times 1000$ | $\left(\frac{13}{4}-\frac{3}{2Y_{pS}}\right)\times MW_H\times 1000$ | | | | | $\rho_{11}$ |
| 12 | Acetogenic Sulphidogen Endogenous Decay | | | | | | $-1\times MW_{NH_4}\times 1000$ | $0.761\times MW_{NH_3}\times 1000$ | | $\left(6-\frac{2}{Y_{aS}}\right)\times MW_H\times 1000$ | | | | | $\rho_{12}$ |
| 13 | Acetoclastic Sulphidogenesis | | | | $-\frac{1}{Y_{aS}}\times MW_{HAc}\times 1000$ | | $-1\times MW_{NH_4}\times 1000$ | $0.761\times MW_{NH_3}\times 1000$ | $-\frac{1}{Y_{hS}}\times MW_{H_2}\times 1000$ | $\left(6-\frac{1}{2Y_{hS}}\right)\times MW_H\times 1000$ | | | | | $\rho_{13}$ |
| 14 | Acetoclastic Sulphidogen Endogenous Decay | | | | | | $-1\times MW_{NH_4}\times 1000$ | $0.761\times MW_{NH_3}\times 1000$ | | $1\times MW_H\times 1000$ | | | | | $\rho_{14}$ |
| 15 | Hydrogenotrophic Sulphidogenesis | | | | | | | | | $-1\times MW_H\times 1000$ | | | | | $\rho_{15}$ |
| 16 | Hydrogenotrophic Sulphidogen Endogenous Decay | | | | | | | | | $1\times MW_H\times 1000$ | | | | | $\rho_{16}$ |
| 17 | Forward Dissociation of $H_2S$(aq) | | | | | | | | | $-1\times MW_H\times 1000$ | | | | | $\rho_{17}$ |
| 18 | Reverse Dissociation of $H_2S$(aq) | | | | | | | | | $1\times MW_H\times 1000$ | | | | | $\rho_{18}$ |
| 19 | Forward Dissociation of $HS^-$ | | | | | | | | | $-1\times MW_H\times 1000$ | | | | | $\rho_{19}$ |
| 20 | Reverse Dissociation of $HS^-$ | | | | | | | | | $1\times MW_H\times 1000$ | | | | | $\rho_{20}$ |
| 21 | Forward Dissociation of $H_3PO_4$ | | | | | | | | | $-1\times MW_H\times 1000$ | | $-1\times MW_{H_3PO_4}\times 1000$ | $1\times MW_{H_2PO_4}\times 1000$ | | $\rho_{21}$ |
| 22 | Reverse Dissociation of $H_3PO_4$ | | | | | | | | | $1\times MW_H\times 1000$ | | $1\times MW_{H_3PO_4}\times 1000$ | $-1\times MW_{H_2PO_4}\times 1000$ | | $\rho_{22}$ |
| 23 | Forward Dissociation of $H_2PO_4^-$ | | | | | | | | | $-1\times MW_H\times 1000$ | | | $-1\times MW_{H_2PO_4}\times 1000$ | $1\times MW_{HPO_4}\times 1000$ | $\rho_{23}$ |
| 24 | Reverse Dissociation of $H_2PO_4^-$ | | | | | | | | | $1\times MW_H\times 1000$ | | | $1\times MW_{H_2PO_4}\times 1000$ | $-1\times MW_{HPO_4}\times 1000$ | $\rho_{24}$ |
| 25 | Forward Dissociation of $HPO_4^{2-}$ | | | | | | | | | $-1\times MW_H\times 1000$ | | | | $-1\times MW_{HPO_4}\times 1000$ | $\rho_{25}$ |
| 26 | Reverse Dissociation of $HPO_4^{2-}$ | | | | | | | | | $1\times MW_H\times 1000$ | | | | $1\times MW_{HPO_4}\times 1000$ | $\rho_{26}$ |
| 27 | Forward Dissociation of $H_2CO_3$ | | | | | | | | | $-1\times MW_H\times 1000$ | | | | | $\rho_{27}$ |
| 28 | Reverse Dissociation of $H_2CO_3$ | | | | | | | | | $1\times MW_H\times 1000$ | | | | | $\rho_{28}$ |
| 29 | Forward Dissociation of $HCO_3^-$ | | | | | | $-1\times MW_{NH_4}\times 1000$ | $1\times MW_{NH_3}\times 1000$ | | $-1\times MW_H\times 1000$ | | | | | $\rho_{29}$ |
| 30 | Reverse Dissociation of $HCO_3^-$ | | | | | | $1\times MW_{NH_4}\times 1000$ | $-1\times MW_{NH_3}\times 1000$ | | $1\times MW_H\times 1000$ | | | | | $\rho_{30}$ |
| 31 | Forward Dissociation of $NH_4^+$ | | | | | | | | | $-1\times MW_H\times 1000$ | | | | | $\rho_{31}$ |
| 32 | Reverse Dissociation of $NH_4^+$ | | | | | | | | | $1\times MW_H\times 1000$ | | | | | $\rho_{32}$ |
| 33 | Forward Dissociation of HPr | | $-1\times MW_{HPr}\times 1000$ | $1\times MW_{Pr}\times 1000$ | | | | | | $-1\times MW_H\times 1000$ | | | | | $\rho_{33}$ |
| 34 | Reverse Dissociation of HPr | | $1\times MW_{HPr}\times 1000$ | $-1\times MW_{Pr}\times 1000$ | | | | | | $1\times MW_H\times 1000$ | | | | | $\rho_{34}$ |
| 35 | Forward Dissociation of HAc | | | | $-1\times MW_{HAc}\times 1000$ | $1\times MW_{Ac}\times 1000$ | | | | $-1\times MW_H\times 1000$ | | | | | $\rho_{35}$ |
| 36 | Reverse Dissociation of HAc | | | | $1\times MW_{HAc}\times 1000$ | $-1\times MW_{Ac}\times 1000$ | | | | $1\times MW_H\times 1000$ | | | | | $\rho_{36}$ |
| 37 | Forward Dissociation of $H_2O$ | | | | | | | | | $-1\times MW_H\times 1000$ | | | | | $\rho_{37}$ |
| 38 | Reverse Dissociation of $H_2O$ | | | | | | | | | $1\times MW_H\times 1000$ | $1\times MW_{OH}\times 1000$ | | | | $\rho_{38}$ |
| 39 | Dissolution of $CO_2$(g) | | | | | | | | | $-1\times MW_H\times 1000$ | $-1\times MW_{OH}\times 1000$ | | | | $\rho_{39}$ |
| 40 | Expulsion of $CO_2$(g) | | | | | | | | | | | | | | $\rho_{40}$ |
| 41 | Dissolution of $H_2S$(g) | | | | | | | | | | | | | | $\rho_{41}$ |
| 42 | Expulsion of $H_2S$(g) | | | | | | | | | | | | | | $\rho_{42}$ |
| | Unit | | $g/m^3$ | $g/m^3$ | $g/m^3$ | $g/m^3$ | $g/m^3$ | $g/m^3$ | $g/m^3$ | $g/m^3$ | $g/m^3$ | $g/m^3$ | $g/m^3$ | $g/m^3$ | |

**Table A-4:** Petersen matrix representation of biochemical rate coefficients ($\upsilon_{i,j}$) and kinetic process rate equations ($\rho_j$) for soluble components (i = 14-22; j = 1-42)

in the UCTADM1 (including sulphate reduction)

| Component → | | 14 | 15 | 16 | 17 | 18 | 19 | 20 | 21 | 22 | |
|---|---|---|---|---|---|---|---|---|---|---|---|
| **j** | **Process ↓ i** | $PO_4^{3-}$ | $H_2CO_3$ | $HCO_3^-$ | $CO_3^{2-}$ | $SO_4^{2-}$ | $H_2S(aq)$ | $HS^-$ | $S^{2-}$ | $S_{bd}$ | **Process Rate ($\rho$)** |
| 1 | Hydrolysis | | $\left(\frac{6 \times Hydrolysis\ Prot \times PsC}{\frac{24}{Hydrolysis\ Prot} \times AW_C + \frac{2}{MW_{CO_2}} \times AW_O}\right) \times MW_{H_2CO_3} \times 1000$ | | | | | | | $\left(\frac{Hydrolysis\ Prot \times MW_{C_5H_7O_2N}}{\frac{24}{Hydrolysis\ Prot} \times AW_C + \frac{2}{MW_{C_5H_7O_2N}} \times AW_O}\right) \times MW_{C_5H_7O_2N} \times 1000$ | $\rho_1$ |
| 2 | Acidogenesis (low and high $pH_2$) | | $\frac{2}{Y_{ac}} \times MW_{H_2CO_3} \times 1000$ | | | | | | | $-\frac{1+\frac{5}{8}Y_{ac}}{Y_{ac}} \times MW_{C_5H_7O_2N} \times 1000$ | $\rho_2$ |
| 3 | Acidogenesis (high $pH_2$ only) | | | | | | | | | $-\frac{1+\frac{5}{8}Y_{ac}}{Y_{ac}} \times MW_{C_5H_7O_2N} \times 1000$ | $\rho_3$ |
| 4 | Acidogen Endogenous Decay | | $(5 - Endogenous\ Prot \times PsC) \times MW_{H_2CO_3} \times 1000$ | | | | | | | | $\rho_4$ |
| 5 | Acetogenesis | | $\left(\frac{1}{Y_{ae}} - \frac{1}{2}\right) \times MW_{H_2CO_3} \times 1000$ | | | | | | | | $\rho_5$ |
| 6 | Acetogen Endogenous Decay | | $(5 - Endogenous\ Prot \times PsC) \times MW_{H_2CO_3} \times 1000$ | | | | | | | | $\rho_6$ |
| 7 | Acetoclastic Methanogenesis | | $\frac{1}{Y_{am}} \times MW_{H_2CO_3} \times 1000$ | | | | | | | | $\rho_7$ |
| 8 | Acetoclastic Methanogen Endogenous Decay | | $(5 - Endogenous\ Prot \times PsC) \times MW_{H_2CO_3} \times 1000$ | | | | | | | | $\rho_8$ |
| 9 | Hydrogenotrophic Methanogenesis | | $\left(-\frac{1+5Y_{hm}}{Y_{hm}}\right) \times MW_{H_2CO_3} \times 1000$ | | | | | | | | $\rho_9$ |
| 10 | Hydrogenotrophic Methanogen Endogenous Decay | | $(5 - Endogenous\ Prot \times PsC) \times MW_{H_2CO_3} \times 1000$ | | | | | | | | $\rho_{10}$ |
| 11 | Acetogenic Sulphidogenesis | | $\left(\frac{1}{Y_{as}} - 2\right) \times MW_{H_2CO_3} \times 1000$ | | | $-\left(\frac{3}{4Y_{as}} - \frac{9}{8}\right) \times MW_{SO_4} \times 1000$ | $\left(\frac{3}{4Y_{as}} - \frac{9}{8}\right) \times MW_{H_2S} \times 1000$ | | | | $\rho_{11}$ |
| 12 | Acetogenic Sulphidogen Endogenous Decay | | $0.7335 \times MW_{H_2CO_3} \times 1000$ | | | | | | | | $\rho_{12}$ |
| 13 | Acetoclastic Sulphidogenesis | | $\left(\frac{2}{Y_{as}} - 5\right) \times MW_{H_2CO_3} \times 1000$ | | | $-\left(\frac{1}{Y_{as}} - \frac{5}{2}\right) \times MW_{SO_4} \times 1000$ | $\left(\frac{1}{Y_{as}} - \frac{5}{2}\right) \times MW_{H_2S} \times 1000$ | | | | $\rho_{13}$ |
| 14 | Acetoclastic Sulphidogen Endogenous Decay | | $0.7335 \times MW_{H_2CO_3} \times 1000$ | | | | | | | | $\rho_{14}$ |
| 15 | Hydrogenotrophic Sulphidogenesis | | $-5 \times MW_{H_2CO_3} \times 1000$ | | | $-\left(\frac{1}{4Y_{hs}} - \frac{5}{2}\right) \times MW_{SO_4} \times 1000$ | $\left(\frac{1}{4Y_{hs}} - \frac{5}{2}\right) \times MW_{H_2S} \times 1000$ | | | | $\rho_{15}$ |
| 16 | Hydrogenotrophic Sulphidogen Endogenous Decay | | $0.7335 \times MW_{H_2CO_3} \times 1000$ | | | | | | | | $\rho_{16}$ |
| 17 | Forward Dissociation of $H_2S(aq)$ | | | | | | $-1 \times MW_{H_2S} \times 1000$ | $1 \times MW_{HS} \times 1000$ | | | $\rho_{17}$ |
| 18 | Reverse Dissociation of $H_2S(aq)$ | | | | | | $1 \times MW_{H_2S} \times 1000$ | $-1 \times MW_{HS} \times 1000$ | | | $\rho_{18}$ |
| 19 | Forward Dissociation of $HS^-$ | | | | | | | $-1 \times MW_{HS} \times 1000$ | $1 \times MW_S \times 1000$ | | $\rho_{19}$ |
| 20 | Reverse Dissociation of $HS^-$ | | | | | | | $1 \times MW_{HS} \times 1000$ | $-1 \times MW_S \times 1000$ | | $\rho_{20}$ |
| 21 | Forward Dissociation of $H_3PO_4$ | | | | | | | | | | $\rho_{21}$ |
| 22 | Reverse Dissociation of $H_3PO_4$ | | | | | | | | | | $\rho_{22}$ |
| 23 | Forward Dissociation of $H_2PO_4^-$ | | | | | | | | | | $\rho_{23}$ |
| 24 | Reverse Dissociation of $H_2PO_4^-$ | | | | | | | | | | $\rho_{24}$ |
| 25 | Forward Dissociation of $HPO_4^{2-}$ | $1 \times MW_{PO_4} \times 1000$ | | | | | | | | | $\rho_{25}$ |
| 26 | Reverse Dissociation of $HPO_4^{2-}$ | $-1 \times MW_{PO_4} \times 1000$ | | | | | | | | | $\rho_{26}$ |
| 27 | Forward Dissociation of $H_2CO_3$ | | $-1 \times MW_{H_2CO_3} \times 1000$ | $1 \times MW_{HCO_3} \times 1000$ | | | | | | | $\rho_{27}$ |
| 28 | Reverse Dissociation of $H_2CO_3$ | | $1 \times MW_{H_2CO_3} \times 1000$ | $-1 \times MW_{HCO_3} \times 1000$ | | | | | | | $\rho_{28}$ |
| 29 | Forward Dissociation of $HCO_3^-$ | | | $-1 \times MW_{HCO_3} \times 1000$ | $1 \times MW_{CO_3} \times 1000$ | | | | | | $\rho_{29}$ |
| 30 | Reverse Dissociation of $HCO_3^-$ | | | $1 \times MW_{HCO_3} \times 1000$ | $-1 \times MW_{CO_3} \times 1000$ | | | | | | $\rho_{30}$ |
| 31 | Forward Dissociation of $NH_4^+$ | | | | | | | | | | $\rho_{31}$ |
| 32 | Reverse Dissociation of $NH_4^+$ | | | | | | | | | | $\rho_{32}$ |
| 33 | Forward Dissociation of HPr | | | | | | | | | | $\rho_{33}$ |
| 34 | Reverse Dissociation of HPr | | | | | | | | | | $\rho_{34}$ |
| 35 | Forward Dissociation of HAc | | | | | | | | | | $\rho_{35}$ |
| 36 | Reverse Dissociation of HAc | | | | | | | | | | $\rho_{36}$ |
| 37 | Forward Dissociation of $H_2O$ | | | | | | | | | | $\rho_{37}$ |
| 38 | Reverse Dissociation of $H_2O$ | | | | | | | | | | $\rho_{38}$ |
| 39 | Dissolution of $CO_2(g)$ | | $1 \times MW_{H_2CO_3} \times 1000$ | | | | | | | | $\rho_{39}$ |
| 40 | Expulsion of $CO_2(g)$ | | $-1 \times MW_{H_2CO_3} \times 1000$ | | | | | | | | $\rho_{40}$ |
| 41 | Dissolution of $H_2S(g)$ | | | | | | $1 \times MW_{H_2S} \times 1000$ | | | | $\rho_{41}$ |
| 42 | Expulsion of $H_2S(g)$ | | | | | | $-1 \times MW_{H_2S} \times 1000$ | | | | $\rho_{42}$ |
| | **Unit** | $g/m^3$ | $g/m^3$ | $g/m^3$ | $g/m^3$ | $g/m^3$ | $g/m^3$ | $g/m^3$ | $g/m^3$ | $g/m^3$ | |

**Table A-5:** Petersen matrix representation of biochemical rate coefficients ($\upsilon_{i,j}$) and kinetic process rate equations ($\rho_j$) for particulate components (i = 23-32; j = 1-42) in the UCTADM1 (including sulphate reduction)

| Component → | i | 23 | 24 | 25 | 26 | 27 | 28 | 29 | 30 | 31 | 32 | Process Rate (ρ) |
|---|---|---|---|---|---|---|---|---|---|---|---|---|
| j | Process ↓ | $S_{su}$ | $S_{bp}$ | $S_{up}$ | $Z_{ai}$ | $Z_{ae}$ | $Z_{am}$ | $Z_{hm}$ | $Z_{pa}$ | $Z_{ac}$ | $Z_{hu}$ | |
| 1 | Hydrolysis | | $-1\times1000$ | | | | | | | | | $\rho_1$ |
| 2 | Acidogenesis (low and high $pH_2$) | | | | $1\times MW_{C_5H_7O_2N}\times1000$ | | | | | | | $\rho_2$ |
| 3 | Acidogenesis (high $pH_2$ only) | | | | $1\times MW_{C_5H_7O_2N}\times1000$ | | | | | | | $\rho_3$ |
| 4 | Acidogen Endogenous Decay | | $160\times1000$ | | $-1\times MW_{C_5H_7O_2N}\times1000$ | | | | | | | $\rho_4$ |
| 5 | Acetogenesis | | | | | $1\times MW_{C_5H_7O_2N}\times1000$ | | | | | | $\rho_5$ |
| 6 | Acetogen Endogenous Decay | | $160\times1000$ | | | $-1\times MW_{C_5H_7O_2N}\times1000$ | | | | | | $\rho_6$ |
| 7 | Acetoclastic Methanogenesis | | | | | | $1\times MW_{C_5H_7O_2N}\times1000$ | | | | | $\rho_7$ |
| 8 | Acetoclastic Methanogen Endogenous Decay | | $160\times1000$ | | | | $-1\times MW_{C_5H_7O_2N}\times1000$ | | | | | $\rho_8$ |
| 9 | Hydrogenotrophic Methanogenesis | | | | | | | $1\times MW_{C_5H_7O_2N}\times1000$ | | | | $\rho_9$ |
| 10 | Hydrogenotrophic Methanogen Endogenous Decay | | $160\times1000$ | | | | | $-1\times MW_{C_5H_7O_2N}\times1000$ | | | | $\rho_{10}$ |
| 11 | Acetogenic Sulphidogenesis | | | | | | | | $1\times MW_{C_5H_7O_2N}\times1000$ | | | $\rho_{11}$ |
| 12 | Acetogenic Sulphidogen Endogenous Decay | | $160\times1000$ | | | | | | $-1\times MW_{C_5H_7O_2N}\times1000$ | | | $\rho_{12}$ |
| 13 | Acetoclastic Sulphidogenesis | | | | | | | | | $1\times MW_{C_5H_7O_2N}\times1000$ | | $\rho_{13}$ |
| 14 | Acetoclastic Sulphidogen Endogenous Decay | | $160\times1000$ | | | | | | | $-1\times MW_{C_5H_7O_2N}\times1000$ | | $\rho_{14}$ |
| 15 | Hydrogenotrophic Sulphidogenesis | | | | | | | | | | $1\times MW_{C_5H_7O_2N}\times1000$ | $\rho_{15}$ |
| 16 | Hydrogenotrophic Sulphidogen Endogenous Decay | | $160\times1000$ | | | | | | | | $-1\times MW_{C_5H_7O_2N}\times1000$ | $\rho_{16}$ |
| 17 | Forward Dissociation of $H_2S$(aq) | | | | | | | | | | | $\rho_{17}$ |
| 18 | Reverse Dissociation of $H_2S$(aq) | | | | | | | | | | | $\rho_{18}$ |
| 19 | Forward Dissociation of $HS^-$ | | | | | | | | | | | $\rho_{19}$ |
| 20 | Reverse Dissociation of $HS^-$ | | | | | | | | | | | $\rho_{20}$ |
| 21 | Forward Dissociation of $H_3PO_4$ | | | | | | | | | | | $\rho_{21}$ |
| 22 | Reverse Dissociation of $H_3PO_4$ | | | | | | | | | | | $\rho_{22}$ |
| 23 | Forward Dissociation of $H_2PO_4^-$ | | | | | | | | | | | $\rho_{23}$ |
| 24 | Reverse Dissociation of $H_2PO_4^-$ | | | | | | | | | | | $\rho_{24}$ |
| 25 | Forward Dissociation of $HPO_4^{2-}$ | | | | | | | | | | | $\rho_{25}$ |
| 26 | Reverse Dissociation of $HPO_4^{2-}$ | | | | | | | | | | | $\rho_{26}$ |
| 27 | Forward Dissociation of $H_2CO_3$ | | | | | | | | | | | $\rho_{27}$ |
| 28 | Reverse Dissociation of $H_2CO_3$ | | | | | | | | | | | $\rho_{28}$ |
| 29 | Forward Dissociation of $HCO_3^-$ | | | | | | | | | | | $\rho_{29}$ |
| 30 | Reverse Dissociation of $HCO_3^-$ | | | | | | | | | | | $\rho_{30}$ |
| 31 | Forward Dissociation of $NH_4^+$ | | | | | | | | | | | $\rho_{31}$ |
| 32 | Reverse Dissociation of $NH_4^+$ | | | | | | | | | | | $\rho_{32}$ |
| 33 | Forward Dissociation of HPr | | | | | | | | | | | $\rho_{33}$ |
| 34 | Reverse Dissociation of HPr | | | | | | | | | | | $\rho_{34}$ |
| 35 | Forward Dissociation of HAc | | | | | | | | | | | $\rho_{35}$ |
| 36 | Reverse Dissociation of HAc | | | | | | | | | | | $\rho_{36}$ |
| 37 | Forward Dissociation of $H_2O$ | | | | | | | | | | | $\rho_{37}$ |
| 38 | Reverse Dissociation of $H_2O$ | | | | | | | | | | | $\rho_{38}$ |
| 39 | Dissolution of $CO_2$(g) | | | | | | | | | | | $\rho_{39}$ |
| 40 | Expulsion of $CO_2$(g) | | | | | | | | | | | $\rho_{40}$ |
| 41 | Dissolution of $H_2S$(g) | | | | | | | | | | | $\rho_{41}$ |
| 42 | Expulsion of $H_2S$(g) | | | | | | | | | | | $\rho_{42}$ |
| | Unit | $gCOD/m^3$ | $gCOD/m^3$ | $gCOD/m^3$ | $g/m^3$ | $g/m^3$ | $g/m^3$ | $g/m^3$ | $g/m^3$ | $g/m^3$ | $g/m^3$ | |

**Table A-6:** Petersen matrix representation of biochemical rate coefficients ($\upsilon_{i,j}$) and kinetic process rate equations ($\rho_j$) for gaseous components (i = 33-35; j = 1-42) in the UCTADM1 (including sulphate reduction)

| Component → | i | 33 | 34 | 35 | Process Rate (ρ) |
|---|---|---|---|---|---|
| j | Process ↓ | $CH_4(g)$ | $CO_2(g)$ | $H_2S(g)$ | |
| 1 | Hydrolysis | | | | $\rho_1$ |
| 2 | Acidogenesis (low and high $pH_2$) | | | | $\rho_2$ |
| 3 | Acidogenesis (high $pH_2$ only) | | | | $\rho_3$ |
| 4 | Acidogen Endogenous Decay | | | | $\rho_4$ |
| 5 | Acetogenesis | | | | $\rho_5$ |
| 6 | Acetogen Endogenous Decay | | | | $\rho_6$ |
| 7 | Acetoclastic Methanogenesis | $\frac{1}{Y_{am}} \times MW_{CH_4} \times 1000$ | | | $\rho_7$ |
| 8 | Acetoclastic Methanogen Endogenous Decay | | | | $\rho_8$ |
| 9 | Hydrogenotrophic Methanogenesis | $\frac{1}{Y_{hm}} \times MW_{CH_4} \times 1000$ | | | $\rho_9$ |
| 10 | Hydrogenotrophic Methanogen Endogenous Decay | | | | $\rho_{10}$ |
| 11 | Acetogenic Sulphidogenesis | | | | $\rho_{11}$ |
| 12 | Acetogenic Sulphidogen Endogenous Decay | | | | $\rho_{12}$ |
| 13 | Acetoclastic Sulphidogenesis | | | | $\rho_{13}$ |
| 14 | Acetoclastic Sulphidogen Endogenous Decay | | | | $\rho_{14}$ |
| 15 | Hydrogenotrophic Sulphidogenesis | | | | $\rho_{15}$ |
| 16 | Hydrogenotrophic Sulphidogen Endogenous Decay | | | | $\rho_{16}$ |
| 17 | Forward Dissociation of $H_2S_{(aq)}$ | | | | $\rho_{17}$ |
| 18 | Reverse Dissociation of $H_2S_{(aq)}$ | | | | $\rho_{18}$ |
| 19 | Forward Dissociation of $HS^-$ | | | | $\rho_{19}$ |
| 20 | Reverse Dissociation of $HS^-$ | | | | $\rho_{20}$ |
| 21 | Forward Dissociation of $H_3PO_4$ | | | | $\rho_{21}$ |
| 22 | Reverse Dissociation of $H_3PO_4$ | | | | $\rho_{22}$ |
| 23 | Forward Dissociation of $H_2PO_4^-$ | | | | $\rho_{23}$ |
| 24 | Reverse Dissociation of $H_2PO_4^-$ | | | | $\rho_{24}$ |
| 25 | Forward Dissociation of $HPO_4^{2-}$ | | | | $\rho_{25}$ |
| 26 | Reverse Dissociation of $HPO_4^{2-}$ | | | | $\rho_{26}$ |
| 27 | Forward Dissociation of $H_2CO_3$ | | | | $\rho_{27}$ |
| 28 | Reverse Dissociation of $H_2CO_3$ | | | | $\rho_{28}$ |
| 29 | Forward Dissociation of $HCO_3^-$ | | | | $\rho_{29}$ |
| 30 | Reverse Dissociation of $HCO_3^-$ | | | | $\rho_{30}$ |
| 31 | Forward Dissociation of $NH_4^+$ | | | | $\rho_{31}$ |
| 32 | Reverse Dissociation of $NH_4^+$ | | | | $\rho_{32}$ |
| 33 | Forward Dissociation of HPr | | | | $\rho_{33}$ |
| 34 | Reverse Dissociation of HPr | | | | $\rho_{34}$ |
| 35 | Forward Dissociation of HAc | | | | $\rho_{35}$ |
| 36 | Reverse Dissociation of HAc | | | | $\rho_{36}$ |
| 37 | Forward Dissociation of $H_2O$ | | | | $\rho_{37}$ |
| 38 | Reverse Dissociation of $H_2O$ | | | | $\rho_{38}$ |
| 39 | Dissolution of $CO_2(g)$ | | $-1 \times MW_{CO_2} \times 1000$ | | $\rho_{39}$ |
| 40 | Expulsion of $CO_2(g)$ | | $1 \times MW_{CO_2} \times 1000$ | | $\rho_{40}$ |
| 41 | Dissolution of $H_2S(g)$ | | | $-1 \times MW_{H_2S} \times 1000$ | $\rho_{41}$ |
| 42 | Expulsion of $H_2S(g)$ | | | $1 \times MW_{H_2S} \times 1000$ | $\rho_{42}$ |
| | Unit | $g/m^3$ | $g/m^3$ | $g/m^3$ | |

$\rho_5$ :

$$\left(\frac{\mu\max_{ae}\times([H\,\mathrm{Pr}]+[\mathrm{Pr}])}{((Ks_{ae}\times MW_{\mathrm{Pr}}\times 1000)+[H\,\mathrm{Pr}]+[\mathrm{Pr}])}\right)\times\left(1-\frac{[H_2]}{(K_{H_2}\times MW_{H_2}\times 1000)+[H_2]}\right)\times\left(\frac{[Z_{ae}]}{(MW_{C_5H_7O_2N}\times 1000)}\right)$$
$$\times\exp\left(-\left(\frac{[H_2Saq]}{0.6065\times Ki_{aes}\times MW_{H_2S}\times 1000}\right)^2\right)$$

$\rho_6$ :

$$\left(\frac{b_{ae}}{\left(MW_{C_5H_7O_2N}\times 1000\right)}\right)\times[Z_{ae}]$$

$\rho_7$ :

$$\left(\frac{\mu\max_{am}\times([HAc]+[Ac])}{((Ks_{am}\times MW_{HAc}\times 1000)+[HAc]+[Ac])\times\left(1+\frac{[H]}{Ki_{am}\times MW_H\times 1000}\right)}\right)\times\left(\frac{[Z_{am}]}{(MW_{C_5H_7O_2N}\times 1000)}\right)$$
$$\times\exp\left(-\left(\frac{[H_2Saq]}{0.6065\times Ki_{ams}\times MW_{H_2S}\times 1000}\right)^2\right)$$

$\rho_8$ :

$$\left(\frac{b_{am}}{(MW_{C_5H_7O_2N}\times 1000)}\right)\times[Z_{am}]$$

$\rho_{14}$ :
$$\left(\frac{b_{as}}{\left(MW_{C_5H_7O_2N}\times 1000\right)}\right)\times[Z_{as}]$$

$\rho_{15}$ :
$$\left(\frac{\mu\max_{hs}\times[H_2]}{(Ks_{hs}\times MW_{H_2}\times 1000)+[H_2]}\right)\times\left(1-\frac{[H_2Saq]}{(Ki_{hs}\times MW_{H_2S}\times 1000)}\right)\times\left(\frac{[SO_4]}{(Kn_{hs}\times MW_{SO_4}\times 1000)+[SO_4]}\right)\times\left(\frac{Z_{hs}}{\left(MW_{C_5H_7O_2N}\times 1000\right)}\right)$$
$$\times\exp\left(-\left(\frac{[H_2Saq]}{0.6065\times Ki_{hs}\times MW_{H_2S}\times 1000}\right)^2\right)$$

$\rho_{16}$ :
$$\left(\frac{b_{hs}}{\left(MW_{C_5H_7O_2N}\times 1000\right)}\right)\times[Z_{hs}]$$

$\rho_{17}$ :
$$\left(\frac{Kf_{HS}}{\left(MW_{H_2S}\times 1000\right)}\right)\times[H_2Saq]$$

$\rho_{18}$ :
$$\left(\frac{Kr_{HS}}{\left(MW_{HS}\times MW_{H}\times 1000000\right)}\right)\times[HS]\times[H]$$

$\rho_{19}$ :
$$\left(\frac{Kf_{S}}{\left(MW_{HS}\times 1000\right)}\right)\times[HS]$$

$\rho_{27}$ : $\left(\frac{Kf_{c1}}{MW_{H_2CO_3}\times 1000}\right)\times[H_2CO_3]$

$\rho_{28}$ : $\left(\frac{Kr_{c1}}{MW_{HCO_3}\times MW_H\times 1000000}\right)\times[HCO_3]\times[H]$

$\rho_{29}$ : $\left(\frac{Kf_{c2}}{MW_{HCO_3}\times 1000}\right)\times[HCO_3]$

$\rho_{30}$ : $\left(\frac{Kr_{c2}}{MW_{CO_3}\times MW_H\times 1000000}\right)\times[CO_3]\times[H]$

$\rho_{31}$ : $\left(\frac{Kf_n}{MW_{NH_4}\times 1000}\right)\times[NH_4]$

$\rho_{32}$ : $\left(\frac{Kr_n}{MW_{NH_3}\times MW_H\times 1000000}\right)\times[NH_3]\times[H]$

$\rho_{33}$ : $\left(\frac{Kf_{\mathrm{Pr}}}{MW_{H\,\mathrm{Pr}}\times 1000}\right)\times[H\,\mathrm{Pr}]$

$\rho_{34}$ : $\left(\frac{Kr_{\mathrm{Pr}}}{MW_{\mathrm{Pr}}\times MW_H\times 1000000}\right)\times[\mathrm{Pr}]\times[H]$

**Table A-8:** Parameters used in UCTADM1

(NB. Kinetic constants apply to modelling and simulation of steady state experiments only)

| Parameter | Value | Unit | Description |
|---|---|---|---|
| PsC | 3.5 | - | Relative proportion of carbon in feed material |
| PsH | 7 | - | Relative proportion of hydrogen in feed material |
| PsN | 0.196 | - | Relative proportion of nitrogen in feed material |
| PsO | 2 | - | Relative proportion of oxygen in feed material |
| $AW_C$ | 12.011 | g/mol | Atomic weight of carbon |
| $AW_H$ | 1.0079 | g/mol | Atomic weight of hydrogen |
| $AW_N$ | 14.007 | g/mol | Atomic weight of nitrogen |
| $AW_O$ | 15.999 | g/mol | Atomic weight of oxygen |
| $AW_P$ | 30.974 | g/mol | Atomic weight of phosphorous |
| $AW_S$ | 32.064 | g/mol | Atomic weight of sulphur |
| HydKmax | 769 | g $S_{bp}$/mol $Z_{ai}$. d | Hydrolysis maximum specific rate constant |
| $\mu max_a$ | 0.8 | $d^{-1}$ | Acidogenic biomass maximum specific growth rate constant |
| $\mu max_{ae}$ | 1.15 | $d^{-1}$ | Acetogenic biomass maximum specific growth rate constant |
| $\mu max_{am}$ | 4.39 | $d^{-1}$ | Acetoclastic methanogen biomass maximum specific growth rate constant |
| $\mu max_{hm}$ | 1.2 | $d^{-1}$ | Hydrogenotrophic methanogen biomass maximum specific growth rate constant |

| | | | |
|---|---|---|---|
| $Y_{ps}$ | 0.0268 | mol VSS/mol COD | Acetogenic sulphidogen biomass yield coefficient |
| $Y_{hs}$ | 0.0071 | mol VSS/mol COD | Hydrogenotrophic sulphidogen biomass yield coefficient |
| $Ks_{Hyd}$ | 1225 | g $S_{bp}$/mol $Z_{ai}$ | Hydrolysis half saturation constant |
| $Ks_a$ | 7.80E-04 | mol/ℓ | Acidogenic biomass half saturation constant |
| $Ks_{ae}$ | 8.90E-05 | mol/ℓ | Acetogenic biomass half saturation constant |
| $Ks_{am}$ | 1.30E-05 | mol/ℓ | Acetoclastic methanogen biomass half saturation constant |
| $Ks_{hm}$ | 1.56E-04 | mol/ℓ | Hydrogenotrophic methanogen biomass half saturation constant |
| $Ks_{as}$ | 3.75E-04 | mol/ℓ | Acetoclastic sulphidogen biomass half saturation constant |
| $Ks_{ps}$ | 2.63E-03 | mol/ℓ | Acetogenic sulphidogen biomass half saturation constant |
| $Ks_{hs}$ | 4.38E-06 | mol/ℓ | Hydrogenotrophic sulphidogen biomass half saturation constant |
| $Kn_{as}$ | 2.00E-04 | mol/ℓ | Acetoclastic sulphidogen biomass half saturation constant for sulphate |
| $Kn_{ps}$ | 7.71E-05 | mol/ℓ | Acetogenic sulphidogen biomass half saturation constant for sulphate |
| $Kn_{hs}$ | 2.00E-04 | mol/ℓ | Hydrogenotrophic sulphidogen biomass half saturation constant for sulphate |
| $K_{H2}$ | 6.25E-04 | mol $H_2$/ℓ | Hydrogen inhibition coefficient for high $pH_2$ |
| $Ki_{am}$ | 1.15E-06 | mol/ℓ | Acetoclastic methanogen biomass hydrogen ion inhibition constant |

| | | | |
|---|---|---|---|
| $Kr_W$ | 1E+11 | - | Reverse dissociation constant for $H_2O \leftrightarrow OH^- + H^+$ |
| $Kr_a$ | 1E+14 | - | Reverse dissociation constant for $HAc \leftrightarrow Ac^- + H^+$ |
| $Kr_{c1}$ | 1E+10 | - | Reverse dissociation constant for $H_2CO_3 \leftrightarrow HCO_3^- + H^+$ |
| $Kr_{c2}$ | 1E+10 | - | Reverse dissociation constant for $HCO_3^- \leftrightarrow CO_3^{2-} + H^+$ |
| $Kr_n$ | 1E+12 | - | Reverse dissociation constant for $NH_4^+ \leftrightarrow NH_3 + H^+$ |
| $Kr_{p1}$ | 1E+08 | - | Reverse dissociation constant for $H_3PO_4 \leftrightarrow H_2PO_4^- + H^+$ |
| $Kr_{p2}$ | 1E+12 | - | Reverse dissociation constant for $H_2PO_4\text{-} \leftrightarrow HPO_4^{2-} + H^+$ |
| $Kr_{p3}$ | 1E+15 | - | Reverse dissociation constant for $HPO_4^{2-} \leftrightarrow PO_4^{3-} + H^+$ |
| $MW_{Ac}$ | 60.0516 | g/mol | Molecular weight of $Ac^-$ |
| $MW_{C5H7O2N}$ | 113.1153 | g/mol | Molecular weight of biomass |
| $MW_{C6H12O6}$ | 180.1548 | g/mol | Molecular weight of $C_6H_{12}O_6$ |
| $MW_{CH4}$ | 16.0426 | g/mol | Molecular weight of $CH_4$ |
| $MW_{CO2}$ | 44.009 | g/mol | Molecular weight of $CO_2$ |
| $MW_{CO3}$ | 60.008 | g/mol | Molecular weight of $CO_3$ |
| $MW_{CaCO3}$ | 100.086 | g/mol | Molecular weight of $CaCO_3$ |
| $MW_H$ | 1.0079 | g/mol | Molecular weight of $H^+$ |
| $MW_{H2}$ | 2.0158 | g/mol | Molecular weight of $H_2$ |
| $MW_{H2CO3}$ | 62.0238 | g/mol | Molecular weight of $H_2CO_3$ |

| | | | |
|---|---|---|---|
| in_f_N_bp | 0.01 | g N/g COD | Fraction of influent Nitrogen content in biodegradable particulate COD |
| in_f_N_up | 0.03 | g N/g COD | Fraction of influent Nitrogen content in unbiodegradable particulate COD |
| in_f_P_bp | 0.0046 | g P/g COD | Fraction of influent Phosphorous content in biodegradable particulate COD |
| in_f_P_up | 0.0046 | g P/g COD | Fraction of influent Phosphorous content in unbiodegradable particulate COD |
| f_$C_5H_7O_2N$COD | 1.4145559 | - | COD/biomass ratio |
| inSC | 284 | mS/m | Conductivity of the influent |
| $k_{CO2}$ | 11.365 | - | Henry's law coefficient for $CO_2$ |
| $k_{H2S}$ | 2.3705 | - | Henry's law coefficient for $H_2S$ |
| $V_r$ | - | ℓ | Reactor volume |

| | | |
|---|---|---|
| $Kf_{HS} = Kr_{HS} \times \frac{10^{-pK_{HS}}}{f_m \times f_m}$ | - | Forward dissociation constant for $H_2S \leftrightarrow HS^- + H^+$ |
| $Kf_{Pr} = Kr_{Pr} \times \frac{10^{-pK_{Pr}}}{f_m \times f_m}$ | - | Forward dissociation constant for $HPr \leftrightarrow Pr^- + H^+$ |
| $Kf_S = Kr_S \times \frac{10^{-pK_S}}{f_d}$ | - | Forward dissociation constant for $HS^- \leftrightarrow S^{2-} + H^+$ |
| $Kf_W = Kr_W \times \frac{10^{-pK_W}}{f_m \times f_m}$ | - | Forward dissociation constant for $H_2O \leftrightarrow OH^- + H^+$ |
| $Kf_a = Kr_a \times \frac{10^{-pK_a}}{f_m \times f_m}$ | - | Forward dissociation constant for $HAc \leftrightarrow Ac^- + H^+$ |
| $Kf_{c1} = Kr_{c1} \times \frac{10^{-pK_{c1}}}{f_m \times f_m}$ | - | Forward dissociation constant for $H_2CO_3 \leftrightarrow HCO_3^- + H^+$ |
| $Kf_{c2} = Kr_{c2} \times \frac{10^{-pK_{c2}}}{f_d}$ | - | Forward dissociation constant for $HCO_3^- \leftrightarrow CO_3^{2-} + H^+$ |

| | | |
|---|---|---|
| $T_k = T_c + 273.15$ | K | Temperature in degrees Kelvin |
| $f_d = 10^{-\left(1825000-(78.3\times T_k)^{-1.5}\right)\times 4\times\left(\left(\frac{(0.000168\times SC)^{0.5}}{1+(0.000168\times SC)^{0.5}}\right)-0.3\times 0.000168\times SC\right)}$ | - | Divalent activity coefficient |
| $f_m = 10^{-\left(1825000-(78.3\times T_k)^{-1.5}\right)\times\left(\left(\frac{(0.000168\times SC)^{0.5}}{1+(0.000168\times SC)^{0.5}}\right)-0.3\times 0.000168\times SC\right)}$ | - | Trivalent activity coefficient |
| $f_t = 10^{-\left(1825000-(78.3\times T_k)^{-1.5}\right)\times 9\times\left(\left(\frac{(0.000168\times SC)^{0.5}}{1+(0.000168\times SC)^{0.5}}\right)-0.3\times 0.000168\times SC\right)}$ | - | Trivalent activity coefficient |
| $outALK = \left(\begin{array}{l} 2\times\frac{[CO_3]}{MW_{CO_3}}+\frac{[HCO_3]}{MW_{HCO_3}}+\frac{[OH]}{MW_{OH}}+\frac{[HS]}{MW_{HS}} \\ +2\times\frac{[S]}{MW_S}+\frac{[NH_3]}{MW_{NH_3}}-\frac{[H]}{MW_H} \end{array}\right)\times\frac{MW_{CaCO_3}}{2}$ | mg/ℓ as $CaCO_3$ | Effluent alkalinity |
| $outCH_4gas = \frac{R\times T_k}{P_{atm}\times MW_{CH_4}}\times\frac{[CH_4]}{1000}\times Q_i$ | ℓ/d | $CH_4$ gas production |
| $outCO_2gas = \frac{R\times T_k}{P_{atm}\times MW_{CO_2}}\times\frac{[CO_2]}{1000}\times Q_i$ | ℓ/d | $CO_2$ gas production |

| | | |
|---|---|---|
| $outFSA = \left( \frac{[NH_3]}{MW_{NH_3}} + \frac{[NH_4]}{MW_{NH_4}} \right) \times AW_N$ | mgN/ℓ | Total effluent free and saline ammonia |
| $outGas\,\mathrm{Pr}odtot = outCH_4gas + outCO_2gas + outH_2Sgas$ | ℓ/d | Total Gas production |
| $outH_2Saq = \frac{[H_2Saq]}{MW_{H_2S}} \times AW_S$ | mgS/ℓ | Effluent sulphide concentration |
| $outHAc\_Ac = [HAc] \times in\_f\_HAcCOD + [Ac] \times in\_f\_HAcCOD$ | mgCOD/ℓ | Total effluent acetate system |
| $outH\,\mathrm{Pr}\_\mathrm{Pr} = [H\,\mathrm{Pr}] \times in\_f\_H\,\mathrm{Pr}COD + [\mathrm{Pr}] \times in\_f\_H\,\mathrm{Pr}COD$ | mgCOD/ℓ | Total effluent propionate system |
| $outNH_3 = \frac{[NH_3]}{MW_{NH_3}} \times AW_N$ | mgN/ℓ | Effluent $NH_3$ |
| $outPO_4 = \frac{[PO_4]}{MW_{PO_4}} \times AW_P$ | mgP/ℓ | Effluent $PO_4$ |
| $outPsol = \left( \frac{[H_3PO_4]}{MW_{H_3PO_4}} + \frac{[H_2PO_4]}{MW_{H_2PO_4}} + \frac{[HPO_4]}{MW_{HPO_4}} + \frac{[PO_4]}{MW_{PO_4}} \right) \times AW_P$ | mgP/ℓ | Total effluent soluble phosphorus system |

| | | |
|---|---|---|
| $outZ_{ae} = [Z_{ae}] \times f\_C_5H_7O_2NCOD$ | mgCOD/ℓ | Effluent acetogenic biomass COD |
| $outZ_{ai} = [Z_{ai}] \times f\_C_5H_7O_2NCOD$ | mgCOD/ℓ | Effluent acidogenic biomass COD |
| $outZ_{am} = [Z_{am}] \times f\_C_5H_7O_2NCOD$ | mgCOD/ℓ | Effluent acetoclastic methanogenic biomass COD |
| $outZ_{hm} = [Z_{hm}] \times f\_C_5H_7O_2NCOD$ | mgCOD/ℓ | Effluent hydrogenotrophic methanogenic biomass COD |
| $outZ_{as} = [Z_{as}] \times f\_C_5H_7O_2NCOD$ | mgCOD/ℓ | Effluent acetoclastic sulphidogenic biomass COD |
| $outZ_{ps} = [Z_{ps}] \times f\_C_5H_7O_2NCOD$ | mgCOD/ℓ | Effluent propionate-degrading sulphidogenic biomass COD |
| $outZ_{hs} = [Z_{hs}] \times f\_C_5H_7O_2NCOD$ | mgCOD/ℓ | Effluent hydrogenotrophic sulphidogenic biomass COD |
| $pCH_4 = \frac{\frac{[CH_4]}{MW_{CH_4}}}{\frac{[CH_4]}{MW_{CH_4}} + \frac{[CO_2gas]}{MW_{CO_2}} + \frac{[H_2Sgas]}{MW_{H_2S}}}$ | - | Partial pressure of $CH_4$ gas |

| | | |
|---|---|---|
| $pK_S = \frac{2642.7}{T_k} + 10.1363$ | - | pK constant for $HS^- \leftrightarrow S^{2-} + H^+$ |
| $pK_W = 14$ | - | pK constant for dissociation of $H_2O$ |
| $pK_a = \frac{1170.5}{T_k} - 3.165 + 0.0134 \times T_k$ | - | pK constant for $HAc \leftrightarrow Ac^- + H^+$ |
| $pK_{c1} = \frac{3404.7}{T_k} - 14.8435 + 0.03279 \times T_k$ | - | pK constant for $H_2CO_3 \leftrightarrow HCO_3^- + H^+$ |
| $pK_{c2} = \frac{2902.4}{T_k} - 6.498 + 0.02379 \times T_k$ | - | pK constant for $HCO_3^- \leftrightarrow CO_3^{2-} + H^+$ |
| $pK_n = \frac{2835.8}{T_k} - 0.6322 + 0.00123 \times T_k$ | - | pK constant for $NH_4^+ \leftrightarrow NH_3 + H^+$ |
| $pK_{p1} = \frac{799.3}{T_k} - 4.5535 + 0.01349 \times T_k$ | - | pK constant for $H_3PO_4 \leftrightarrow H_2PO_4^- + H^+$ |
| $pK_{p2} = \frac{1979.5}{T_k} - 5.3541 + 0.01984 \times T_k$ | - | pK constant for $H_2PO_4^- \leftrightarrow HPO_4^{2-} + H^+$ |
| $pK_{p3} = 12.023$ | - | pK constant for $HPO_4^{2-} \leftrightarrow PO_4^{3-} + H^+$ |

**Table B-2:** Influent characterisation for steady state numbers 1-11

| Steady state number | 1 | 2 | 3 | 4 | 5 | 6 | 7 | 8 | 9 | 10 | 11 |
|---|---|---|---|---|---|---|---|---|---|---|---|
| **Feed batch number** | F12 | F12 | F12 | F12 | F12 | F12 | F13 | F13 | F13 | F13 | F13 |
| **Reactor volume (ℓ)** | 16 | 16 | 20 | 20 | 20 | 16 | 16 | 16 | 16 | 20 | 20 |
| **Retention time (d)** | 10 | 8 | 20 | 15 | 15 | 10 | 6.67 | 5.71 | 5 | 15 | 15 |
| **Flowrate (ℓ/d)** | 1.6 | 2 | 1 | 1.33 | 1.33 | 1.6 | 2.40 | 2.80 | 3.2 | 1.33 | 1.33 |
| $H_20$ (g/d) | 1600 | 2000 | 1000 | 1333.33 | 1333.33 | 1600 | 2398.80 | 2802.10 | 3200 | 1333.33 | 1333.33 |
| **pH** | 4.91 | 4.91 | 4.91 | 4.91 | 4.91 | 4.91 | 5.73 | 5.73 | 5.73 | 5.73 | 5.73 |
| $H^+$ (g/d) | 1.98E-05 | 2.48E-05 | 1.24E-05 | 1.65E-05 | 1.65E-05 | 1.98E-05 | 4.50E-06 | 5.26E-06 | 6.01E-06 | 2.50E-06 | 2.50E-06 |
| $OH^-$ (g/d) | 2.21E-08 | 2.76E-08 | 1.38E-08 | 1.84E-08 | 1.84E-08 | 2.21E-08 | 2.19E-07 | 2.56E-07 | 2.92E-07 | 1.22E-07 | 1.22E-07 |
| **$S_{VFAi}$ (mg COD/ℓ)** | 4000 | 1740 | 1775 | 1900 | 1060 | 4000 | 1260 | 1250 | 1196 | 1830 | 2020 |
| $Ac^-$ (g/d) | 3.53E+00 | 1.92E+00 | 9.78E-01 | 1.40E+00 | 7.79E-01 | 3.53E+00 | 2.56E+00 | 2.97E+00 | 3.25E+00 | 2.07E+00 | 2.28E+00 |
| HAc (g/d) | 2.52E+00 | 1.37E+00 | 6.99E-01 | 9.98E-01 | 5.57E-01 | 2.52E+00 | 2.77E-01 | 3.21E-01 | 3.51E-01 | 2.24E-01 | 2.47E-01 |
| $Pr^-$ (g/d) | 0 | 0 | 0 | 0 | 0 | 0 | 0 | 0 | 0 | 0 | 0 |
| HPr (g/d) | 0 | 0 | 0 | 0 | 0 | 0 | 0 | 0 | 0 | 0 | 0 |
| **FSA (mg N/ℓ)** | 39 | 39 | 39 | 39 | 20 | 39 | 106 | 124 | 131 | 180 | 198 |
| $NH_3$ (g/d) | 3.45E-06 | 4.32E-06 | 2.16E-06 | 2.88E-06 | 1.48E-06 | 3.45E-06 | 9.29E-05 | 1.27E-04 | 1.53E-04 | 8.77E-05 | 9.65E-05 |
| $NH_4^+$ (g/d) | 8.04E-02 | 1.00E-01 | 5.02E-02 | 6.70E-02 | 3.43E-02 | 8.04E-02 | 3.27E-01 | 4.47E-01 | 5.40E-01 | 3.09E-01 | 3.40E-01 |
| **Alkalinity (mg/ℓ as $CaCO_3$)** | 47.3 | 47.3 | 47.3 | 47.3 | 47.3 | 47.3 | 151.6 | 151.6 | 151.6 | 151.6 | 151.6 |
| $CO_3^{2-}$ (g/d) | 3.50E-07 | 4.38E-07 | 2.19E-07 | 2.92E-07 | 2.92E-07 | 3.50E-07 | 1.10E-05 | 1.28E-05 | 1.47E-05 | 6.11E-06 | 6.11E-06 |
| $HCO_3^-$ (g/d) | 9.35E-02 | 1.17E-01 | 5.84E-02 | 7.79E-02 | 7.79E-02 | 9.35E-02 | 4.44E-01 | 5.18E-01 | 5.92E-01 | 2.47E-01 | 2.47E-01 |
| $H_2CO_3$ (g/d) | 2.69 | 3.36 | 1.68 | 2.24 | 2.24 | 2.69 | 1.93 | 2.26 | 2.58 | 1.07 | 1.07 |
| **Sulphate (mg/ℓ)** | 0 | 0 | 0 | 0 | 0 | 1000 | 0 | 0 | 0 | 0 | 0 |
| $SO_4^{2+}$ (g/d) | 0 | 0 | 0 | 0 | 0 | 1.6 | 0 | 0 | 0 | 0 | 0 |
| **COD Fractionation** | | | | | | | | | | | |
| $S_{bp}$ (mg COD/ℓ) | 14940.72 | 14596.72 | 14945.72 | 14624.72 | 7630.78 | 14624.72 | 14531.31 | 14107.88 | 13864.31 | 22959.25 | 22490.25 |
| $S_{bp}$ (g COD/d) | 23.91 | 29.19 | 14.95 | 19.50 | 10.17 | 23.40 | 34.86 | 39.53 | 44.37 | 30.61 | 29.99 |
| $S_{up}$ (mg COD/ℓ) | 8681.28 | 8681.28 | 8681.28 | 8681.28 | 4555.22 | 8681.28 | 8322.69 | 8349.12 | 8322.69 | 13309.76 | 13309.76 |
| $S_{up}$ (g COD/d) | 13.89 | 17.36 | 8.68 | 11.58 | 6.07 | 13.89 | 19.96 | 23.40 | 26.63 | 17.75 | 17.75 |
| $S_{bs}$ (mg COD/ℓ) | 1076 | 1253 | 1073 | 1245 | 668 | 1076 | 914 | 1149 | 1196 | 1635 | 1846 |
| $S_{bs}$ (g/d) | 1.62 | 2.35 | 1.01 | 1.56 | 0.84 | 1.62 | 2.06 | 3.02 | 3.59 | 2.05 | 2.31 |
| $S_{us}$ (mg COD/ℓ) | 178 | 168 | 179 | 157 | 97 | 178 | 200 | 205 | 301 | 250 | 299 |
| $S_{us}$ (g COD/d) | 2.85E-01 | 3.36E-01 | 1.79E-01 | 2.09E-01 | 1.29E-01 | 2.85E-01 | 4.80E-01 | 5.74E-01 | 9.63E-01 | 3.33E-01 | 3.99E-01 |

**Table B-4:** Influent characterisation for steady state numbers 24-28, 31, 36, 41, 42, 46 and 47

| Steady state number | 24 | 25 | 26 | 27 | 28 | 31 | 36 | 41 | 42 | 46 | 47 |
|---|---|---|---|---|---|---|---|---|---|---|---|
| **Feed batch number** | F14 | F14 | F14 | F15 | F15 | F15 | F15 | F15 | F15 | F15 | F15 |
| **Reactor volume (ℓ)** | 20 | 20 | 20 | 16 | 20 | 20 | 16 | 20 | 20 | 20 | 16 |
| **Retention time (d)** | 6.67 | 10 | 8 | 8 | 5.71 | 5.71 | 8 | 16 | 13.3 | 10 | 8 |
| **Flowrate (ℓ/d)** | 3.00 | 2 | 2.5 | 2 | 3.50 | 3.50 | 2 | 1.25 | 1.50 | 2 | 2 |
| $H_20$ (g/d) | 2998.50 | 2000 | 2500 | 2000 | 3502.63 | 3502.63 | 2000 | 1250 | 1503.76 | 2000 | 2000 |
| **pH** | 5.38 | 5.38 | 5.38 | 5.38 | 5.38 | 5.38 | 5.38 | 5.38 | 5.38 | 5.38 | 5.38 |
| $H^+$ (g/d) | 1.26E-05 | 8.40E-06 | 1.05E-05 | 8.40E-06 | 1.47E-05 | 1.47E-05 | 8.40E-06 | 5.25E-06 | 6.32E-06 | 8.40E-06 | 8.40E-06 |
| $OH^-$ (g/d) | 1.22E-07 | 8.16E-08 | 1.02E-07 | 8.16E-08 | 1.43E-07 | 1.43E-07 | 8.16E-08 | 5.10E-08 | 6.13E-08 | 8.16E-08 | 8.16E-08 |
| **$S_{VFAi}$ (mg COD/ℓ)** | 875 | 111 | 116 | 104 | 1144 | 418 | 116 | 98 | 104 | 47 | 94 |
| $Ac^-$ (g/d) | 1.99E+00 | 1.68E-01 | 2.20E-01 | 1.58E-01 | 3.04E+00 | 1.11E+00 | 1.76E-01 | 9.28E-02 | 1.19E-01 | 7.12E-02 | 1.42E-01 |
| HAc (g/d) | 4.82E-01 | 4.07E-02 | 5.32E-02 | 3.82E-02 | 7.35E-01 | 2.69E-01 | 4.26E-02 | 2.25E-02 | 2.87E-02 | 1.73E-02 | 3.45E-02 |
| $Pr^-$ (g/d) | 0 | 0 | 0 | 0 | 0 | 0 | 0 | 0 | 0 | 0 | 0 |
| HPr (g/d) | 0 | 0 | 0 | 0 | 0 | 0 | 0 | 0 | 0 | 0 | 0 |
| **FSA (mg N/ℓ)** | 37 | 5 | 7 | 8 | 40 | 18 | 13 | 6 | 10 | 7 | 4 |
| $NH_3$ (g/d) | 1.81E-05 | 1.63E-06 | 2.86E-06 | 2.61E-06 | 2.29E-05 | 1.03E-05 | 4.25E-06 | 1.22E-06 | 2.46E-06 | 2.29E-06 | 1.31E-06 |
| $NH_4^+$ (g/d) | 1.43E-01 | 1.29E-02 | 2.25E-02 | 2.06E-02 | 1.80E-01 | 8.12E-02 | 3.35E-02 | 9.66E-03 | 1.94E-02 | 1.80E-02 | 1.03E-02 |
| **Alkalinity (mg/ℓ as $CaCO_3$)** | 90.28 | 90.28 | 90.28 | 90.28 | 90.28 | 90.28 | 90.28 | 90.28 | 90.28 | 90.28 | 90.28 |
| $CO_3^{2-}$ (g/d) | 3.66E-06 | 2.44E-06 | 3.05E-06 | 2.44E-06 | 4.28E-06 | 4.28E-06 | 2.44E-06 | 1.53E-06 | 1.84E-06 | 2.44E-06 | 2.44E-06 |
| $HCO_3^-$ (g/d) | 3.31E-01 | 2.21E-01 | 2.76E-01 | 2.21E-01 | 3.86E-01 | 3.86E-01 | 2.21E-01 | 1.38E-01 | 1.66E-01 | 2.21E-01 | 2.21E-01 |
| $H_2CO_3$ (g/d) | 3.22 | 2.15 | 2.69 | 2.15 | 3.76 | 3.76 | 2.15 | 1.34 | 1.62 | 2.15 | 2.15 |
| **Sulphate (mg/ℓ)** | 0 | 0 | 0 | 0 | 0 | 0 | 2000 | 2000 | 2000 | 2000 | 2000 |
| $SO_4^{2+}$ (g/d) | 0 | 0 | 0 | 0 | 0 | 0 | 4 | 2.5 | 3.01 | 4 | 4 |
| **COD Fractionation** | | | | | | | | | | | |
| $S_{bp}$ (mg COD/ℓ) | 7191.82 | 1043.73 | 1013.73 | 1118.31 | 24996.99 | 7819.28 | 1013.73 | 1127.32 | 1118.31 | 556.18 | 1061.45 |
| $S_{bp}$ (g COD/d) | 21.56 | 2.09 | 2.53 | 2.24 | 87.56 | 27.39 | 2.03 | 1.41 | 1.68 | 1.11 | 2.12 |
| $S_{up}$ (mg COD/ℓ) | 4542.18 | 652.28 | 652.28 | 674.69 | 13862.01 | 4410.72 | 652.28 | 672.68 | 674.69 | 330.82 | 635.55 |
| $S_{up}$ (g COD/d) | 13.62 | 1.30 | 1.63 | 1.35 | 48.55 | 15.45 | 1.30 | 0.84 | 1.01 | 0.66 | 1.27 |
| $S_{bs}$ (mg COD/ℓ) | 875 | 111 | 116 | 104 | 1144 | 418 | 116 | 98 | 104 | 47 | 94 |
| $S_{bs}$ (g/d) | 2.46 | 0.21 | 0.27 | 0.20 | 3.76 | 1.37 | 0.22 | 0.11 | 0.15 | 0.09 | 0.18 |
| $S_{us}$ (mg COD/ℓ) | 96 | 32 | 51 | 16 | 295 | 120 | 51 | 16 | 16 | 8 | 15 |
| $S_{us}$ (g COD/d) | 2.88E-01 | 6.40E-02 | 1.28E-01 | 3.20E-02 | 1.03E+00 | 4.20E-01 | 1.02E-01 | 2.00E-02 | 2.41E-02 | 1.60E-02 | 3.00E-02 |

# APPENDIX C

## SIMULATION RESULTS OF MODELLING STEADY STATE EXPERIMENTS

### Steady State Number 1

**Table C-1:** Operating conditions for steady state number 1

| | |
|---|---|
| **Feed Batch Number** | F12 |
| **Reactor Volume (ℓ)** | 16 |
| **Retention Time (d)** | 10 |
| **pH** | steady state |
| **Biological Groups Present** | acidogenic, acetogenic and methanogenic |

**Table C-2:** Results summary for steady state number 1

| | Measured | Model | Relative error (%) |
|---|---|---|---|
| **Feed Total COD (mg COD/ℓ)** | 25952 | 28876 | - |
| **Feed Soluble COD (mg COD/ℓ)** | 2330 | 5254 | - |
| **Feed TKN (mg N/ℓ)** | 482 | 482 | - |
| **Feed FSA (mg N/ℓ)** | 39 | 39 | - |
| **Effluent Total COD (mg COD/ℓ)** | 10849 ± 304 | 11079.48 | 2.08 |
| **Effluent Soluble COD (mg COD/ℓ)** | 178 ± 14 | 215.73 | 17.49 |
| **Reactor pH** | 7.00 ± 0.01 | 6.83 | -2.55 |
| **Effluent VFA (mg HAc/ℓ)** | 24 ± 14 | 1.01 | -2276.68 |
| **Effluent Alkalinity (mg/ℓ as $CaCO_3$)** | 2424 ± 127 | 2475.25 | 2.07 |
| **Sulphate Addition (mg SO4/ℓ)** | 0 | 0 | - |
| **Effluent Sulphate (mg SO4/ℓ)** | 0 | 0 | - |
| **% Sulphate Conversion** | - | - | - |
| **Methane Production (ℓ/d)** | 10.69 | 12.23 | 12.57 |

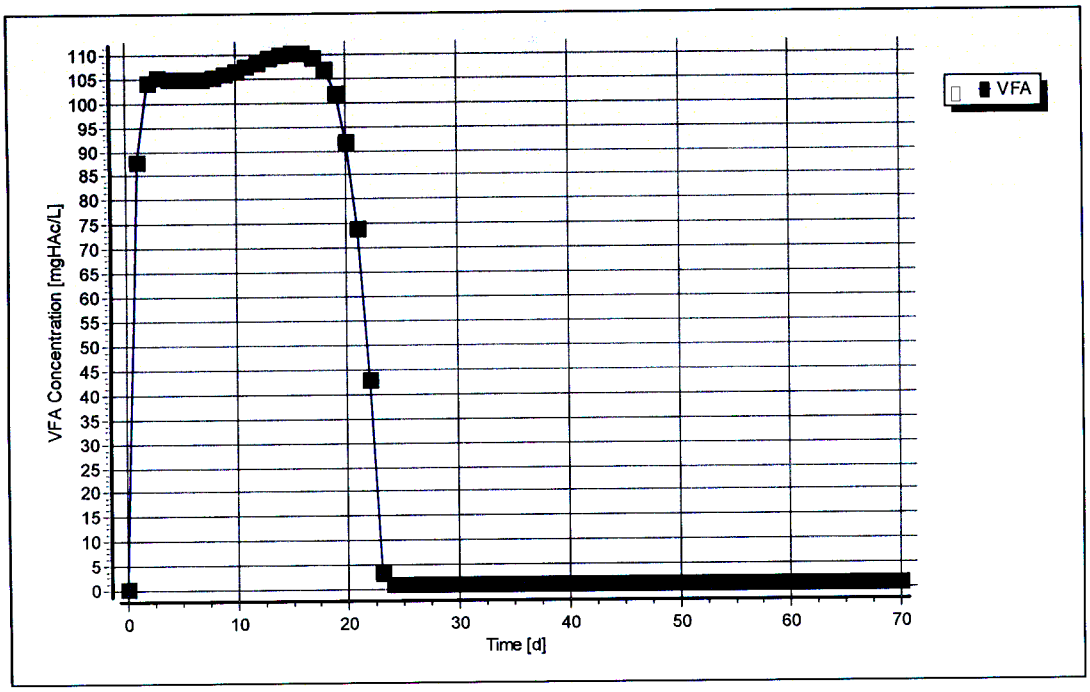


**Figure C-2:** Simulated VFA concentration profile for steady state number 1

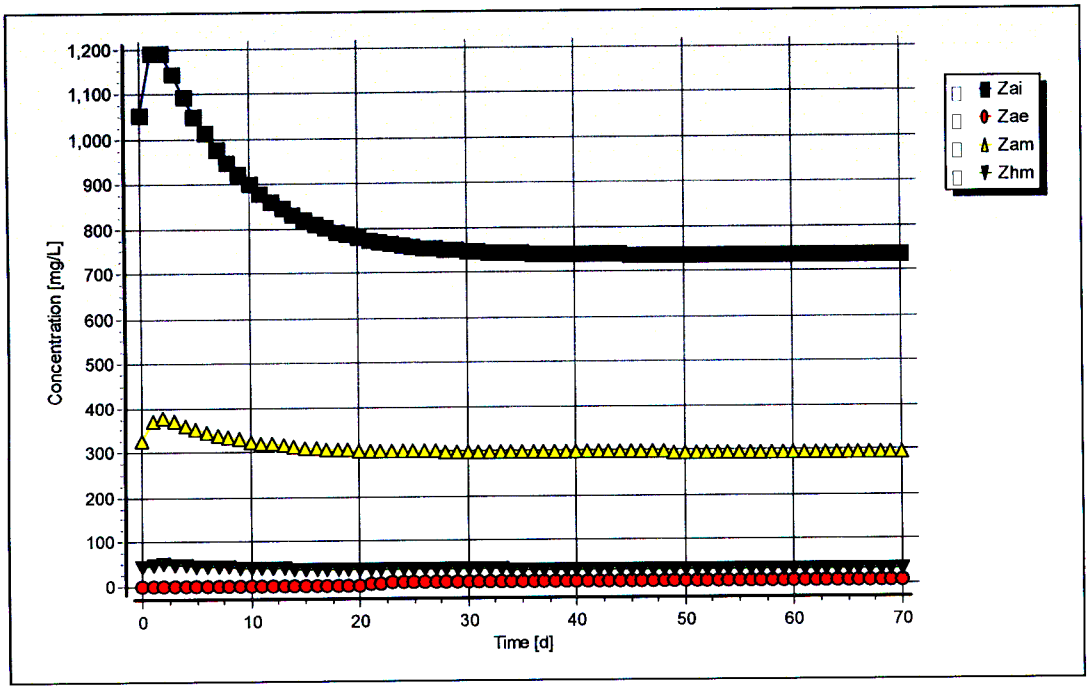


**Figure C-3:** Simulated biomass concentration profiles for steady state number 1

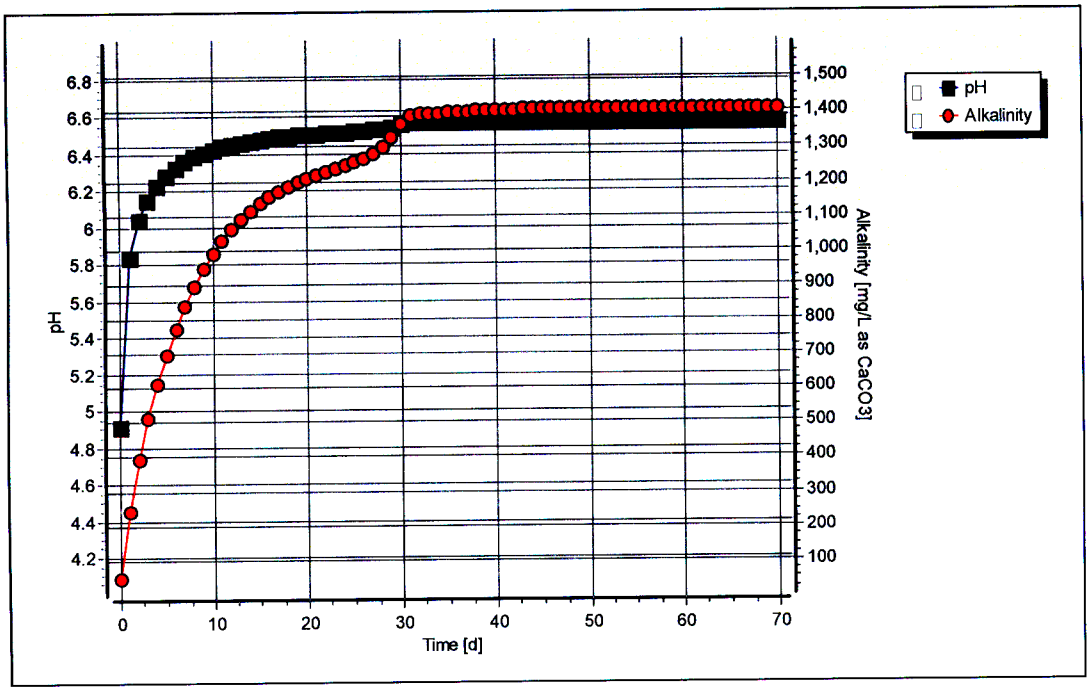


**Figure C-4:** Simulated pH and alkalinity profiles for steady state number 2

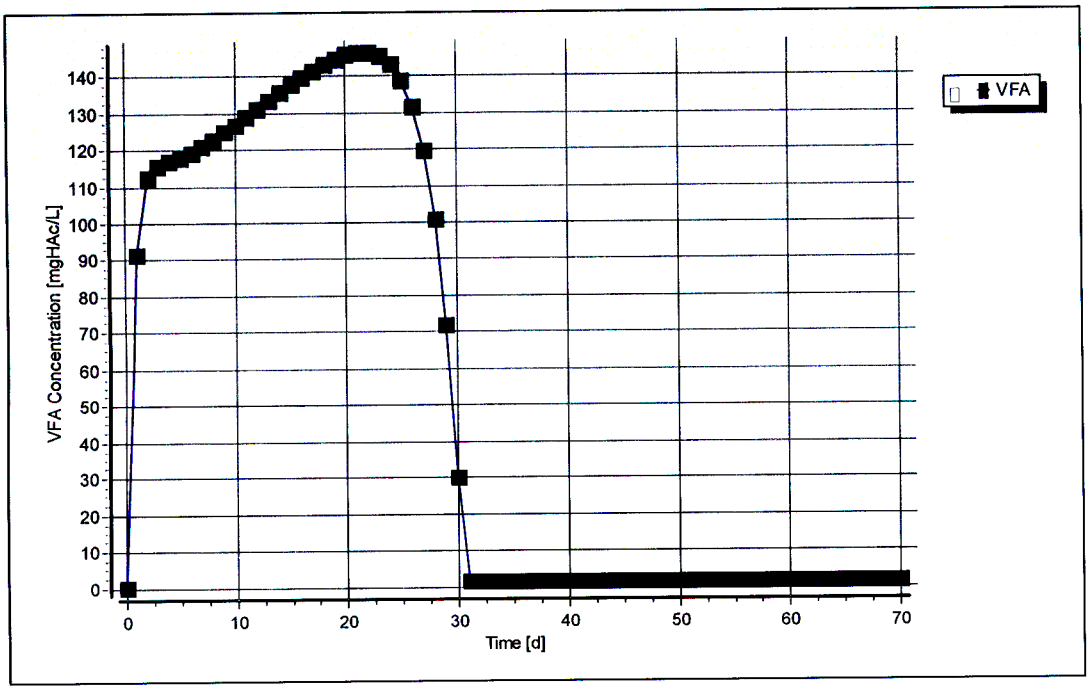


**Figure C-5:** Simulated VFA concentration profile for steady state number 2

## Steady State Number 3

**Table C-5:** Operating conditions for steady state number 3

| | |
|---|---|
| **Feed Batch Number** | F12 |
| **Reactor Volume (ℓ)** | 20 |
| **Retention Time (d)** | 20 |
| **pH** | steady state |
| **Biological Groups Present** | acidogenic, acetogenic and methanogenic |

**Table C-6:** Results summary for steady state number 3

| | **Measured** | **Model** | **Relative error (%)** |
|---|---|---|---|
| **Feed Total COD (mg COD/ℓ)** | 25952 | 26654 | - |
| **Feed Soluble COD (mg COD/ℓ)** | 2325 | 3027 | - |
| **Feed TKN (mg N/ℓ)** | 482 | 482 | - |
| **Feed FSA (mg N/ℓ)** | 39 | 39 | - |
| **Effluent Total COD (mg COD/ℓ)** | 10525 ± 166 | 10402.06 | -1.18 |
| **Effluent Soluble COD (mg COD/ℓ)** | 179 ± 8 | 200.76 | 10.84 |
| **Reactor pH** | 6.89 ± 0.02 | 6.62 | -4.08 |
| **Effluent VFA (mg HAc/ℓ)** | 11 ± 7 | 0.60 | -1724.48 |
| **Effluent Alkalinity (mg/ℓ as $CaCO_3$)** | 1577 ± 20 | 1576.84 | -0.01 |
| **Sulphate Addition (mg SO4/ℓ)** | 0 | 0 | - |
| **Effluent Sulphate (mg SO4/ℓ)** | 0 | 0 | - |
| **% Sulphate Conversion** | - | - | - |
| **Methane Production (ℓ/d)** | 5.41 | 7.05 | 23.29 |
| **Gas Composition (% $CH_4$)** | 63.11 | 58.70 | -7.52 |
| **Effluent FSA (mg N/ℓ)** | 231 ± 6 | 240.00 | 3.75 |
| **Effluent TKN (mg N/ℓ)** | 518 ± 6 | 516.39 | -0.31 |

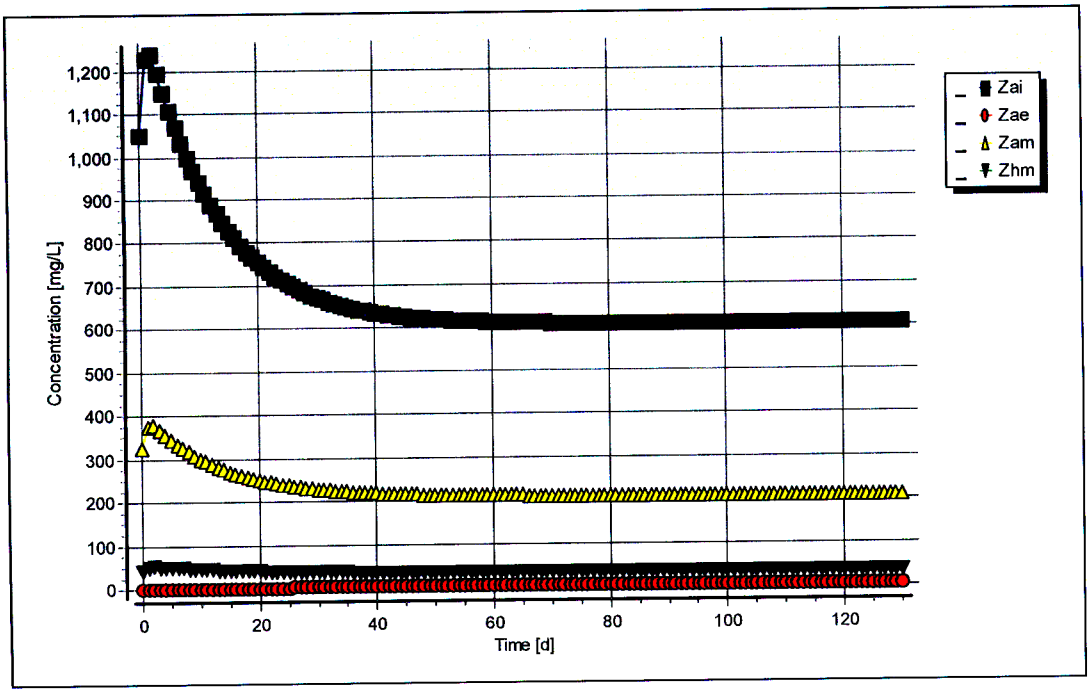


**Figure C-9:** Simulated biomass concentration profiles for steady state number 3

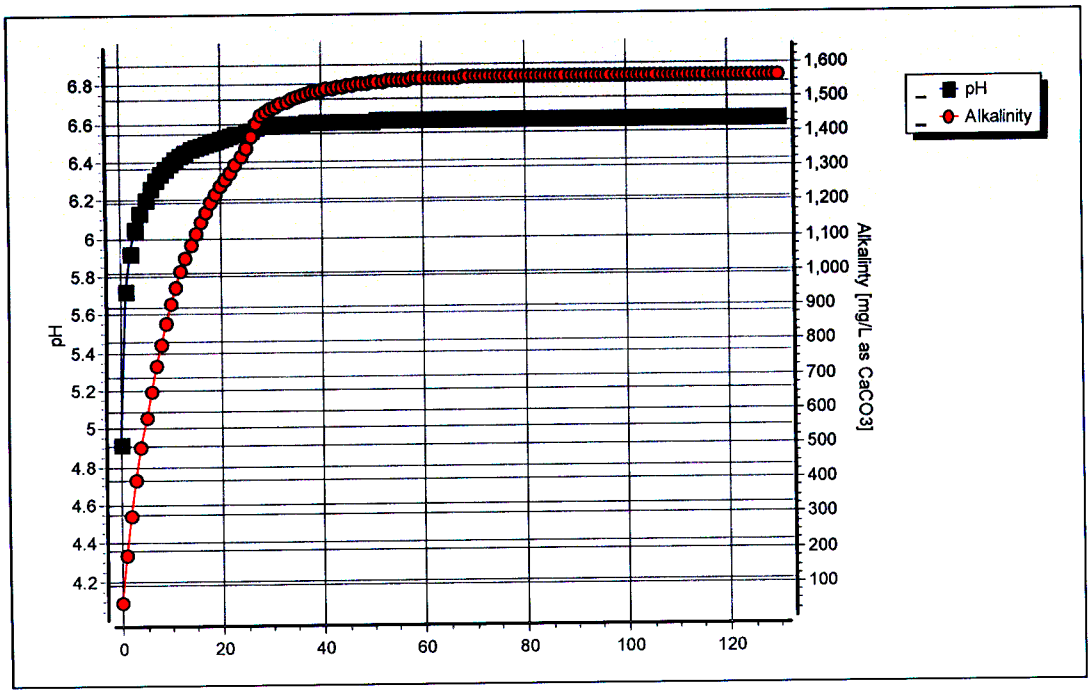


**Figure C-10:** Simulated pH and alkalinity profiles for steady state number 4

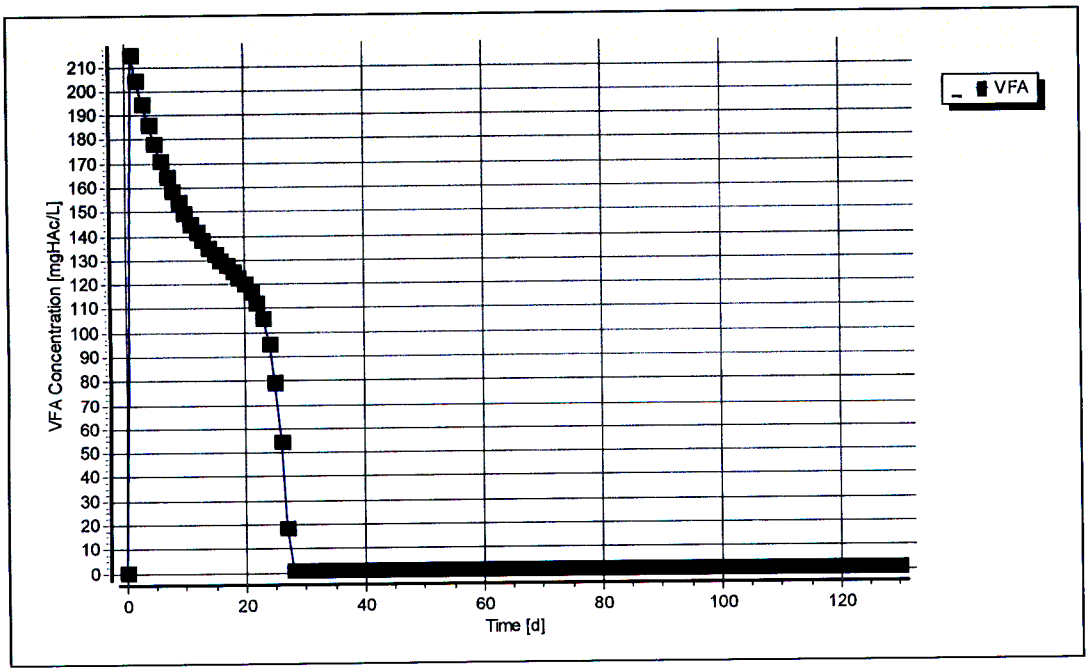


**Figure C-11:** Simulated VFA concentration profile for steady state number 4

## Steady State Number 5

**Table C-9:** Operating conditions for steady state number 5

| | |
|---|---|
| **Feed Batch Number** | F12 |
| **Reactor Volume (ℓ)** | 20 |
| **Retention Time (d)** | 15 |
| **pH** | steady state |
| **Biological Groups Present** | acidogenic, acetogenic and methanogenic |

**Table C-10:** Results summary for steady state number 5

| | Measured | Model | Relative error (%) |
|---|---|---|---|
| **Feed Total COD (mg COD/ℓ)** | 13619 | 14011 | - |
| **Feed Soluble COD (mg COD/ℓ)** | 1433 | 1825 | - |
| **Feed TKN (mg N/ℓ)** | 253 | 253 | - |
| **Feed FSA (mg N/ℓ)** | 20 | 20 | - |
| **Effluent Total COD (mg COD/ℓ)** | 5751 ± 106 | 5711.95 | -0.68 |
| **Effluent Soluble COD (mg COD/ℓ)** | 97 ± 3 | 129.93 | 25.34 |
| **Reactor pH** | 6.80 ± 0.02 | 6.34 | -7.26 |
| **Effluent VFA (mg HAc/ℓ)** | 6 ± 6 | 1.38 | -333.39 |
| **Effluent Alkalinity (mg/ℓ as $CaCO_3$)** | 845 ± 22 | 854.83 | 1.15 |
| **Sulphate Addition (mg SO4/ℓ)** | 0 | 0 | - |
| **Effluent Sulphate (mg SO4/ℓ)** | 0 | 0 | - |
| **% Sulphate Conversion** | - | - | - |
| **Methane Production (ℓ/d)** | 3.95 | 4.83 | 18.25 |
| **Gas Composition (% $CH_4$)** | 63.26 | 57.01 | -10.96 |
| **Effluent FSA (mg N/ℓ)** | 114 ± 3 | 111.53 | -2.21 |
| **Effluent TKN (mg N/ℓ)** | 294 ± 7 | 259.35 | -13.36 |

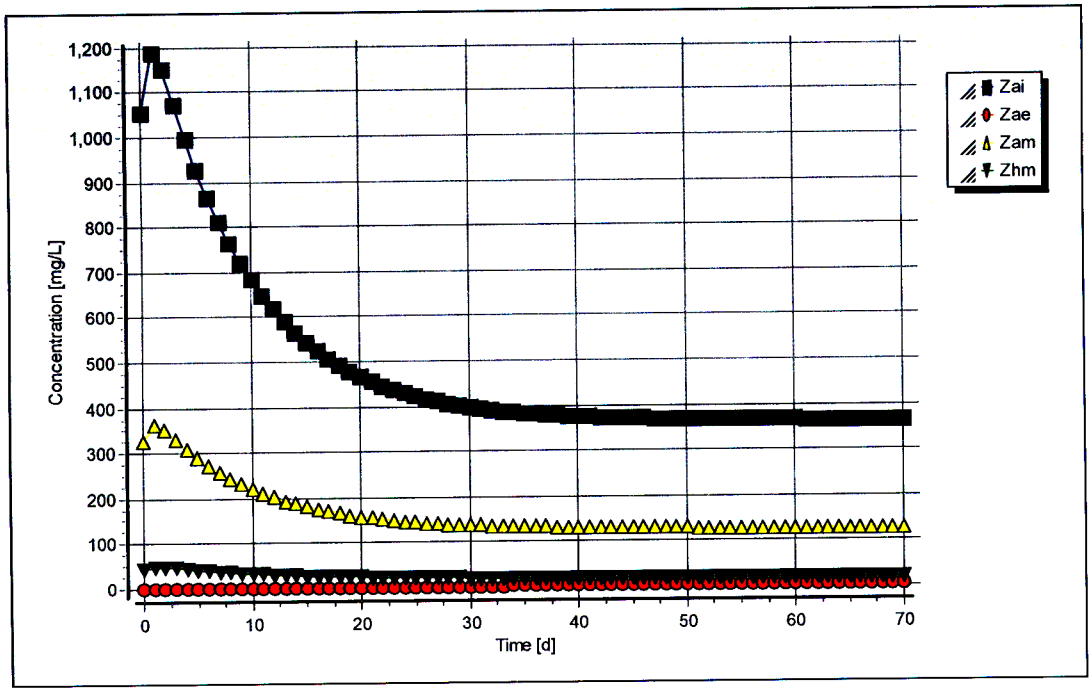


**Figure C-15:** Simulated biomass concentration profiles for steady state number 5

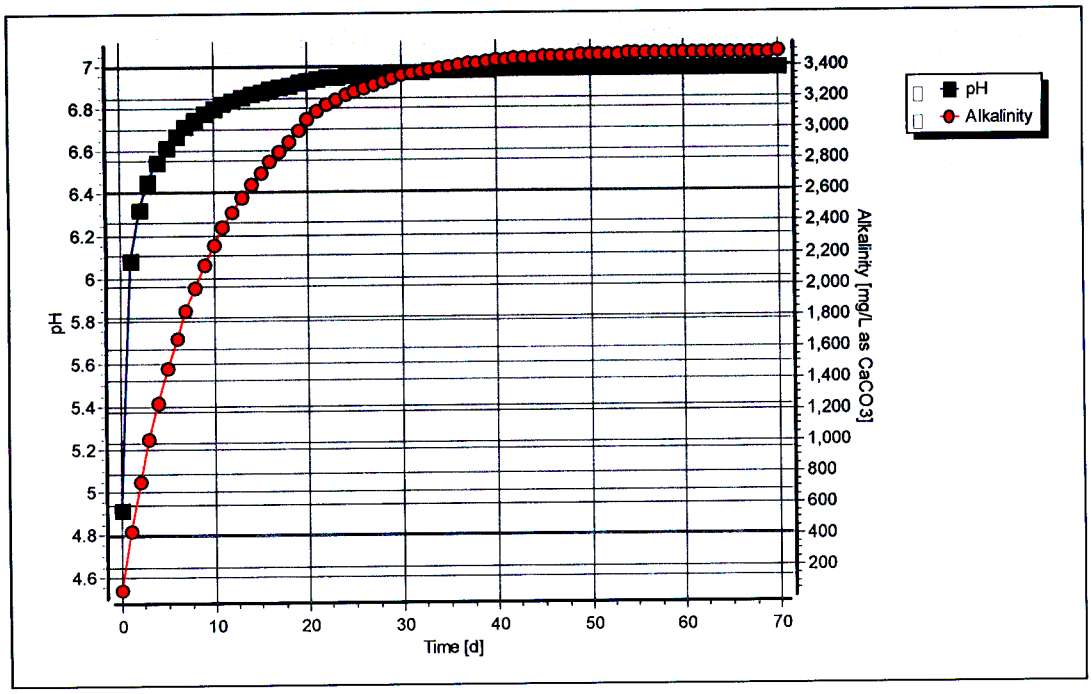


**Figure C-16:** Simulated pH and alkalinity profiles for steady state number 6

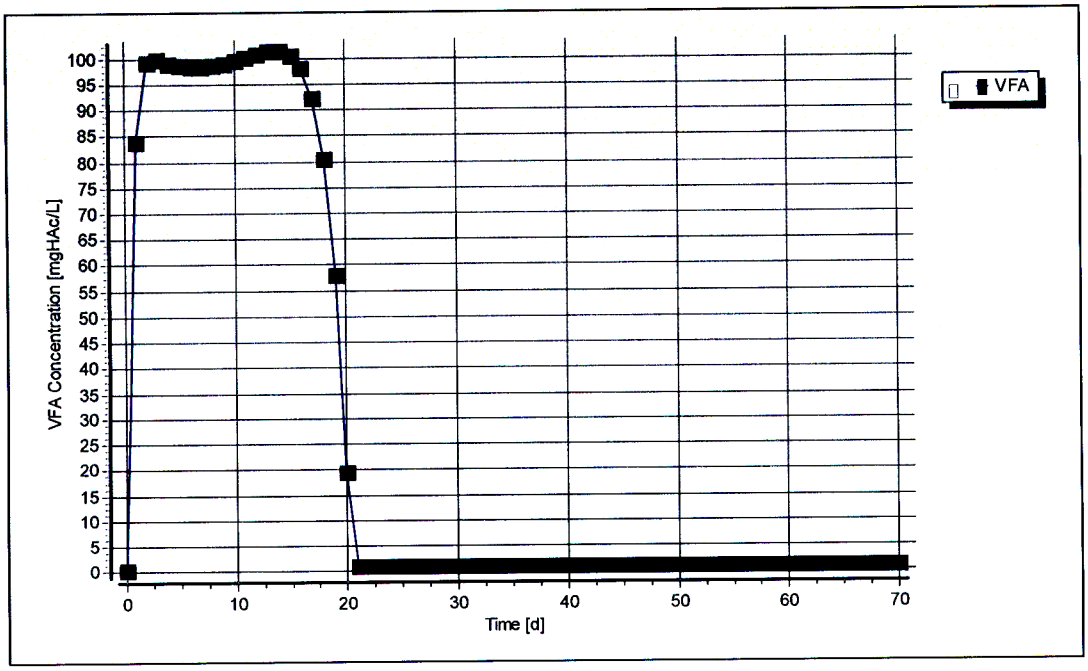


**Figure C-17:** Simulated VFA concentration profile for steady state number 6

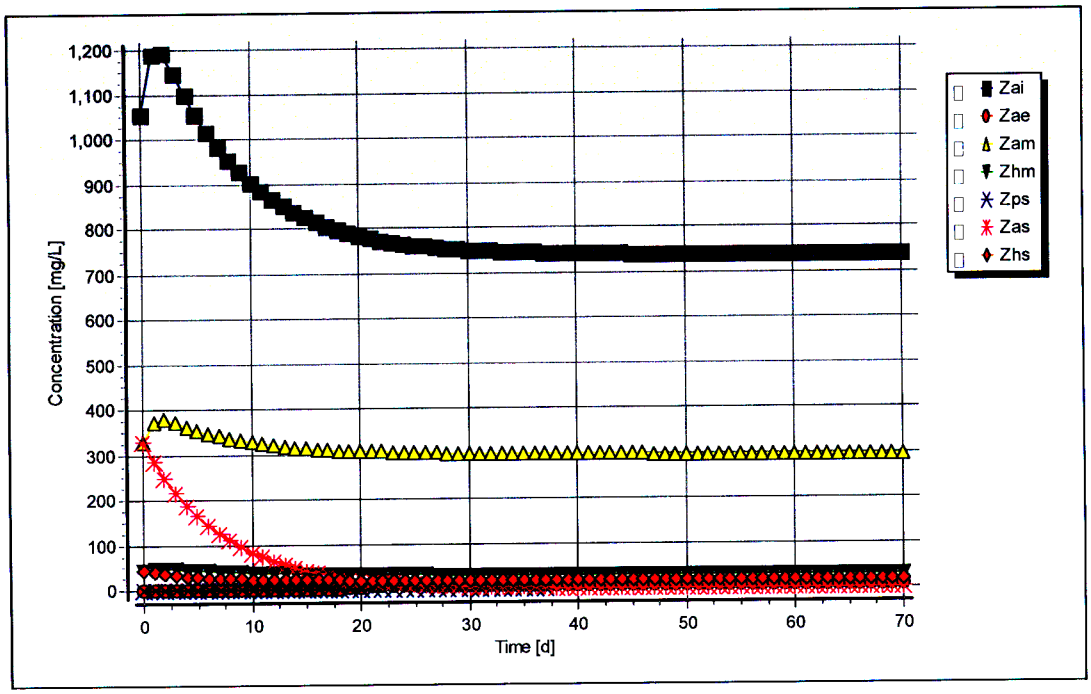


**Figure C-20:** Simulated biomass concentration profiles for steady state number 6

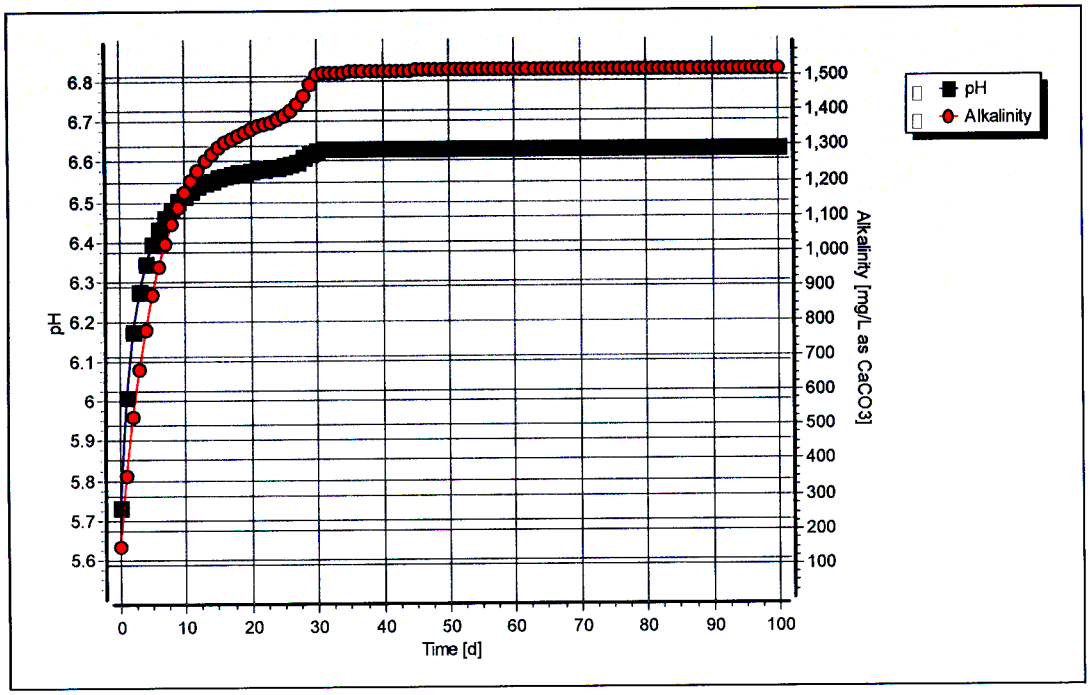


**Figure C-21:** Simulated pH and alkalinity profiles for steady state number 7

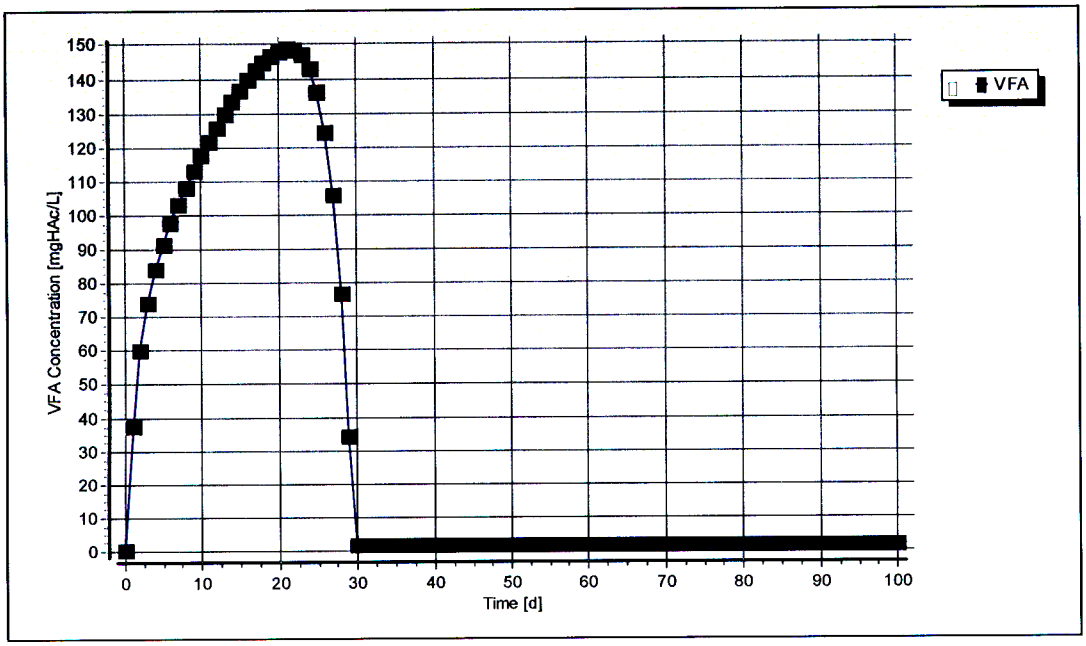


**Figure C-22:** Simulated VFA concentration profile for steady state number 7

## Steady State Number 8

**Table C-15:** Operating conditions for steady state number 8

| | |
|---|---|
| **Feed Batch Number** | F13 |
| **Reactor Volume (ℓ)** | 16 |
| **Retention Time (d)** | 5.71 |
| **pH** | steady state |
| **Biological Groups Present** | acidogenic, acetogenic and methanogenic |

**Table C-16:** Results summary for steady state number 8

| | **Measured** | **Model** | **Relative error (%)** |
|---|---|---|---|
| **Feed Total COD (mg COD/ℓ)** | 24960 | 25061 | - |
| **Feed Soluble COD (mg COD/ℓ)** | 2503 | 2604 | - |
| **Feed TKN (mg N/ℓ)** | 616 | 616 | - |
| **Feed FSA (mg N/ℓ)** | 124 | 124 | - |
| **Effluent Total COD (mg COD/ℓ)** | 12729 ± 297 | 12713.84 | -0.12 |
| **Effluent Soluble COD (mg COD/ℓ)** | 205 ± 12 | 273.94 | 25.17 |
| **Reactor pH** | 6.93 ± 0.01 | 6.62 | -4.74 |
| **Effluent VFA (mg HAc/ℓ)** | 32 ± 10 | 2.38 | -1242.13 |
| **Effluent Alkalinity (mg/ℓ as $CaCO_3$)** | 1463 ± 16 | 1470.85 | 0.53 |
| **Sulphate Addition (mg SO4/ℓ)** | 0 | 0 | - |
| **Effluent Sulphate (mg SO4/ℓ)** | 0 | 0 | - |
| **% Sulphate Conversion** | - | - | - |
| **Methane Production (ℓ/d)** | 13.24 | 15.01 | 11.79 |
| **Gas Composition (% $CH_4$)** | 61.67 | 61.37 | -0.49 |
| **Effluent FSA (mg N/ℓ)** | 200 ± 4 | 246.47 | 18.85 |
| **Effluent TKN (mg N/ℓ)** | 574 ± 6 | 538.51 | -6.59 |

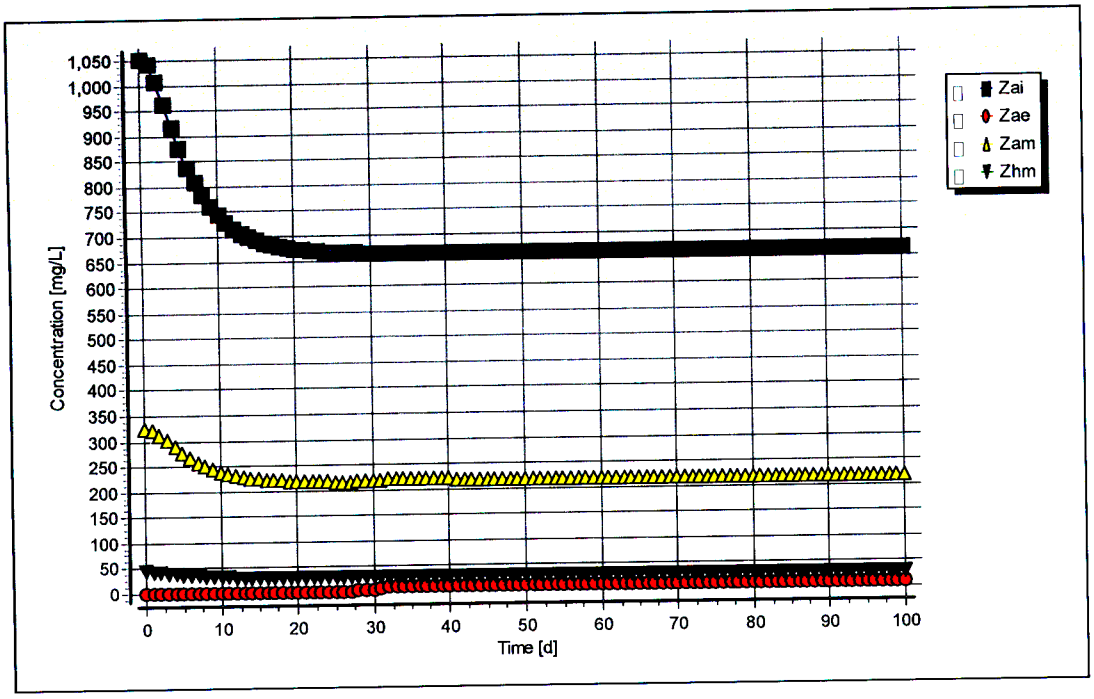


**Figure C-26:** Simulated biomass concentration profiles for steady state number 8

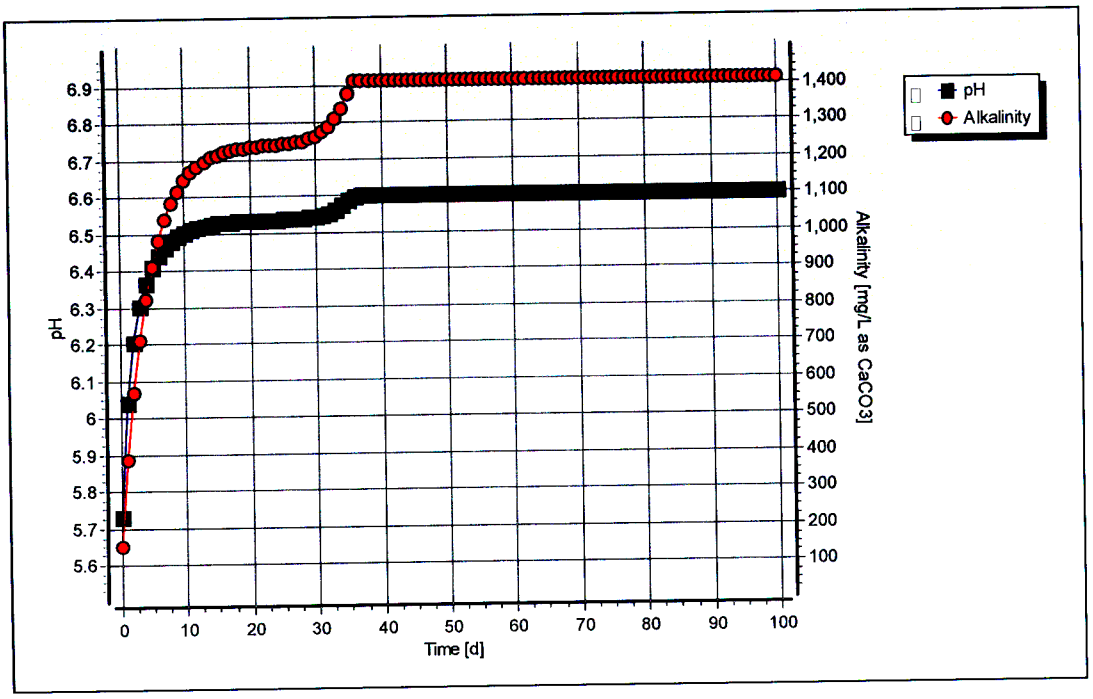


**Figure C-27:** Simulated pH and alkalinity profiles for steady state number 9

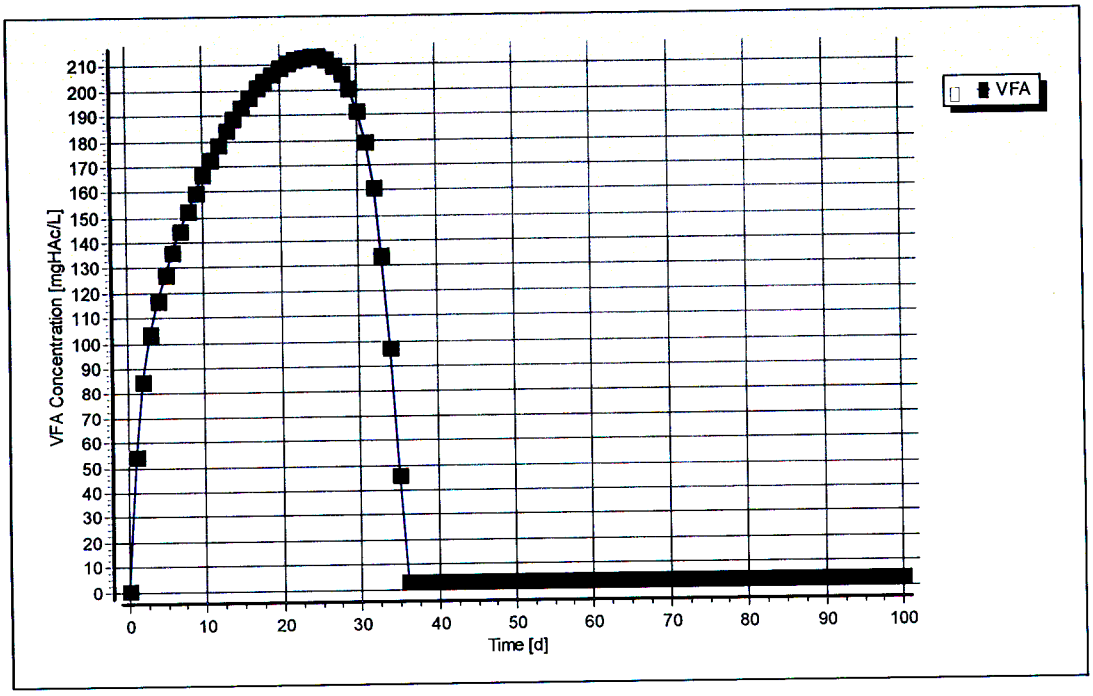


**Figure C-28:** Simulated VFA concentration profile for steady state number 9

## Steady State Number 10

**Table C-19:** Operating conditions for steady state number 10

| | |
|---|---|
| **Feed Batch Number** | F13 |
| **Reactor Volume (ℓ)** | 20 |
| **Retention Time (d)** | 15 |
| **pH** | steady state |
| **Biological Groups Present** | acidogenic, acetogenic and methanogenic |

**Table C-20:** Results summary for steady state number 10

| | Measured | Model | Relative error (%) |
|---|---|---|---|
| **Feed Total COD (mg COD/ℓ)** | 39789 | 39984 | - |
| **Feed Soluble COD (mg COD/ℓ)** | 3520 | 3715 | - |
| **Feed TKN (mg N/ℓ)** | 982 | 982 | - |
| **Feed FSA (mg N/ℓ)** | 180 | 180 | - |
| **Effluent Total COD (mg COD/ℓ)** | 16972 ± 322 | 17033.63 | 0.36 |
| **Effluent Soluble COD (mg COD/ℓ)** | 250 ± 7 | 276.86 | 9.70 |
| **Reactor pH** | 6.98 ± 0.02 | 6.83 | -2.16 |
| **Effluent VFA (mg HAc/ℓ)** | 28 ± 7 | 0.67 | -4093.73 |
| **Effluent Alkalinity (mg/ℓ as $CaCO_3$)** | 2446 ± 25 | 2442.00 | -0.16 |
| **Sulphate Addition (mg SO4/ℓ)** | 0 | 0 | - |
| **Effluent Sulphate (mg SO4/ℓ)** | 0 | 0 | - |
| **% Sulphate Conversion** | - | - | - |
| **Methane Production (ℓ/d)** | 12.12 | 13.30 | 8.86 |
| **Gas Composition (% $CH_4$)** | 61.4 | 61.11 | -0.47 |
| **Effluent FSA (mg N/ℓ)** | 347 ± 8 | 459.10 | 24.42 |
| **Effluent TKN (mg N/ℓ)** | 854 ± 14 | 893.84 | 4.46 |

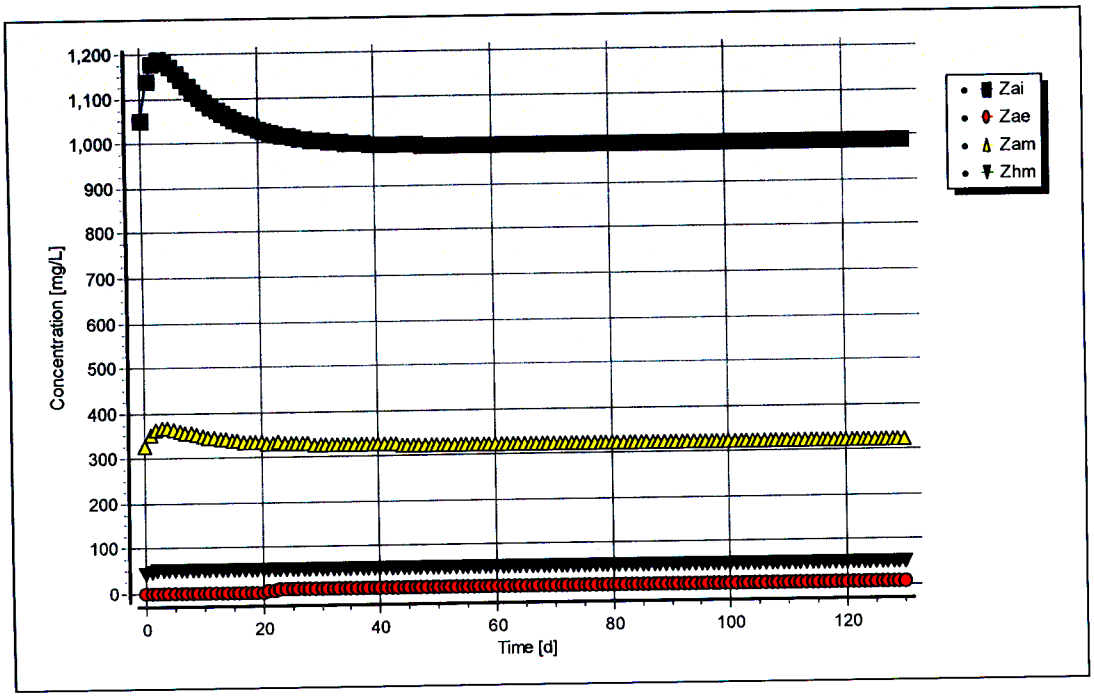


**Figure C-32:** Simulated biomass concentration profiles for steady state number 10

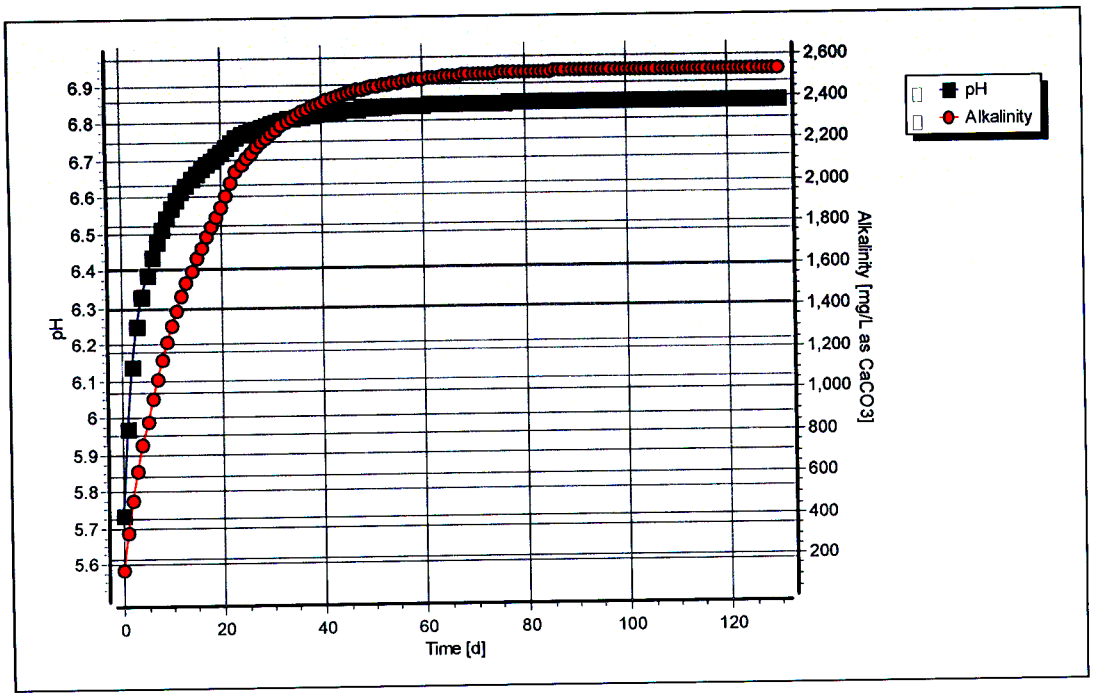


**Figure C-33:** Simulated pH and alkalinity profiles for steady state number 11

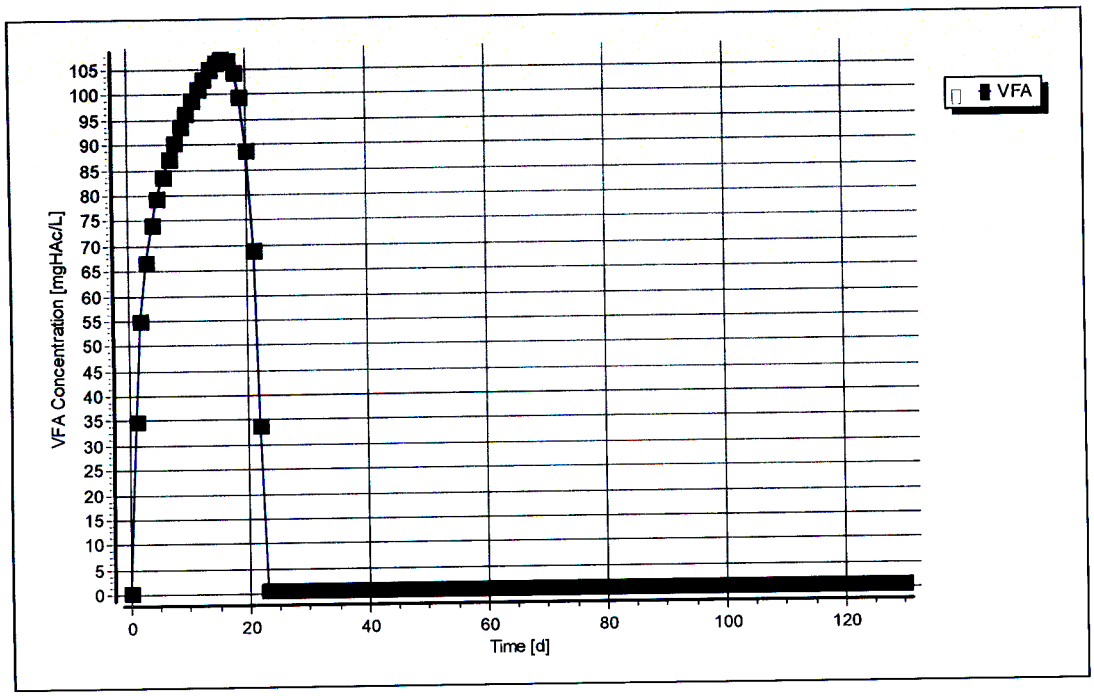


**Figure C-34:** Simulated VFA concentration profile for steady state number 11

## Steady State Number 12

**Table C-23:** Operating conditions for steady state number 12

| | |
|---|---|
| **Feed Batch Number** | F13 |
| **Reactor Volume (ℓ)** | 20 |
| **Retention Time (d)** | 10 |
| **pH** | steady state |
| **Biological Groups Present** | acidogenic, acetogenic and methanogenic |

**Table C-24:** Results summary for steady state number 12

| | Measured | Model | Relative error (%) |
|---|---|---|---|
| **Feed Total COD (mg COD/ℓ)** | 39810 | 39810 | - |
| **Feed Soluble COD (mg COD/ℓ)** | 4436 | 4436 | - |
| **Feed TKN (mg N/ℓ)** | 983 | 983 | - |
| **Feed FSA (mg N/ℓ)** | 214 | 214 | - |
| **Effluent Total COD (mg COD/ℓ)** | 18085 ± 589 | 18629.35 | 2.92 |
| **Effluent Soluble COD (mg COD/ℓ)** | 256 ± 10 | 293.88 | 12.89 |
| **Reactor pH** | 6.92 ± 0.01 | 6.83 | -1.32 |
| **Effluent VFA (mg HAc/ℓ)** | 27 ± 8 | 1.01 | -2586.05 |
| **Effluent Alkalinity (mg/ℓ as $CaCO_3$)** | 2362 ± 25 | 2425.72 | 2.63 |
| **Sulphate Addition (mg SO4/ℓ)** | 0 | 0 | - |
| **Effluent Sulphate (mg SO4/ℓ)** | 0 | 0 | - |
| **% Sulphate Conversion** | - | - | - |
| **Methane Production (ℓ/d)** | 17.33 | 18.38 | 5.70 |
| **Gas Composition (% $CH_4$)** | 62.73 | 61.17 | -2.55 |
| **Effluent FSA (mg N/ℓ)** | 260 ± 22 | 437.82 | 40.61 |
| **Effluent TKN (mg N/ℓ)** | 770 ± 14 | 888.51 | 13.34 |

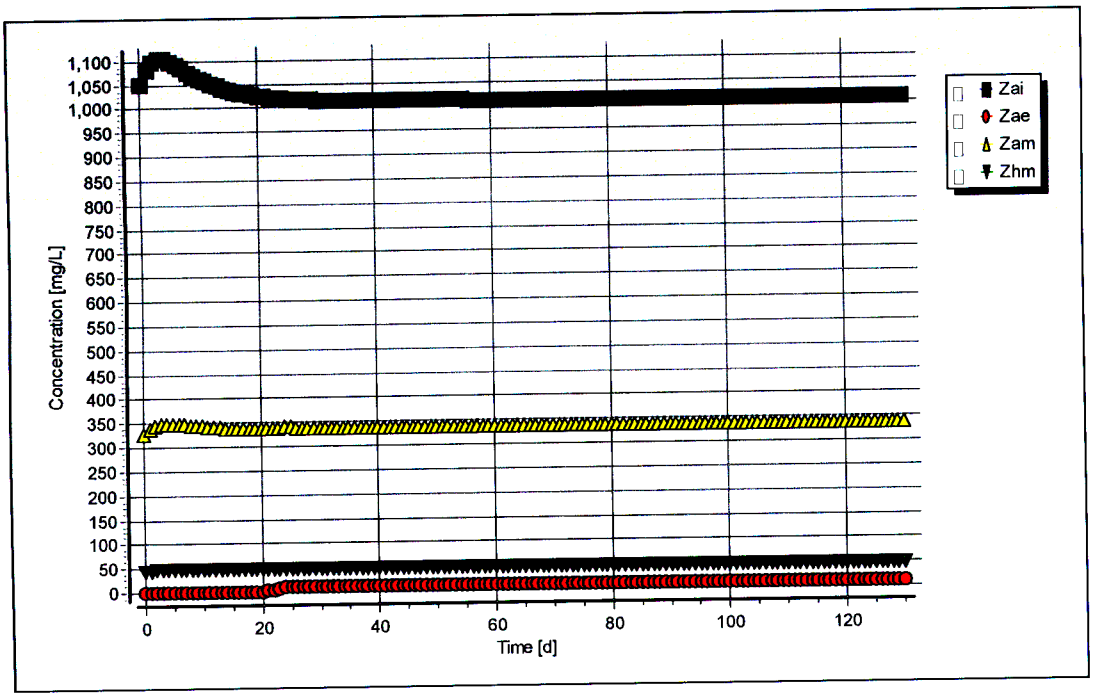


**Figure C-38:** Simulated biomass concentration profiles for steady state number 12

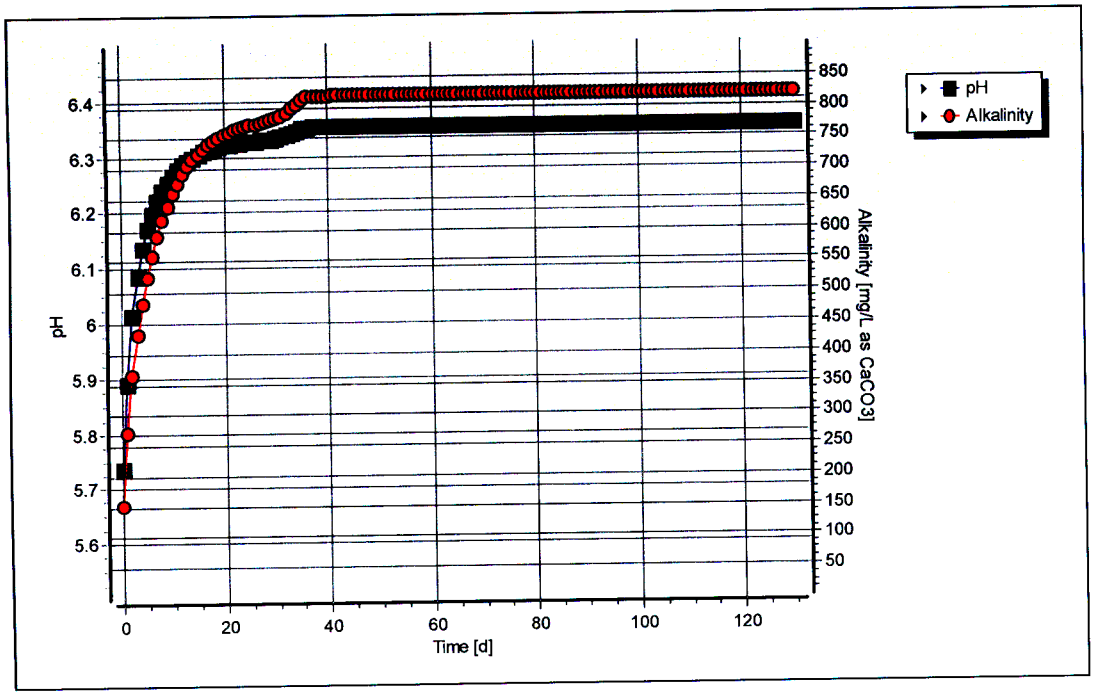


**Figure C-39:** Simulated pH and alkalinity profiles for steady state number 13

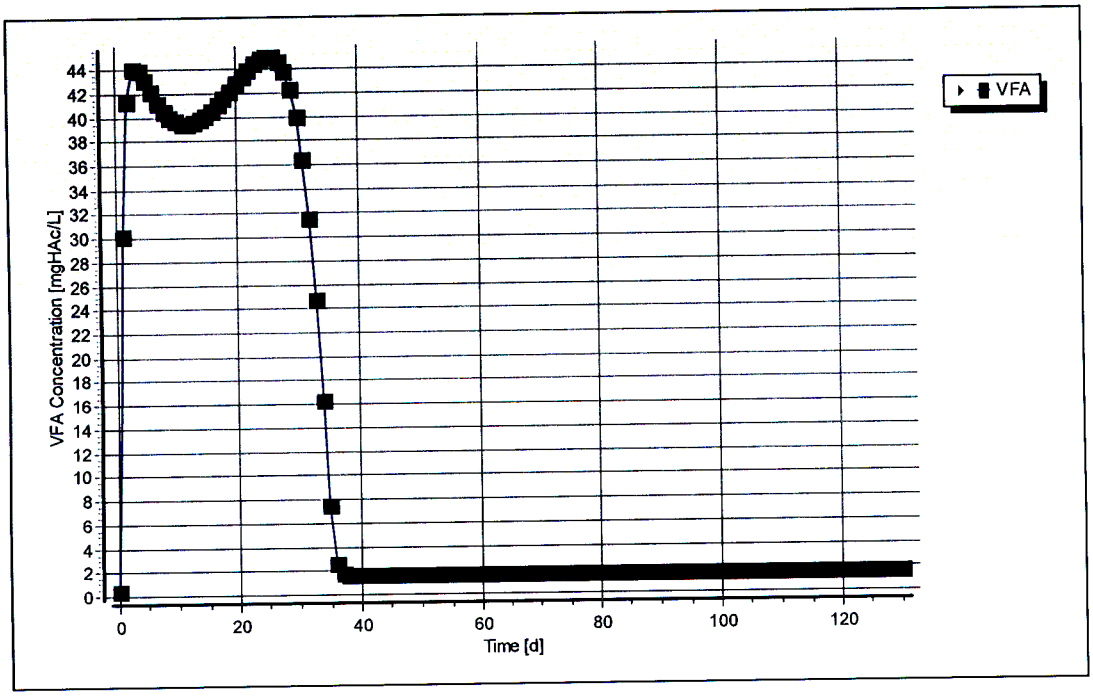


**Figure C-40:** Simulated VFA concentration profile for steady state number 13

## Steady State Number 14

**Table C-27:** Operating conditions for steady state number 14

| | |
|---|---|
| **Feed Batch Number** | F13 |
| **Reactor Volume (ℓ)** | 20 |
| **Retention Time (d)** | 8 |
| **pH** | steady state |
| **Biological Groups Present** | acidogenic, acetogenic and methanogenic |

**Table C-28:** Results summary for steady state number 14

| | Measured | Model | Relative error (%) |
|---|---|---|---|
| **Feed Total COD (mg COD/ℓ)** | 13269 | 13269 | - |
| **Feed Soluble COD (mg COD/ℓ)** | 1524 | 1524 | - |
| **Feed TKN (mg N/ℓ)** | 328 | 328 | - |
| **Feed FSA (mg N/ℓ)** | 73 | 73 | - |
| **Effluent Total COD (mg COD/ℓ)** | 6299 ± 86 | 6384.39 | 1.34 |
| **Effluent Soluble COD (mg COD/ℓ)** | 104 ± 4 | 152.34 | 31.73 |
| **Reactor pH** | 6.78 ± 0.01 | 6.40 | -5.96 |
| **Effluent VFA (mg HAc/ℓ)** | 7 ± 6 | 2.01 | -247.56 |
| **Effluent Alkalinity (mg/ℓ as $CaCO_3$)** | 863 ± 7 | 903.30 | 4.46 |
| **Sulphate Addition (mg SO4/ℓ)** | 0 | 0 | - |
| **Effluent Sulphate (mg SO4/ℓ)** | 0 | 0 | - |
| **% Sulphate Conversion** | - | - | - |
| **Methane Production (ℓ/d)** | 6.4 | 7.47 | 14.29 |
| **Gas Composition (% $CH_4$)** | 63.06 | 60.76 | -3.78 |
| **Effluent FSA (mg N/ℓ)** | 112 ± 3 | 143.00 | 21.68 |
| **Effluent TKN (mg N/ℓ)** | 143 ± 28 | 295.88 | 51.67 |

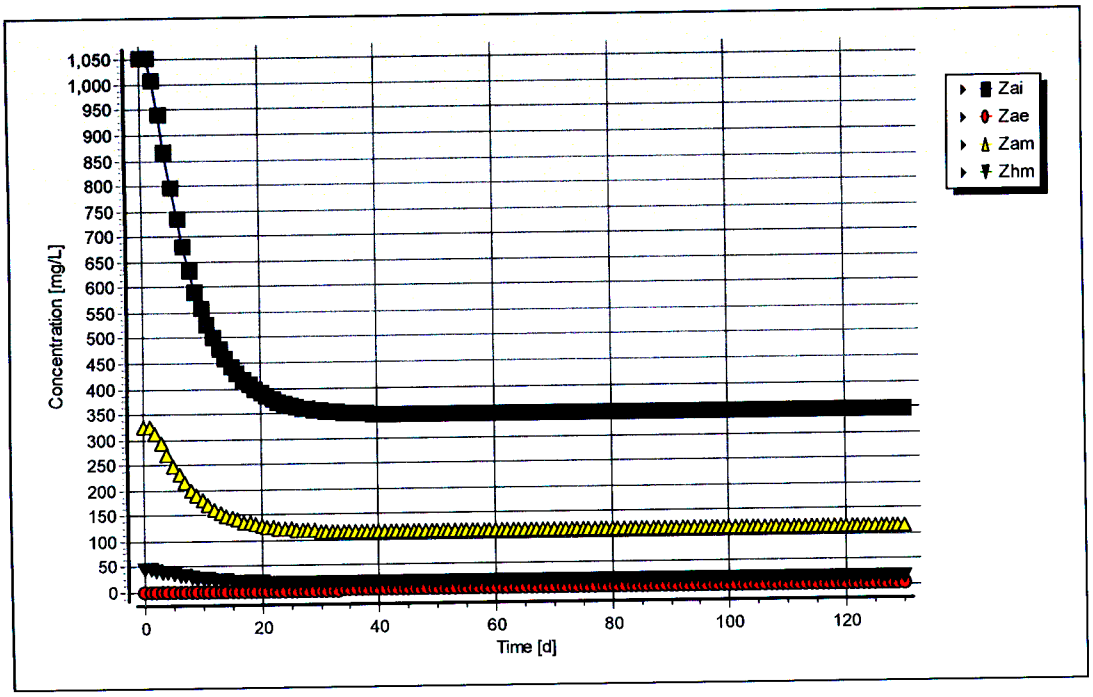


**Figure C-44:** Simulated biomass concentration profiles for steady state number 14

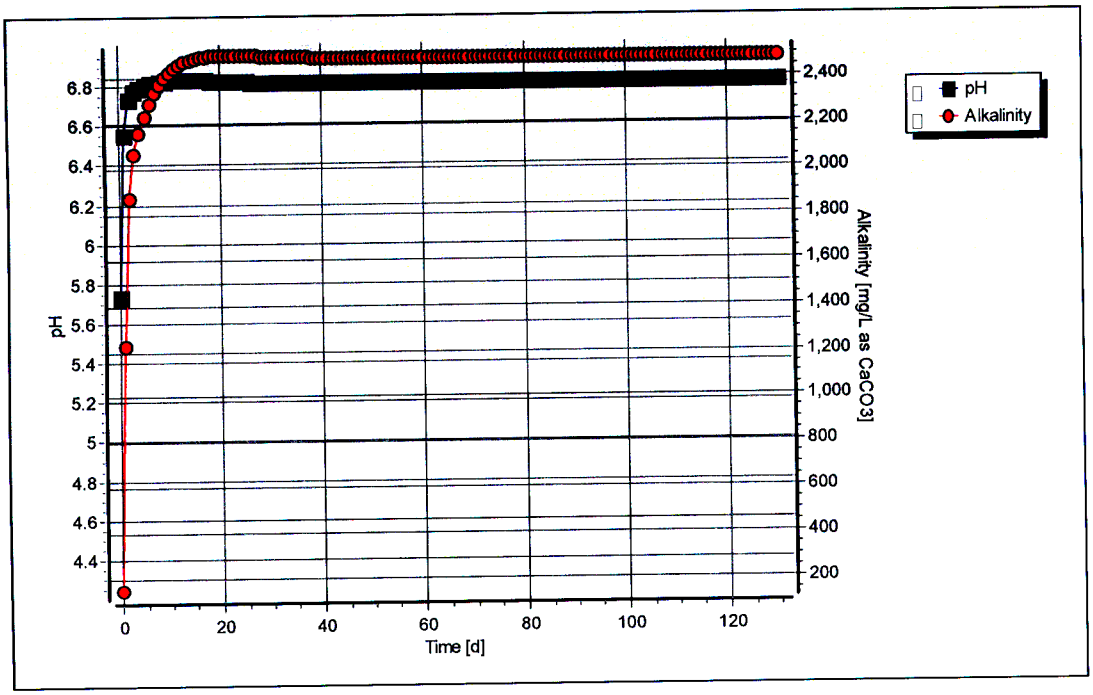


**Figure C-45:** Simulated pH and alkalinity profiles for steady state number 15

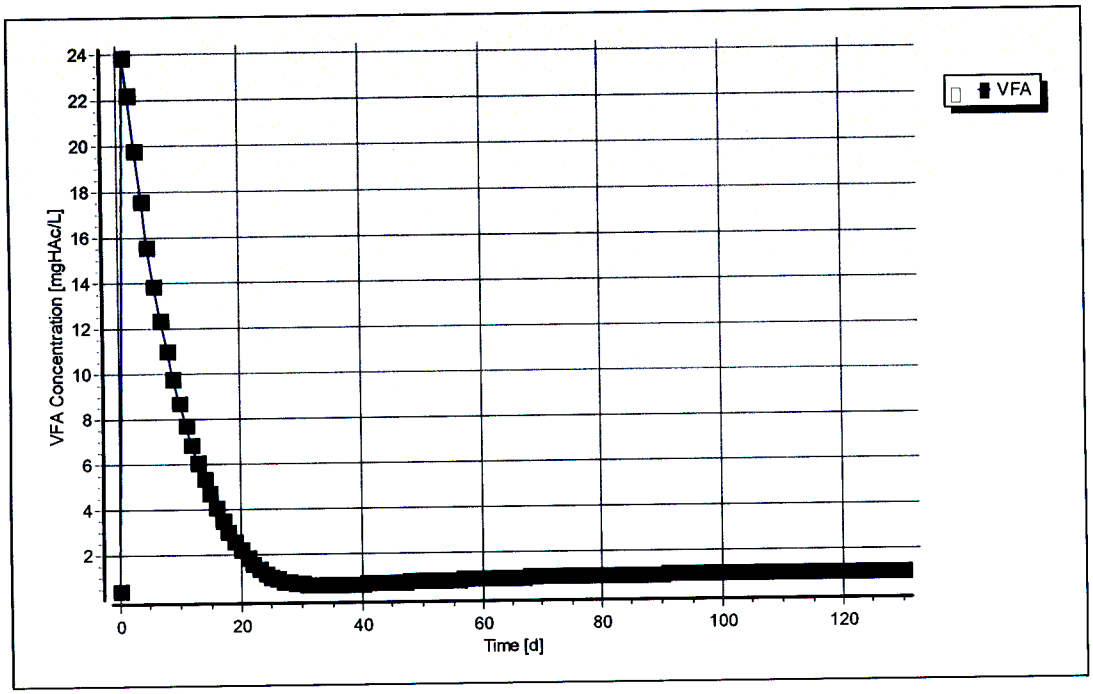


**Figure C-46:** Simulated VFA concentration profile for steady state number 15

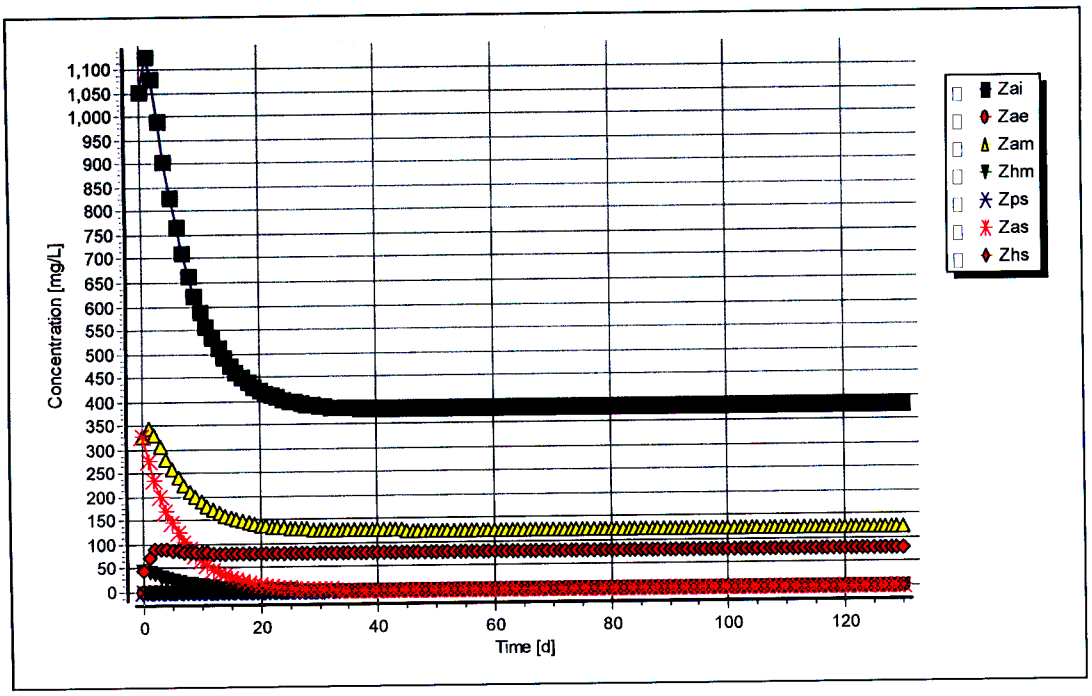


**Figure C-49:** Simulated biomass concentration profiles for steady state number 15

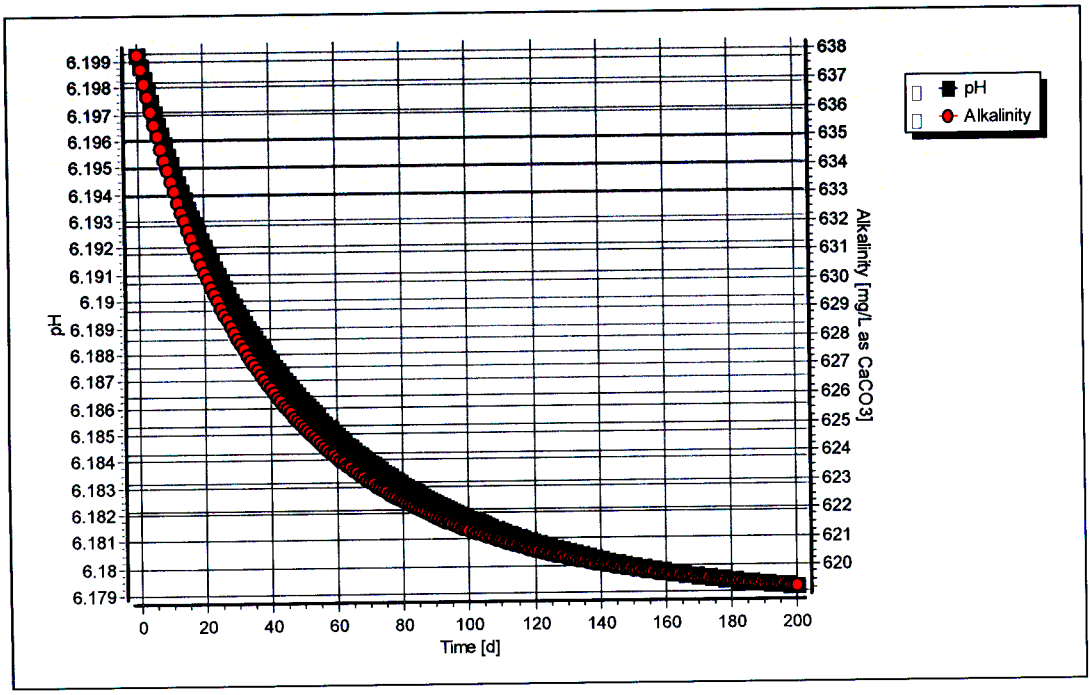


**Figure C-50:** Simulated pH and alkalinity profiles for steady state number 17

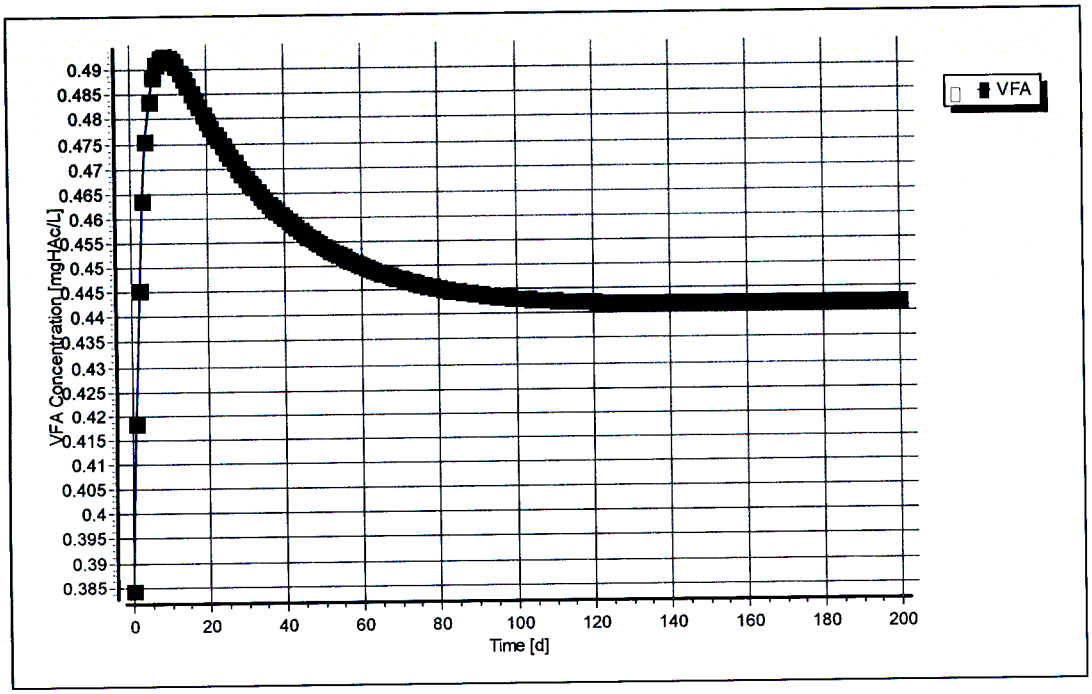


**Figure C-51:** Simulated VFA concentration profile for steady state number 17

## Steady State Number 18

**Table C-33:** Operating conditions for steady state number 18

| | |
|---|---|
| **Feed Batch Number** | F14 |
| **Reactor Volume (ℓ)** | 16 |
| **Retention Time (d)** | 8 |
| **pH** | Controlled to ~ 7.5 |
| **Biological Groups Present** | acidogenic, acetogenic and methanogenic |

**Table C-34:** Results summary for steady state number 18

| | Measured | Model | Relative error (%) |
|---|---|---|---|
| **Feed Total COD (mg COD/ℓ)** | 1949 | 1949 | - |
| **Feed Soluble COD (mg COD/ℓ)** | 283 | 283 | - |
| **Feed TKN (mg N/ℓ)** | 43 | 43 | - |
| **Feed FSA (mg N/ℓ)** | 7 | 7 | - |
| **Effluent Total COD (mg COD/ℓ)** | 827 ± 29 | 864.43 | 4.33 |
| **Effluent Soluble COD (mg COD/ℓ)** | 43 ± 6 | 97.48 | 55.89 |
| **Reactor pH** | 7.48 ± 0.02 | 7.50 | 0.23 |
| **Effluent VFA (mg HAc/ℓ)** | 0 | 1.00 | 100.00 |
| **Effluent Alkalinity (mg/ℓ as $CaCO_3$)** | 571 ± 13 | 1536.15 | 62.83 |
| **Sulphate Addition (mg SO4/ℓ)** | 0 | 0 | - |
| **Effluent Sulphate (mg SO4/ℓ)** | 0 | 0 | - |
| **% Sulphate Conversion** | - | - | - |
| **Methane Production (ℓ/d)** | 0.84 | 0.94 | 10.69 |
| **Gas Composition (% $CH_4$)** | 84.69 | 94.72 | 10.59 |
| **Effluent FSA (mg N/ℓ)** | 18 ± 2 | 18.67 | 3.61 |
| **Effluent TKN (mg N/ℓ)** | 17 ± 1 | 39.44 | 56.90 |

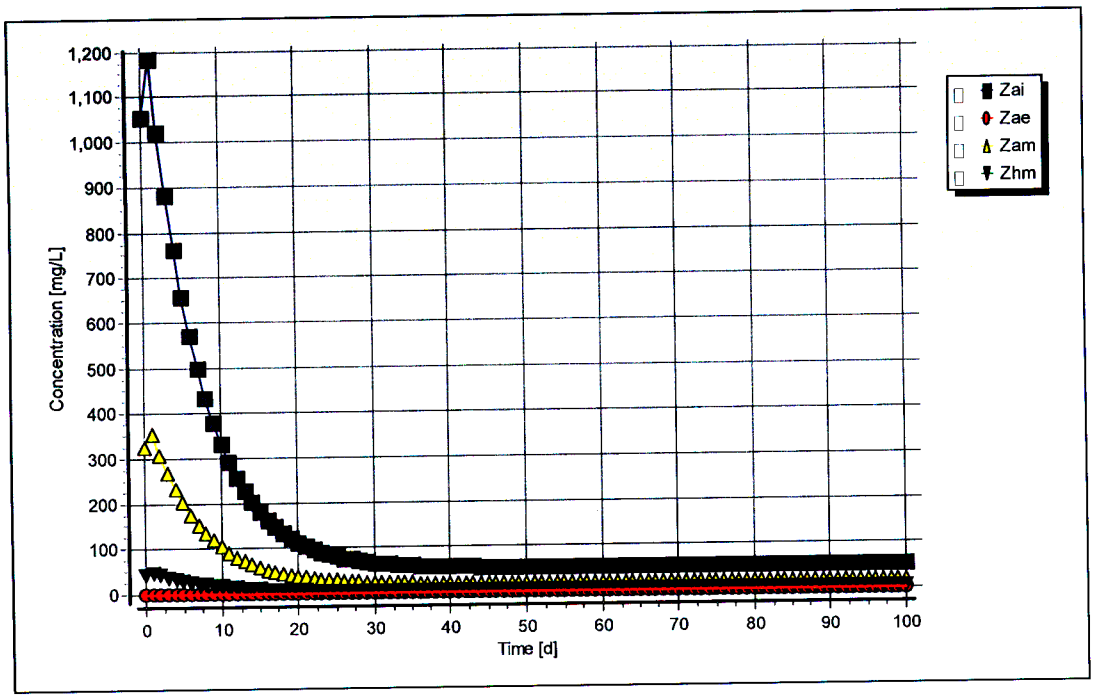


**Figure C-55:** Simulated biomass concentration profiles for steady state number 18

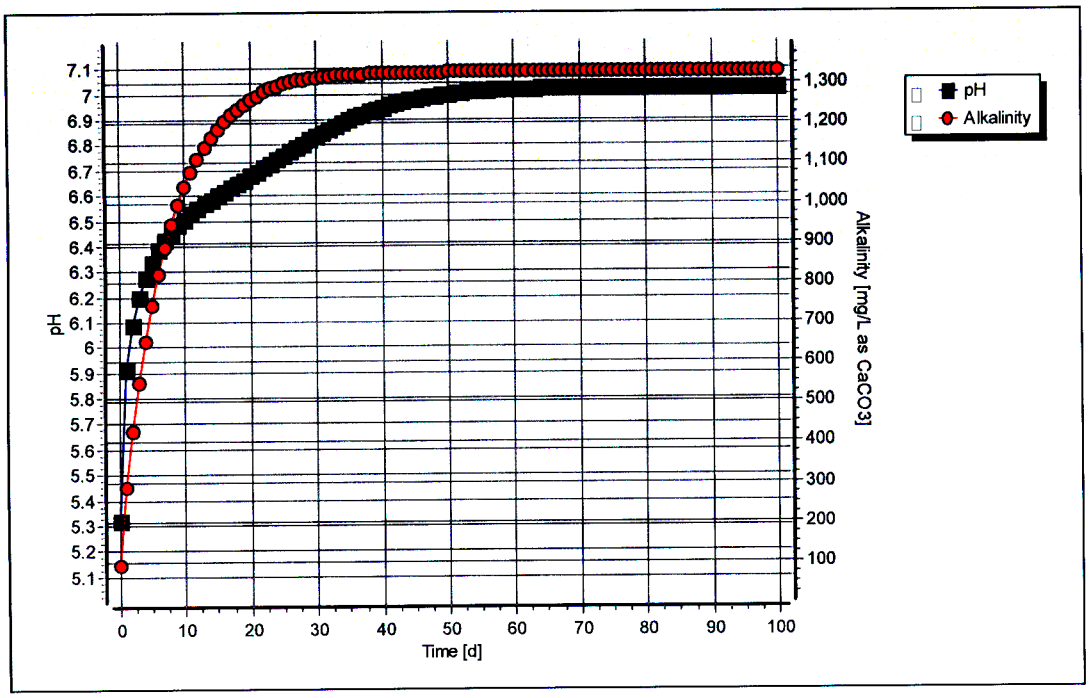


**Figure C-56:** Simulated pH and alkalinity profiles for steady state number 19

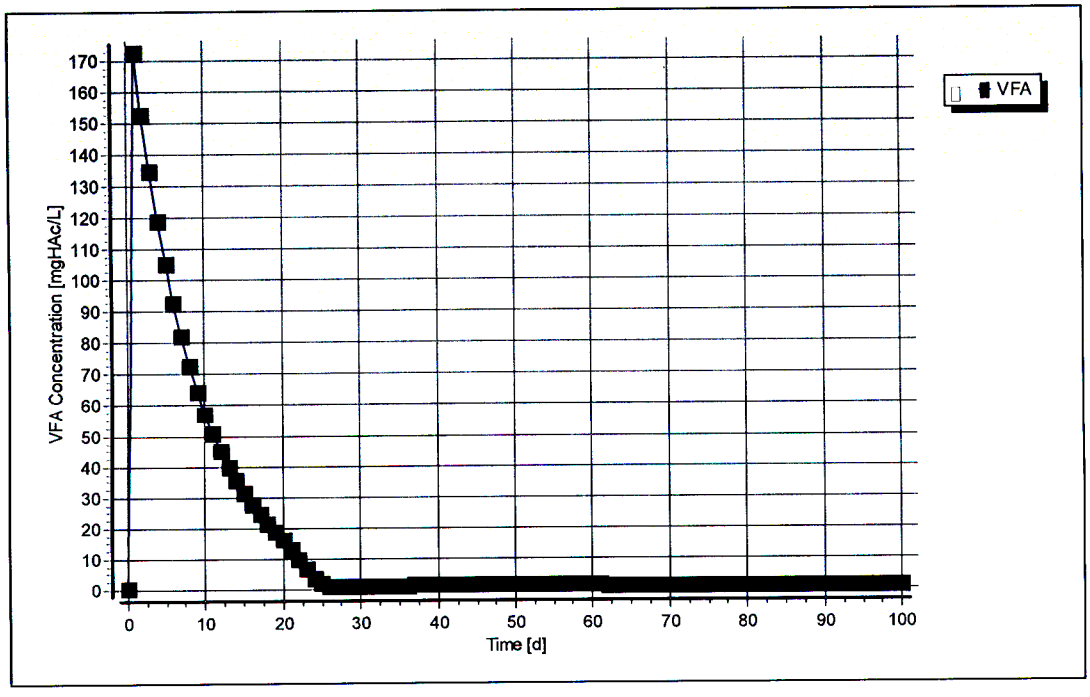


**Figure C-57:** Simulated VFA concentration profile for steady state number 19

## Steady State Number 20

**Table C-37:** Operating conditions for steady state number 20

| | |
|---|---|
| **Feed Batch Number** | F14 |
| **Reactor Volume (ℓ)** | 16 |
| **Retention Time (d)** | 8 |
| **pH** | Controlled to ~ 7.5 |
| **Biological Groups Present** | acidogenic, acetogenic, methanogenic and sulphidogenic |

**Table C-38:** Results summary for steady state number 20

| | **Measured** | **Model** | **Relative error (%)** |
|---|---|---|---|
| **Feed Total COD (mg COD/ℓ)** | 1949 | 1949 | - |
| **Feed Soluble COD (mg COD/ℓ)** | 283 | 283 | - |
| **Feed TKN (mg N/ℓ)** | 43 | 43 | - |
| **Feed FSA (mg N/ℓ)** | 8 | 8 | - |
| **Effluent Total COD (mg COD/ℓ)** | 1532 ± 58 | 1117.75 | -37.06 |
| **Effluent Soluble COD (mg COD/ℓ)** | 790 ± 40 | 247.63 | -219.03 |
| **Reactor pH** | 7.52 ± 0.03 | 7.52 | - |
| **Effluent VFA (mg HAc/ℓ)** | 0 | 0.16 | 100 |
| **Effluent Alkalinity (mg/ℓ as $CaCO_3$)** | 1386 ± 36 | 1812.58 | 23.53 |
| **Sulphate Addition (mg SO4/ℓ)** | 2000 | 2000 | - |
| **Effluent Sulphate (mg SO4/ℓ)** | 530 ± 26 | 1523 | 65.19 |
| **% Sulphate Conversion** | 73.50 | 23.87 | - |
| **Methane Production (ℓ/d)** | 0 | 0.48 | 100 |
| **Gas Composition (% $CH_4$)** | 0 | 75.11 | 100 |
| **Effluent FSA (mg N/ℓ)** | 18 ± 1 | 17.41 | -3.41 |
| **Effluent TKN (mg N/ℓ)** | 44 ± 1 | 39.21 | -12.22 |

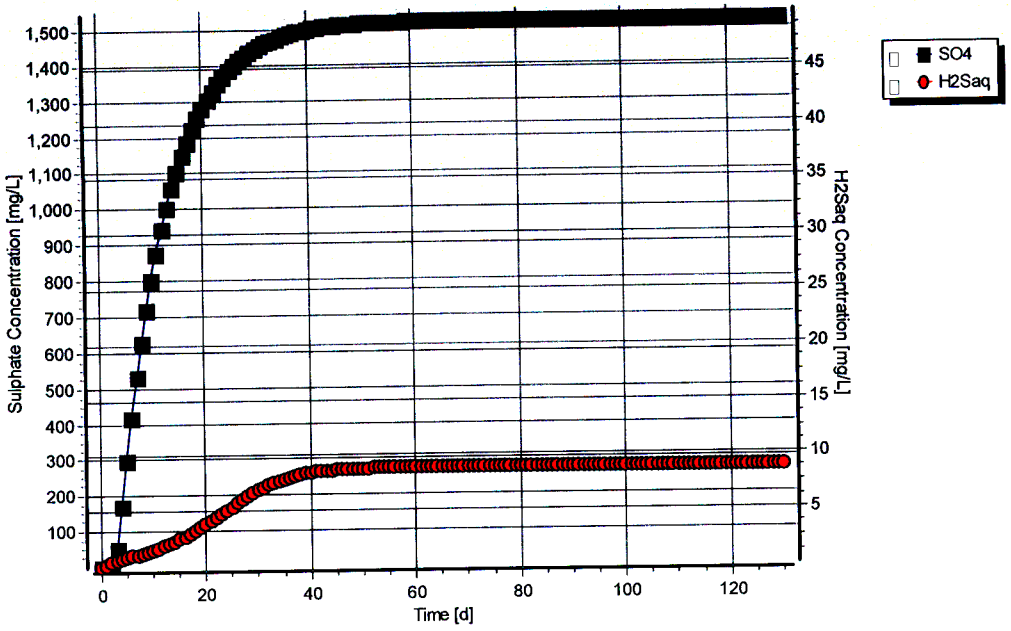


**Figure C-61:** Simulated sulphate and aqueous hydrogen sulphide concentration profiles for steady state number 20

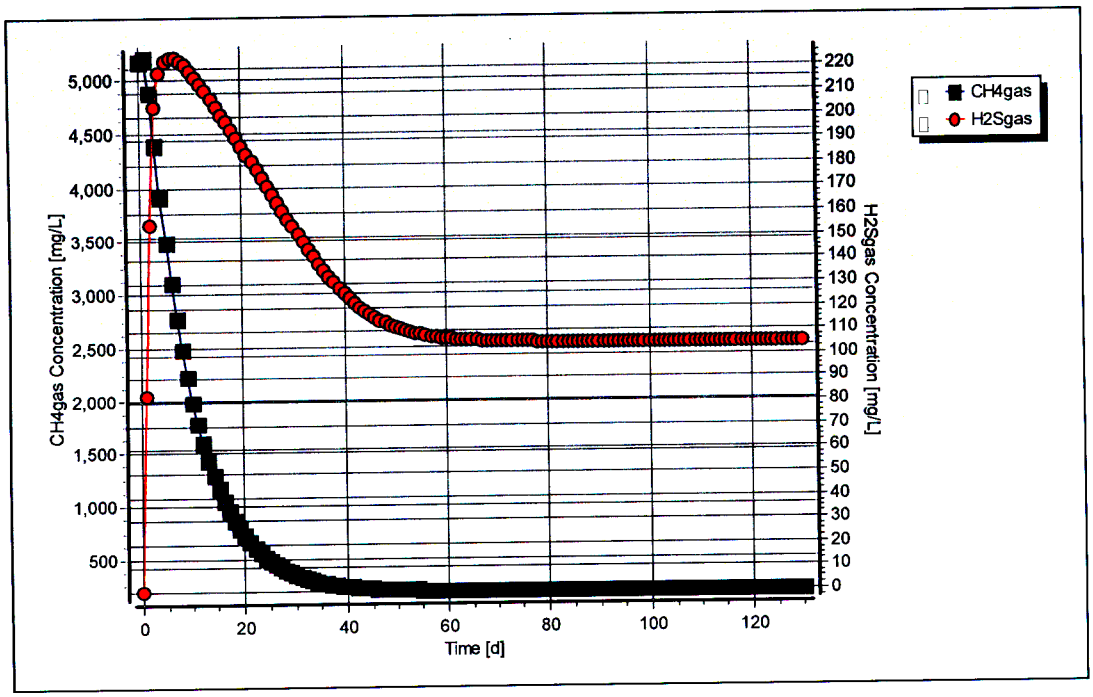


**Figure C-62:** Simulated methane and hydrogen sulphide gas concentration profiles for steady state number 20

## Steady State Number 21

**Table C-39:** Operating conditions for steady state number 21

| | |
|---|---|
| **Feed Batch Number** | F14 |
| **Reactor Volume (ℓ)** | 20 |
| **Retention Time (d)** | 8 |
| **pH** | steady state |
| **Biological Groups Present** | acidogenic, acetogenic and methanogenic |

**Table C-40:** Results summary for steady state number 21

| | Measured | Model | Relative error (%) |
|---|---|---|---|
| **Feed Total COD (mg COD/ℓ)** | 34819 | 34819 | - |
| **Feed Soluble COD (mg COD/ℓ)** | 3829 | 3829 | - |
| **Feed TKN (mg N/ℓ)** | 770 | 770 | - |
| **Feed FSA (mg N/ℓ)** | 44 | 44 | - |
| **Effluent Total COD (mg COD/ℓ)** | 15094 ± 493 | 15490.07 | 2.56 |
| **Effluent Soluble COD (mg COD/ℓ)** | 205 ± 8 | 252.20 | 18.71 |
| **Reactor pH** | 6.90 ± 0.01 | 6.73 | -2.53 |
| **Effluent VFA (mg HAc/ℓ)** | 22 ± 10 | 1.39 | -1482.43 |
| **Effluent Alkalinity (mg/ℓ as $CaCO_3$)** | 1868 ± 74 | 1952.11 | 4.31 |
| **Sulphate Addition (mg SO4/ℓ)** | 0 | 0 | - |
| **Effluent Sulphate (mg SO4/ℓ)** | 0 | 0 | - |
| **% Sulphate Conversion** | - | - | - |
| **Methane Production (ℓ/d)** | 19.39 | 20.97 | 7.55 |
| **Gas Composition (% $CH_4$)** | 58.85 | 60.45 | 2.64 |
| **Effluent FSA (mg N/ℓ)** | 258 ± 10 | 245.52 | -5.08 |
| **Effluent TKN (mg N/ℓ)** | 651 ± 14 | 631.80 | -3.04 |

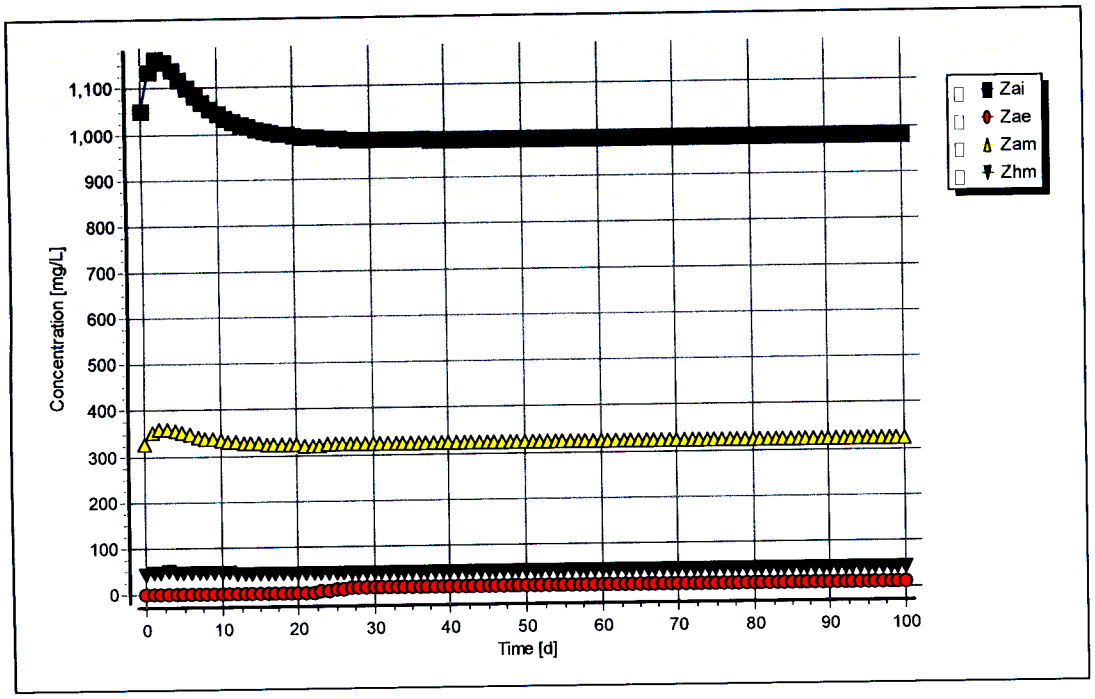


**Figure C-66:** Simulated biomass concentration profiles for steady state number 21

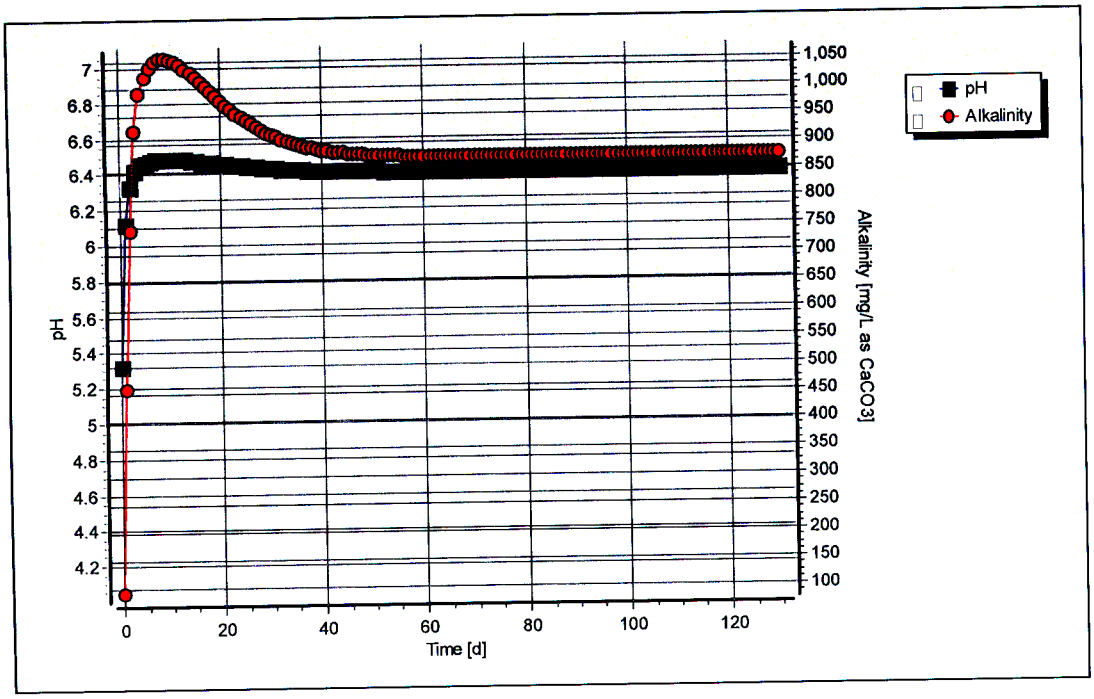


**Figure C-67:** Simulated pH and alkalinity profiles for steady state number 22

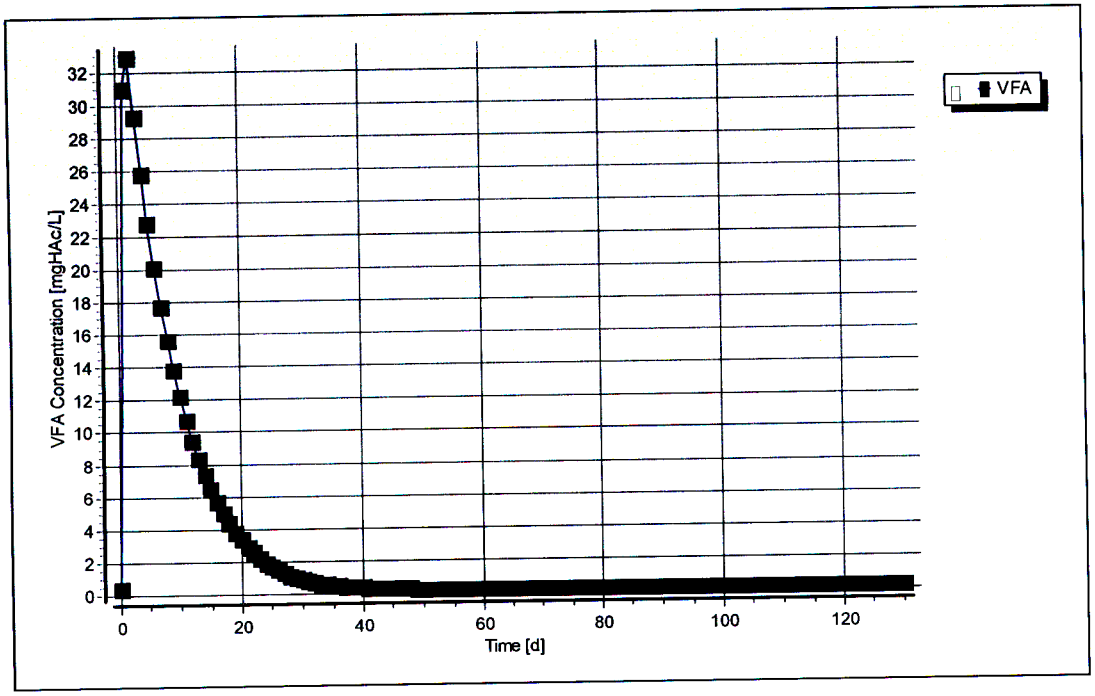


**Figure C-68:** Simulated VFA concentration profile for steady state number 22

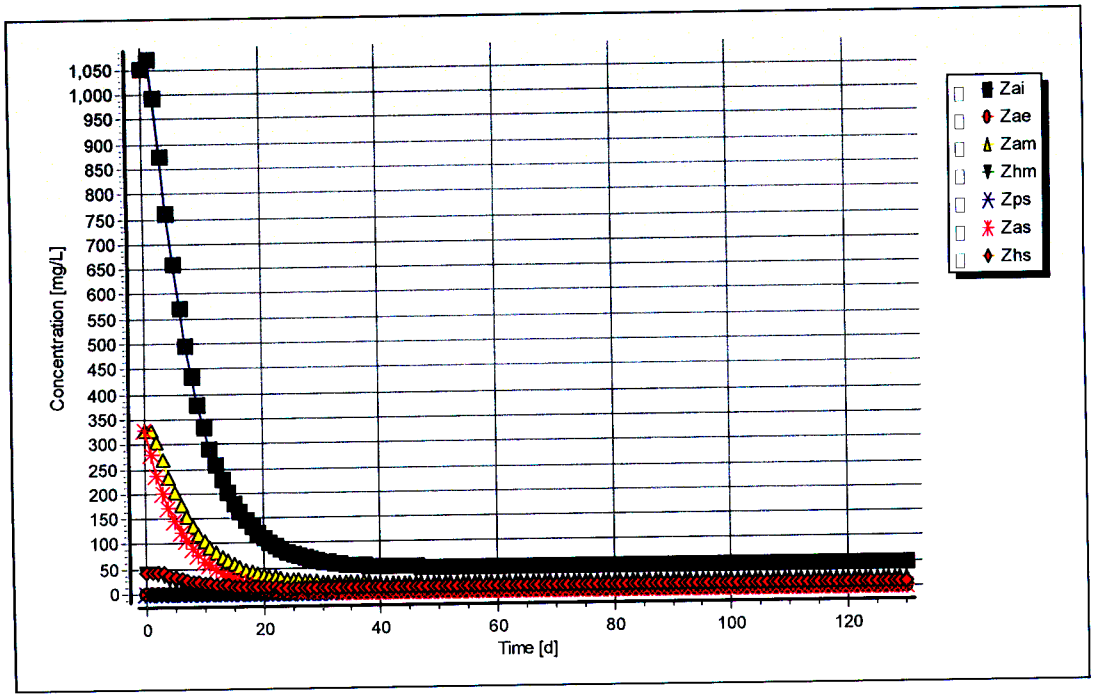


**Figure C-71:** Simulated biomass concentration profiles for steady state number 22

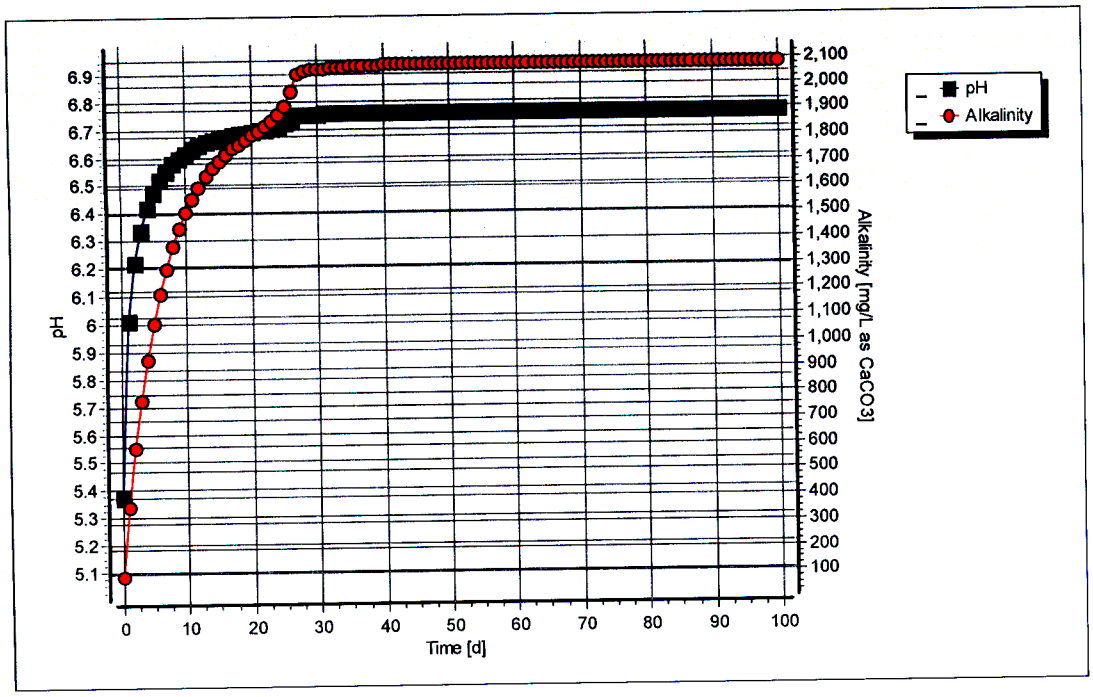


**Figure C-72:** Simulated pH and alkalinity profiles for steady state number 23

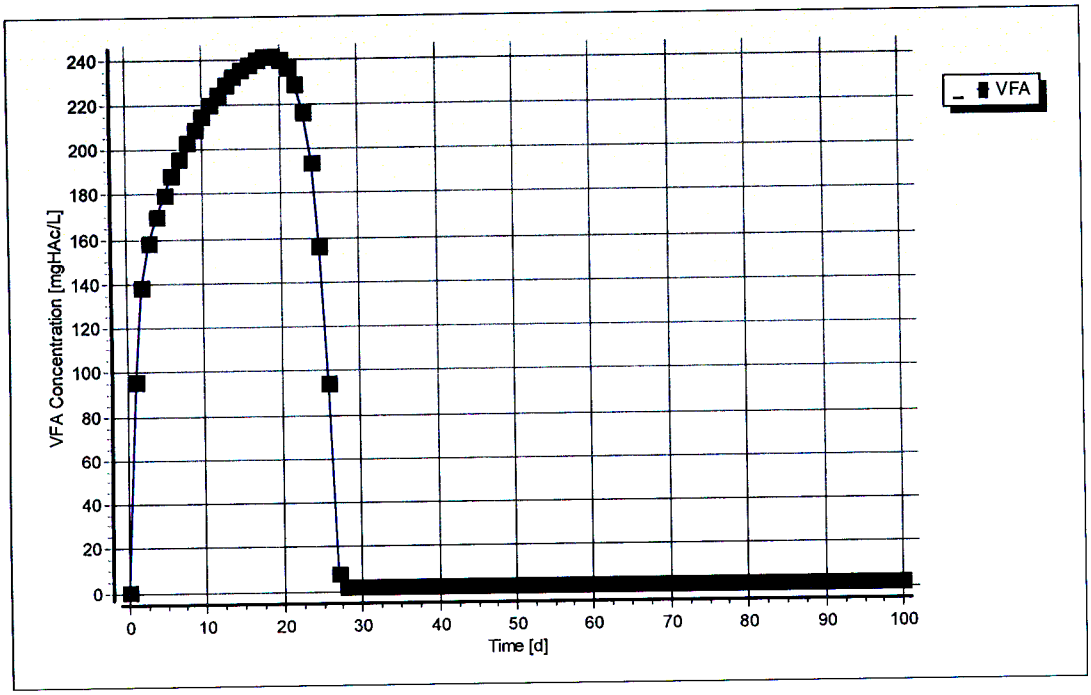


**Figure C-73:** Simulated VFA concentration profile for steady state number 23

## Steady State Number 24

**Table C-45:** Operating conditions for steady state number 24

| | |
|---|---|
| **Feed Batch Number** | F14 |
| **Reactor Volume (ℓ)** | 20 |
| **Retention Time (d)** | 6.67 |
| **pH** | steady state |
| **Biological Groups Present** | acidogenic, acetogenic and methanogenic |

**Table C-46:** Results summary for steady state number 24

| | **Measured** | **Model** | **Relative error (%)** |
|---|---|---|---|
| **Feed Total COD (mg COD/ℓ)** | 13580 | 13580 | - |
| **Feed Soluble COD (mg COD/ℓ)** | 1846 | 1846 | - |
| **Feed TKN (mg N/ℓ)** | 300 | 300 | - |
| **Feed FSA (mg N/ℓ)** | 37 | 37 | - |
| **Effluent Total COD (mg COD/ℓ)** | 5944 ± 140 | 6094.14 | 2.46 |
| **Effluent Soluble COD (mg COD/ℓ)** | 96 ± 14 | 154.92 | 38.03 |
| **Reactor pH** | 6.57 ± 0.01 | 6.38 | -2.98 |
| **Effluent VFA (mg HAc/ℓ)** | 5 ± 3 | 2.65 | -88.86 |
| **Effluent Alkalinity (mg/ℓ as $CaCO_3$)** | 789 ± 11 | 893.28 | 11.67 |
| **Sulphate Addition (mg SO4/ℓ)** | 0 | 0 | - |
| **Effluent Sulphate (mg SO4/ℓ)** | 0 | 0 | - |
| **% Sulphate Conversion** | - | - | - |
| **Methane Production (ℓ/d)** | 8.74 | 9.73 | 10.13 |
| **Gas Composition (% $CH_4$)** | 60.95 | 59.48 | -2.47 |
| **Effluent FSA (mg N/ℓ)** | 104 ± 3 | 107.58 | 3.33 |
| **Effluent TKN (mg N/ℓ)** | 246 ± 1 | 258.20 | 4.73 |

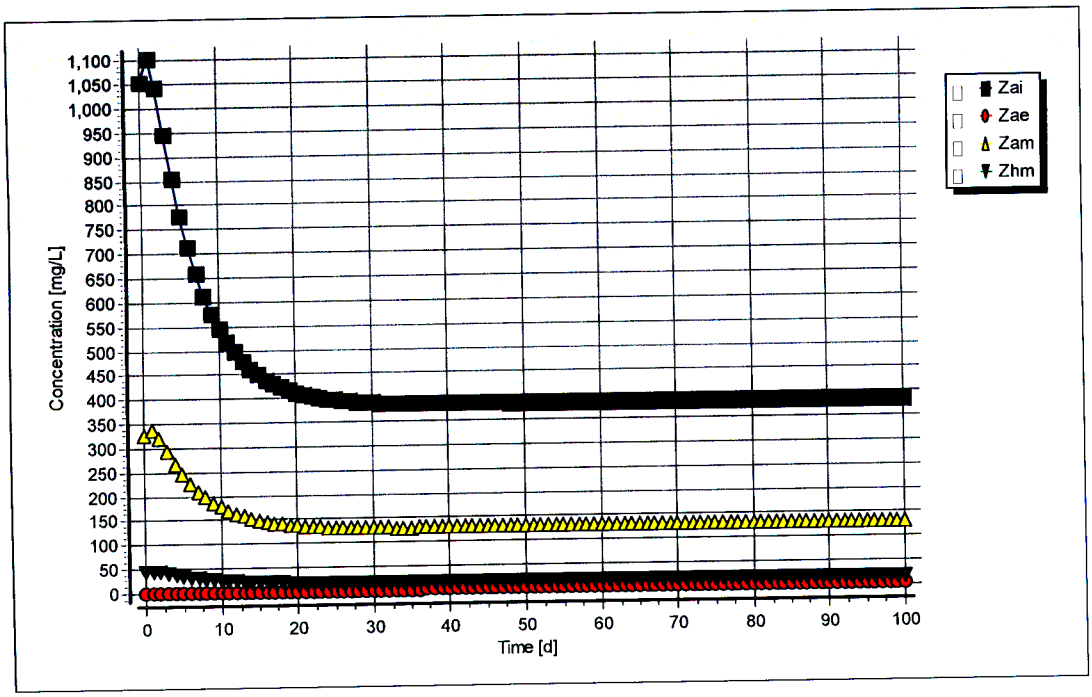


**Figure C-77:** Simulated biomass concentration profiles for steady state number 24

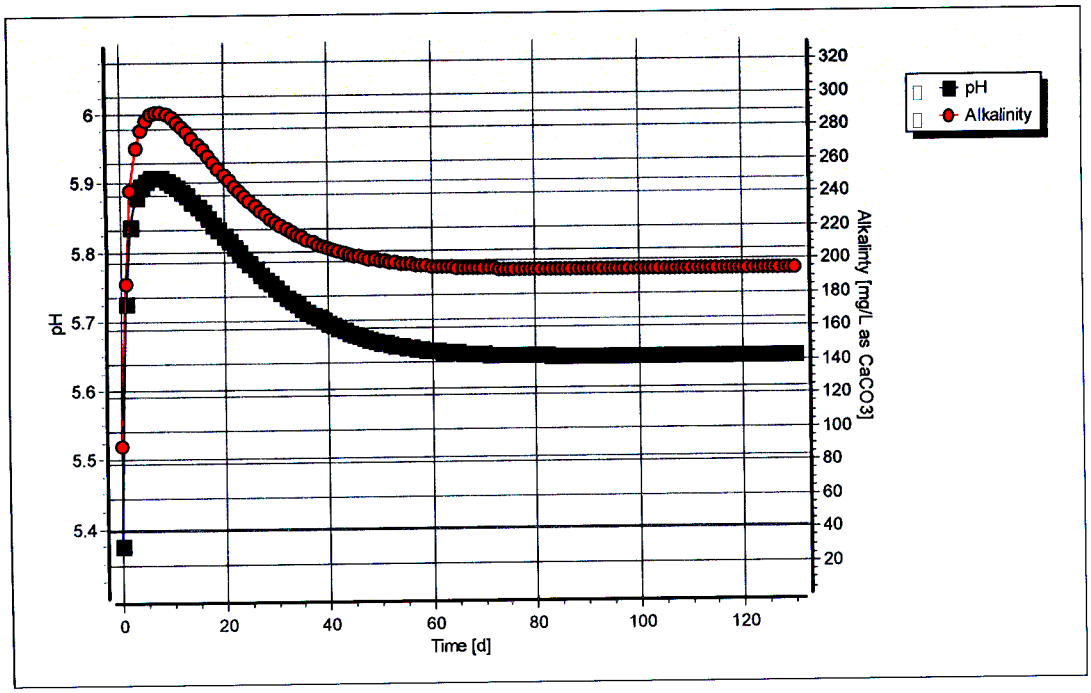


**Figure C-78:** Simulated pH and alkalinity profiles for steady state number 25

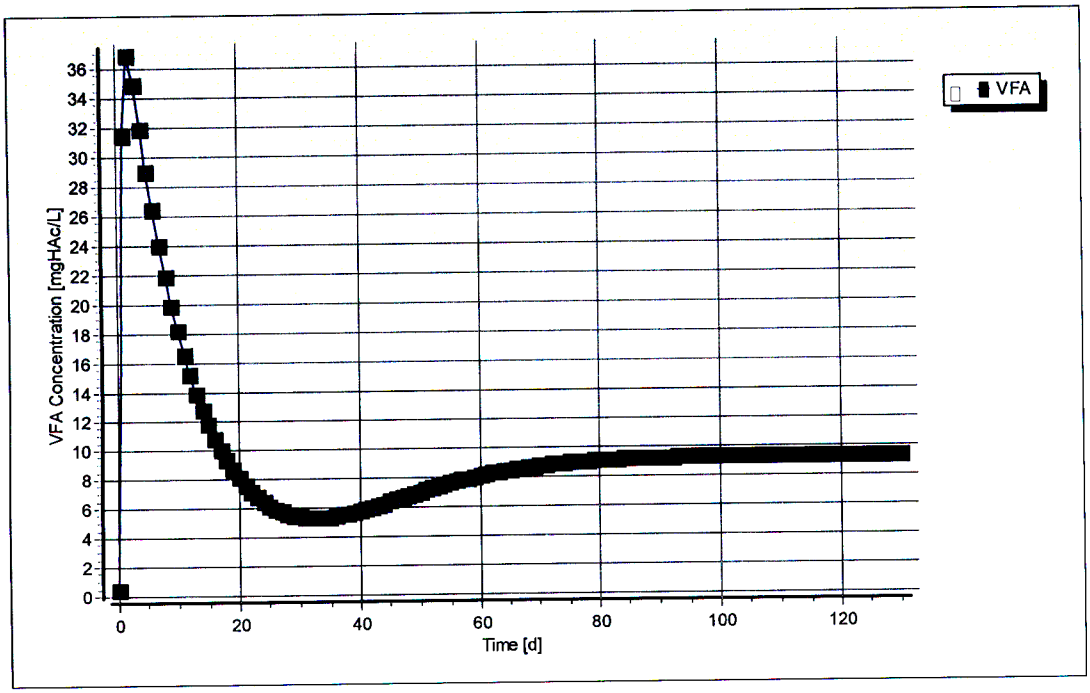


**Figure C-79:** Simulated VFA concentration profile for steady state number 25

## Steady State Number 26

**Table C-49:** Operating conditions for steady state number 26

| | |
|---|---|
| **Feed Batch Number** | F14 |
| **Reactor Volume (ℓ)** | 20 |
| **Retention Time (d)** | 8 |
| **pH** | steady state |
| **Biological Groups Present** | acidogenic, acetogenic and methanogenic |

**Table C-50:** Results summary for steady state number 26

| | Measured | Model | Relative error (%) |
|---|---|---|---|
| **Feed Total COD (mg COD/ℓ)** | 1949 | 1949 | - |
| **Feed Soluble COD (mg COD/ℓ)** | 283 | 283 | - |
| **Feed TKN (mg N/ℓ)** | 43 | 43 | - |
| **Feed FSA (mg N/ℓ)** | 7 | 7 | - |
| **Effluent Total COD (mg COD/ℓ)** | 892 ± 21 | 921.82 | 3.24 |
| **Effluent Soluble COD (mg COD/ℓ)** | 51 ± 8 | 117.40 | 56.56 |
| **Reactor pH** | 6.38 ± 0.02 | 5.65 | -12.92 |
| **Effluent VFA (mg HAc/ℓ)** | 10 ± 3 | 11.89 | 15.90 |
| **Effluent Alkalinity (mg/ℓ as $CaCO_3$)** | 144 ± 1 | 194.80 | 26.08 |
| **Sulphate Addition (mg SO4/ℓ)** | 0 | 0 | - |
| **Effluent Sulphate (mg SO4/ℓ)** | 0 | 0 | - |
| **% Sulphate Conversion** | - | - | - |
| **Methane Production (ℓ/d)** | 0.84 | 1.11 | 24.60 |
| **Gas Composition (% $CH_4$)** | 59.3 | -13.34 | -13.34 |
| **Effluent FSA (mg N/ℓ)** | 15 ± 1 | 18.24 | 17.75 |
| **Effluent TKN (mg N/ℓ)** | 36 ± 1 | 39.38 | 8.58 |

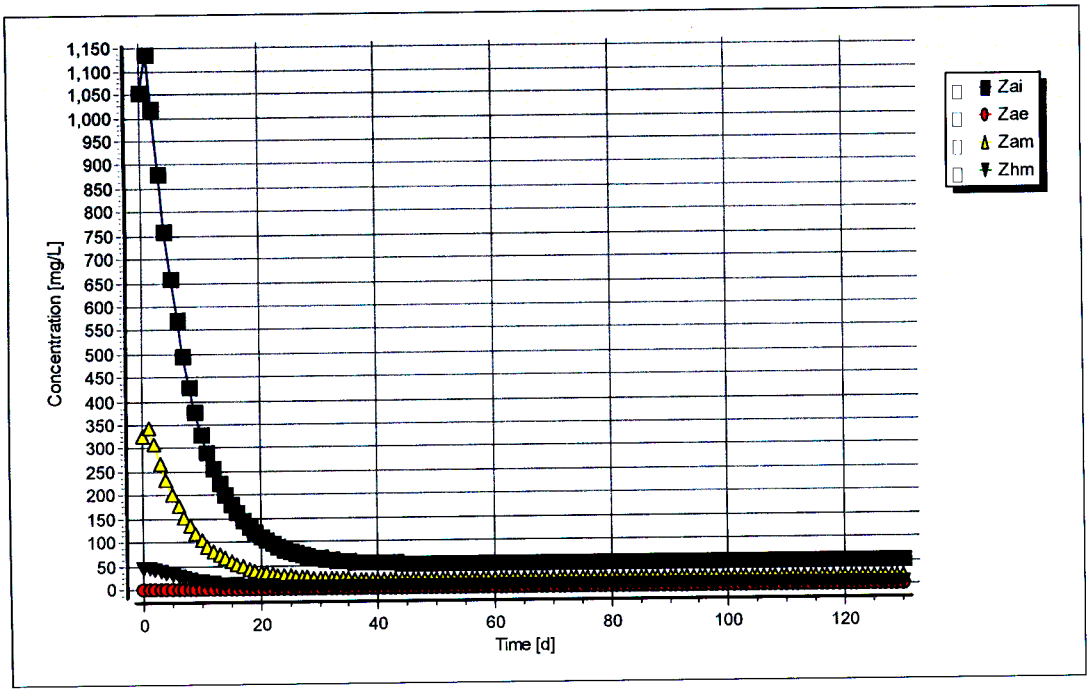


**Figure C-83:** Simulated biomass concentration profiles for steady state number 26

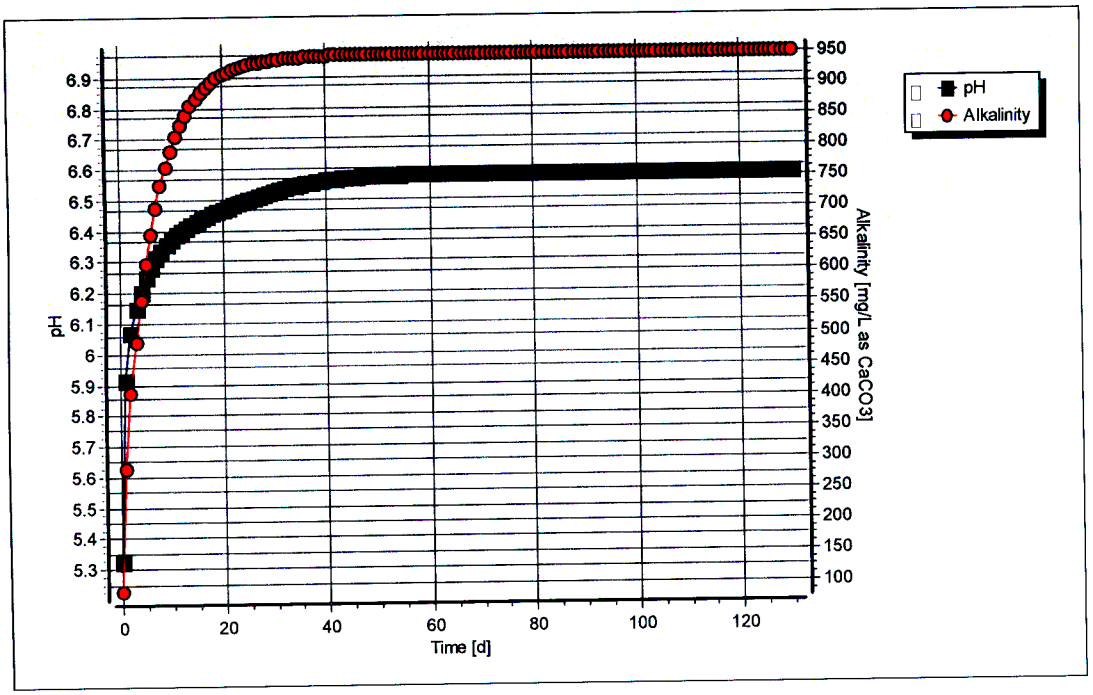


**Figure C-84:** Simulated pH and alkalinity profiles for steady state number 27

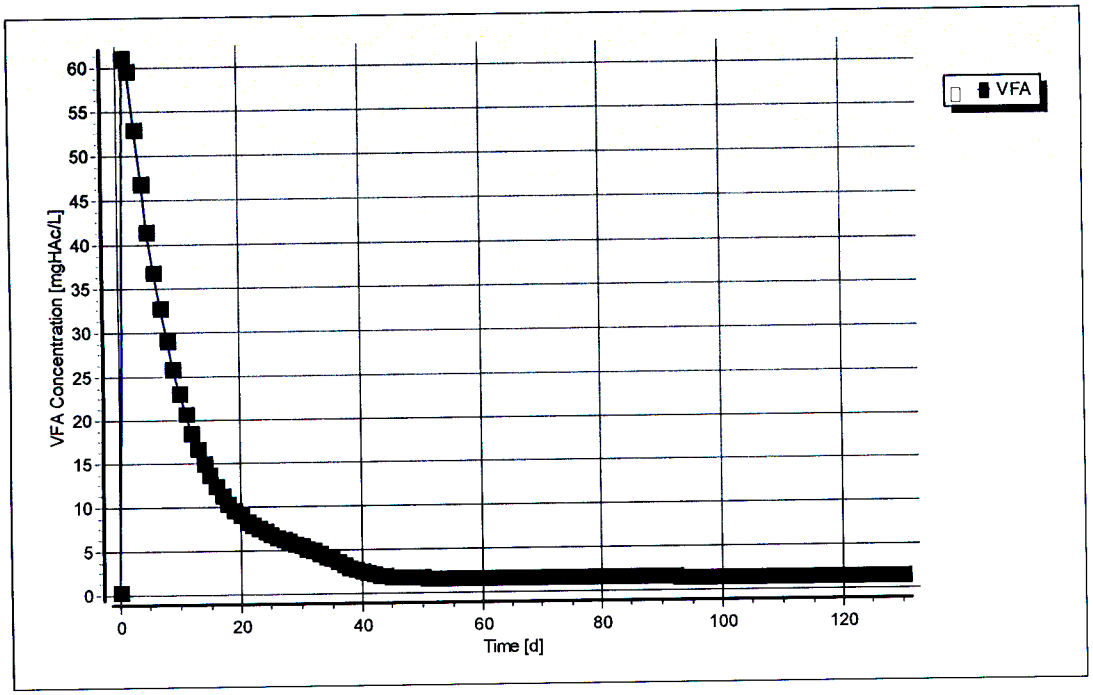


**Figure C-85:** Simulated VFA concentration profile for steady state number 27

## Steady State Number 28

**Table C-53:** Operating conditions for steady state number 28

| | |
|---|---|
| **Feed Batch Number** | F15 |
| **Reactor Volume (ℓ)** | 20 |
| **Retention Time (d)** | 5.71 |
| **pH** | steady state |
| **Biological Groups Present** | acidogenic, acetogenic and methanogenic |

**Table C-54:** Results summary for steady state number 28

| | Measured | Model | Relative error (%) |
|---|---|---|---|
| **Feed Total COD (mg COD/ℓ)** | 41442 | 41442 | - |
| **Feed Soluble COD (mg COD/ℓ)** | 2583 | 2583 | - |
| **Feed TKN (mg N/ℓ)** | 792 | 792 | - |
| **Feed FSA (mg N/ℓ)** | 40 | 40 | - |
| **Effluent Total COD (mg COD/ℓ)** | 19737 ± 732 | 20388.97 | 3.20 |
| **Effluent Soluble COD (mg COD/ℓ)** | 295 ± 36 | 363.72 | 18.89 |
| **Reactor pH** | 6.75 ± 0.01 | 6.66 | -1.30 |
| **Effluent VFA (mg HAc/ℓ)** | 26 ± 16 | 2.27 | -1047.88 |
| **Effluent Alkalinity (mg/ℓ as $CaCO_3$)** | 1612 ± 25 | 1671.18 | 3.54 |
| **Sulphate Addition (mg SO4/ℓ)** | 0 | 0 | - |
| **Effluent Sulphate (mg SO4/ℓ)** | 0 | 0 | - |
| **% Sulphate Conversion** | - | - | - |
| **Methane Production (ℓ/d)** | 30.32 | 32.13 | 5.62 |
| **Gas Composition (% $CH_4$)** | 63.76 | 60.63 | -5.16 |
| **Effluent FSA (mg N/ℓ)** | 183 ± 5 | 280.51 | 34.76 |
| **Effluent TKN (mg N/ℓ)** | 648 ± 22 | 759.16 | 14.64 |

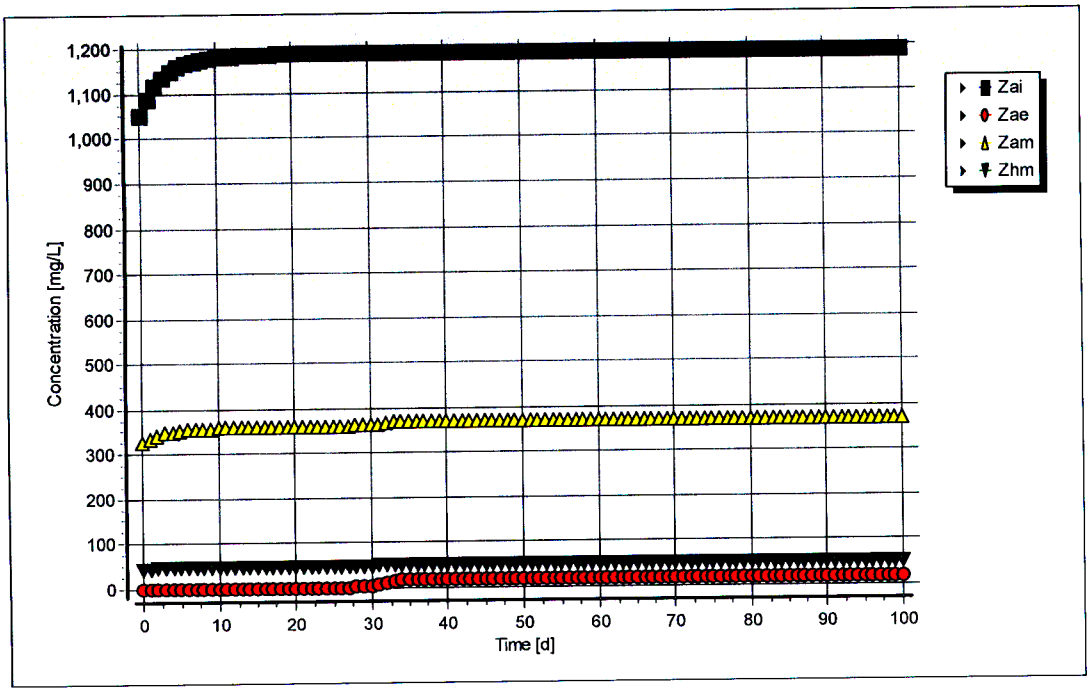


**Figure C-89:** Simulated biomass concentration profiles for steady state number 28

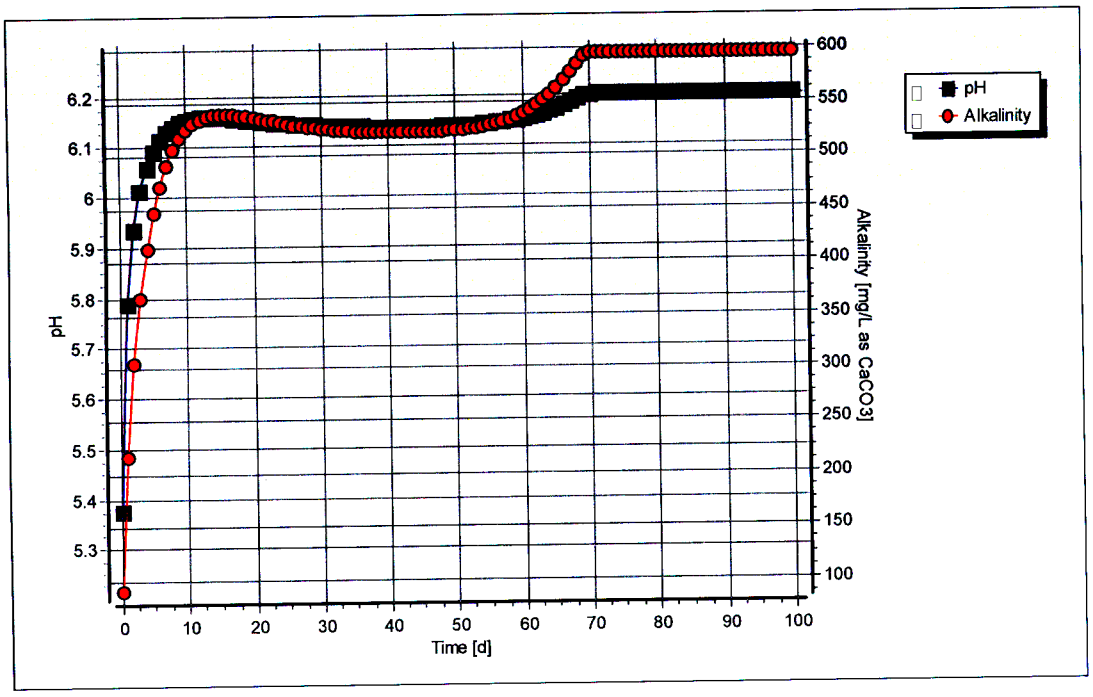


**Figure C-90:** Simulated pH and alkalinity profiles for steady state number 31

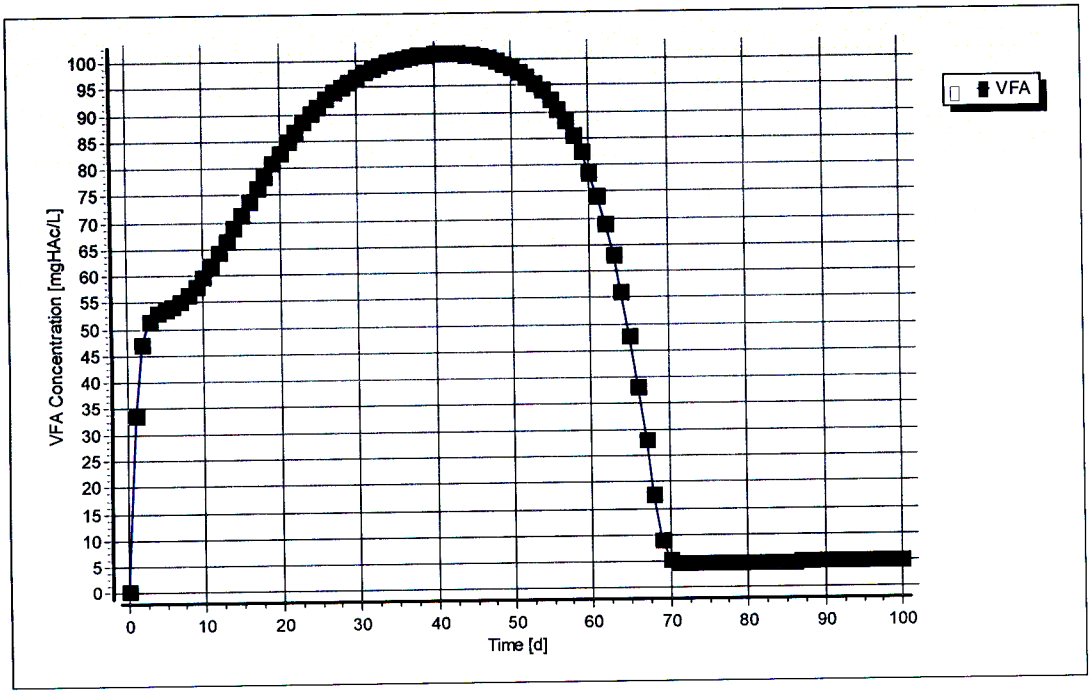


**Figure C-91:** Simulated VFA concentration profile for steady state number 31

## Steady State Number 36

**Table C-57:** Operating conditions for steady state number 36

| | |
|---|---|
| **Feed Batch Number** | F15 |
| **Reactor Volume (ℓ)** | 16 |
| **Retention Time (d)** | 8 |
| **pH** | Controlled to ~ 6.5 |
| **Biological Groups Present** | acidogenic, acetogenic, methanogenic and sulphidogenic |

**Table C-58:** Results summary for steady state number 36

| | **Measured** | **Model** | **Relative error (%)** |
|---|---|---|---|
| **Feed Total COD (mg COD/ℓ)** | 1949 | 1949 | - |
| **Feed Soluble COD (mg COD/ℓ)** | 283 | 283 | - |
| **Feed TKN (mg N/ℓ)** | 43 | 43 | - |
| **Feed FSA (mg N/ℓ)** | 13 | 13 | - |
| **Effluent Total COD (mg COD/ℓ)** | 1304 ± 48 | 996.00 | -30.92 |
| **Effluent Soluble COD (mg COD/ℓ)** | 521 ± 24 | 125.87 | -313.91 |
| **Reactor pH** | 6.47 ± 0.01 | 6.46 | -0.15 |
| **Effluent VFA (mg HAc/ℓ)** | 0 ± 1 | 0.17 | 100 |
| **Effluent Alkalinity (mg/ℓ as $CaCO_3$)** | 354 ± 10 | 937.84 | 62.25 |
| **Sulphate Addition (mg SO4/ℓ)** | 2000 | 2000 | - |
| **Effluent Sulphate (mg SO4/ℓ)** | 436 ± 20 | 1523 | 71.37 |
| **% Sulphate Conversion** | 78.20 | 23.87 | - |
| **Methane Production (ℓ/d)** | 0 | 0.61 | 100 |
| **Gas Composition (% $CH_4$)** | 0 | 46.76 | 100 |
| **Effluent FSA (mg N/ℓ)** | 16 ± 3 | 22.42 | 28.62 |
| **Effluent TKN (mg N/ℓ)** | 46 ± 1 | 44.22 | -4.03 |

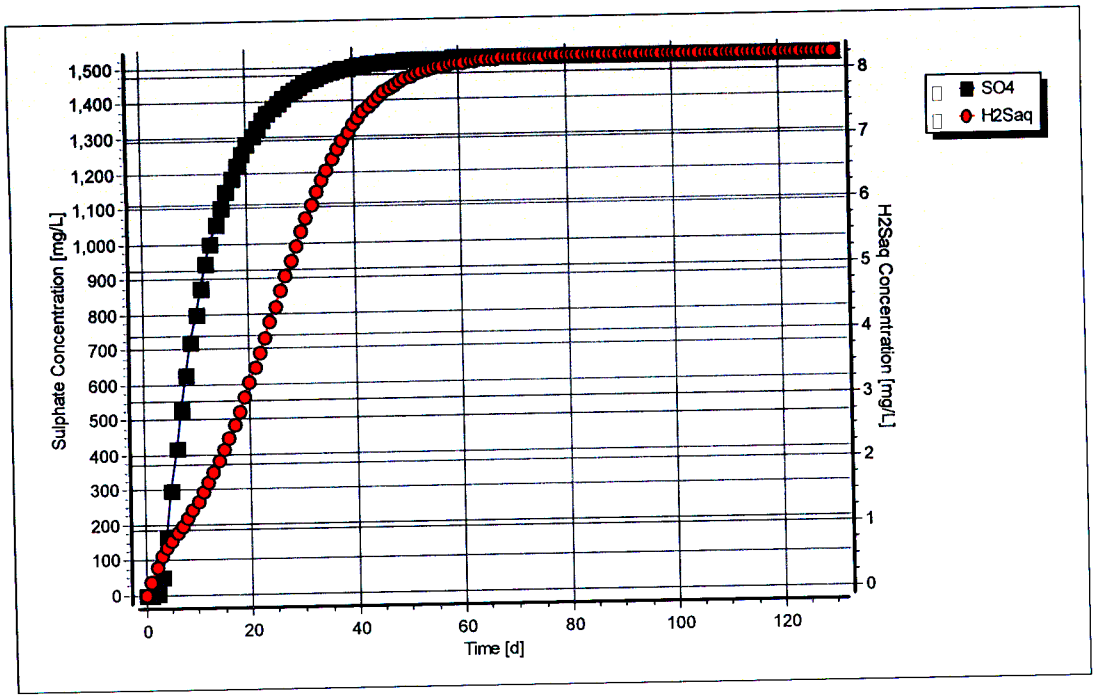


**Figure C-95:** Simulated sulphate and aqueous hydrogen sulphide concentration profiles for steady state number 36

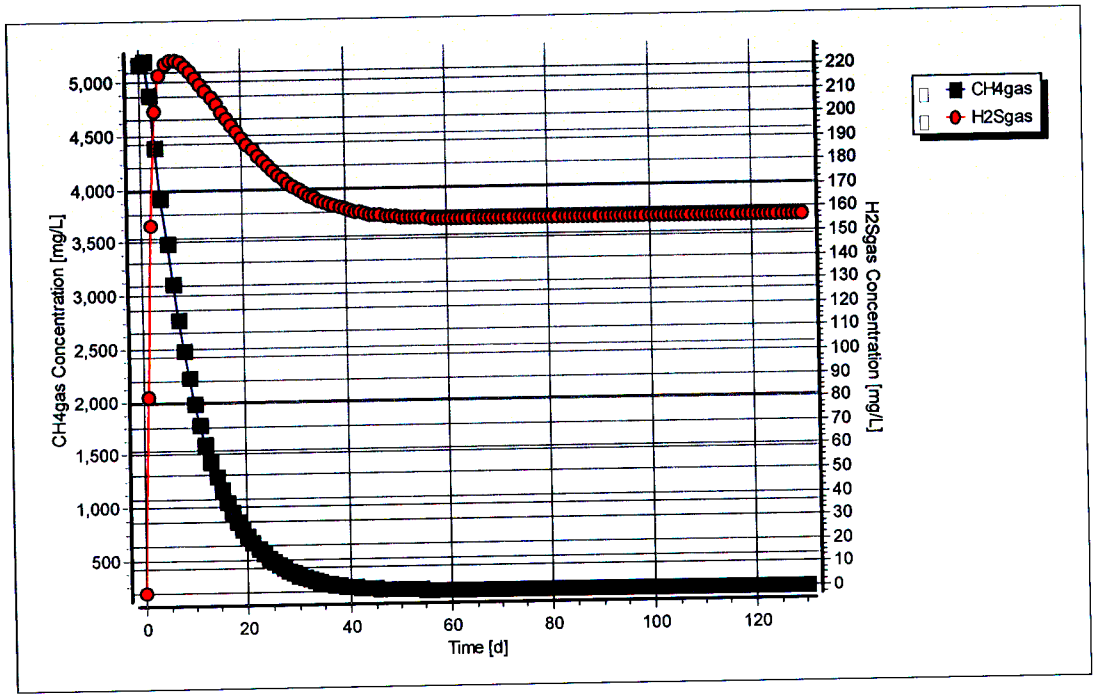


**Figure C-96:** Simulated methane and hydrogen sulphide gas concentration profiles for steady state number 36

## Steady State Number 41

**Table C-59:** Operating conditions for steady state number 41

| | |
|---|---|
| **Feed Batch Number** | F15 |
| **Reactor Volume (ℓ)** | 20 |
| **Retention Time (d)** | 16 |
| **pH** | steady state |
| **Biological Groups Present** | acidogenic, acetogenic, methanogenic and sulphidogenic |

**Table C-60:** Results summary for steady state number 41

| | **Measured** | **Model** | **Relative error (%)** |
|---|---|---|---|
| **Feed Total COD (mg COD/ℓ)** | 2012 | 2012 | - |
| **Feed Soluble COD (mg COD/ℓ)** | 212 | 212 | - |
| **Feed TKN (mg N/ℓ)** | 39 | 39 | - |
| **Feed FSA (mg N/ℓ)** | 6 | 6 | - |
| **Effluent Total COD (mg COD/ℓ)** | 1697 ± 41 | 898.94 | -54.67 |
| **Effluent Soluble COD (mg COD/ℓ)** | 897 ± 41 | 66.44 | -241.19 |
| **Reactor pH** | 7.64 ± 0.01 | 6.32 | -20.88 |
| **Effluent VFA (mg HAc/ℓ)** | 0 ± 1 | 0.13 | 100 |
| **Effluent Alkalinity (mg/ℓ as $CaCO_3$)** | 1633 ± 41 | 789.57 | -106.82 |
| **Sulphate Addition (mg SO4/ℓ)** | 2000 | 2000 | - |
| **Effluent Sulphate (mg SO4/ℓ)** | - | 1425 | - |
| **% Sulphate Conversion** | - | 28.75 | - |
| **Methane Production (ℓ/d)** | 0 | 0.44 | 100 |
| **Gas Composition (% $CH_4$)** | 0 | 42.00 | 100 |
| **Effluent FSA (mg N/ℓ)** | 11 ± 1 | 19.55 | 43.74 |
| **Effluent TKN (mg N/ℓ)** | 45 ± 1 | 41.46 | -8.54 |

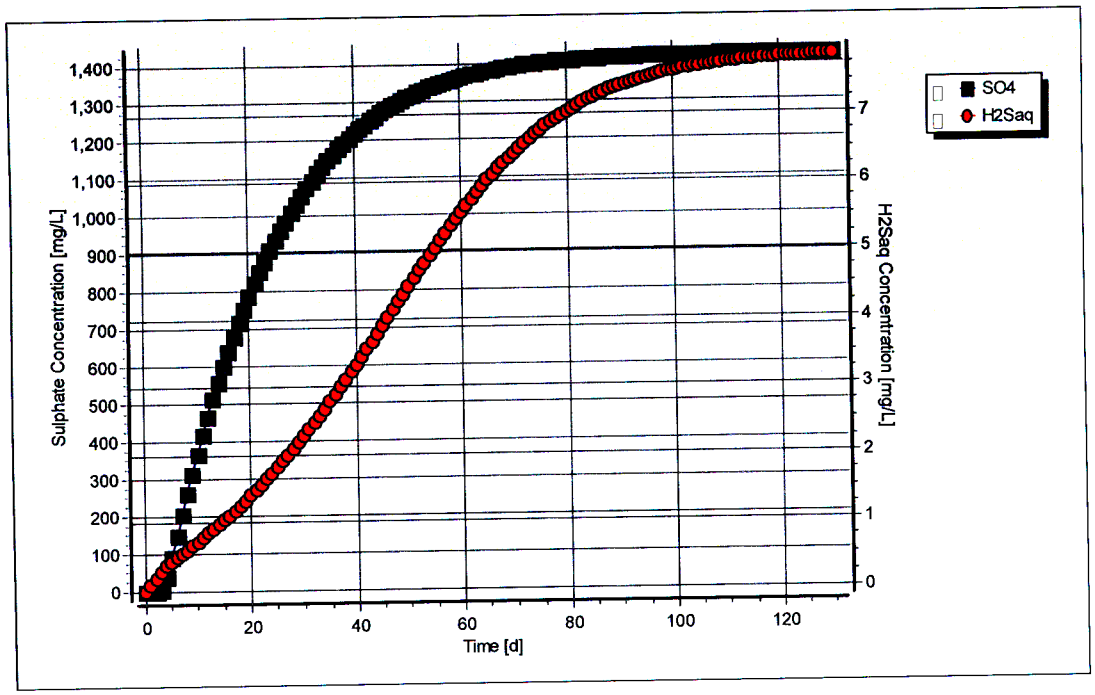


**Figure C-100:** Simulated sulphate and aqueous hydrogen sulphide concentration profiles for steady state number 41

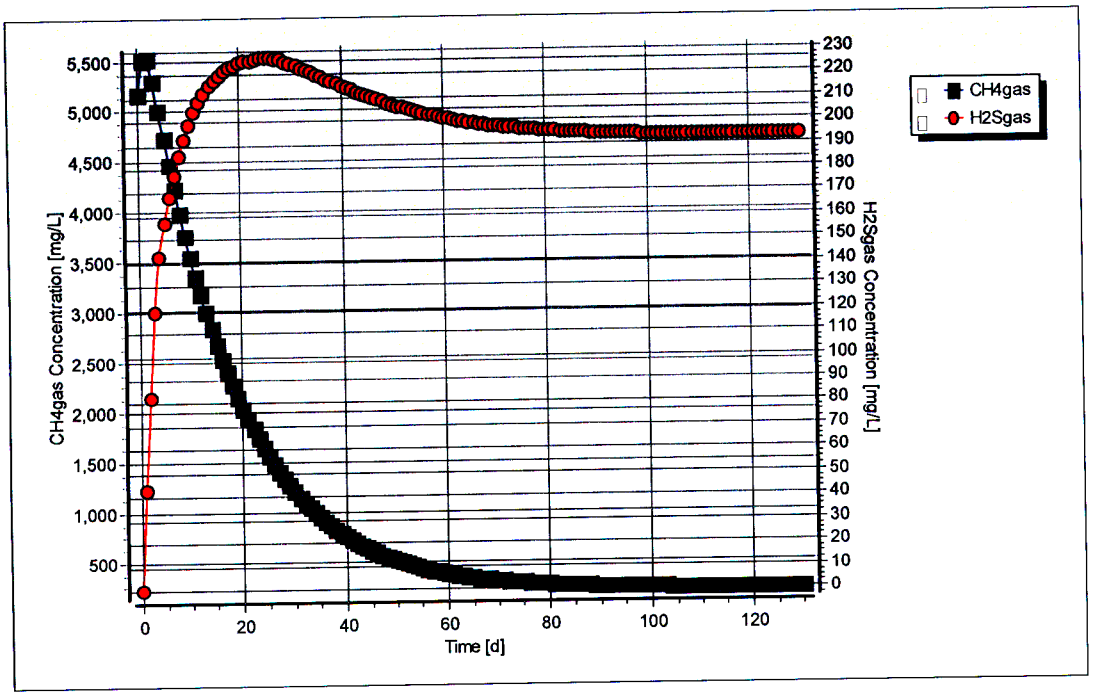


**Figure C-101:** Simulated methane and hydrogen sulphide gas concentration profiles for steady state number 41

## Steady State Number 42

**Table C-61:** Operating conditions for steady state number 42

| | |
|---|---|
| **Feed Batch Number** | F15 |
| **Reactor Volume (ℓ)** | 20 |
| **Retention Time (d)** | 13.3 |
| **pH** | steady state |
| **Biological Groups Present** | acidogenic, acetogenic, methanogenic and sulphidogenic |

**Table C-62:** Results summary for steady state number 42

| | Measured | Model | Relative error (%) |
|---|---|---|---|
| **Feed Total COD (mg COD/ℓ)** | 2017 | 2017 | - |
| **Feed Soluble COD (mg COD/ℓ)** | 224 | 224 | - |
| **Feed TKN (mg N/ℓ)** | 38 | 38 | - |
| **Feed FSA (mg N/ℓ)** | 10 | 10 | - |
| **Effluent Total COD (mg COD/ℓ)** | 1749 ± 34 | 918.44 | -90.43 |
| **Effluent Soluble COD (mg COD/ℓ)** | 964 ± 63 | 69.90 | -1279.16 |
| **Reactor pH** | 7.75 ± 0.01 | 6.31 | -22.81 |
| **Effluent VFA (mg HAc/ℓ)** | 57 ± 16 | 0.14 | -39417.78 |
| **Effluent Alkalinity (mg/ℓ as $CaCO_3$)** | 1573 ± 41 | 776.91 | -102.47 |
| **Sulphate Addition (mg SO4/ℓ)** | 2000 | 2000 | - |
| **Effluent Sulphate (mg SO4/ℓ)** | 147 ± 39 | 1439 | 89.78 |
| **% Sulphate Conversion** | 92.65 | 28.07 | - |
| **Methane Production (ℓ/d)** | 0 | 0.52 | 100 |
| **Gas Composition (% $CH_4$)** | 0 | 41.86 | 100 |
| **Effluent FSA (mg N/ℓ)** | 19 ± 1 | 22.54 | 15.71 |
| **Effluent TKN (mg N/ℓ)** | 127 ± 3 | 44.59 | -184.82 |

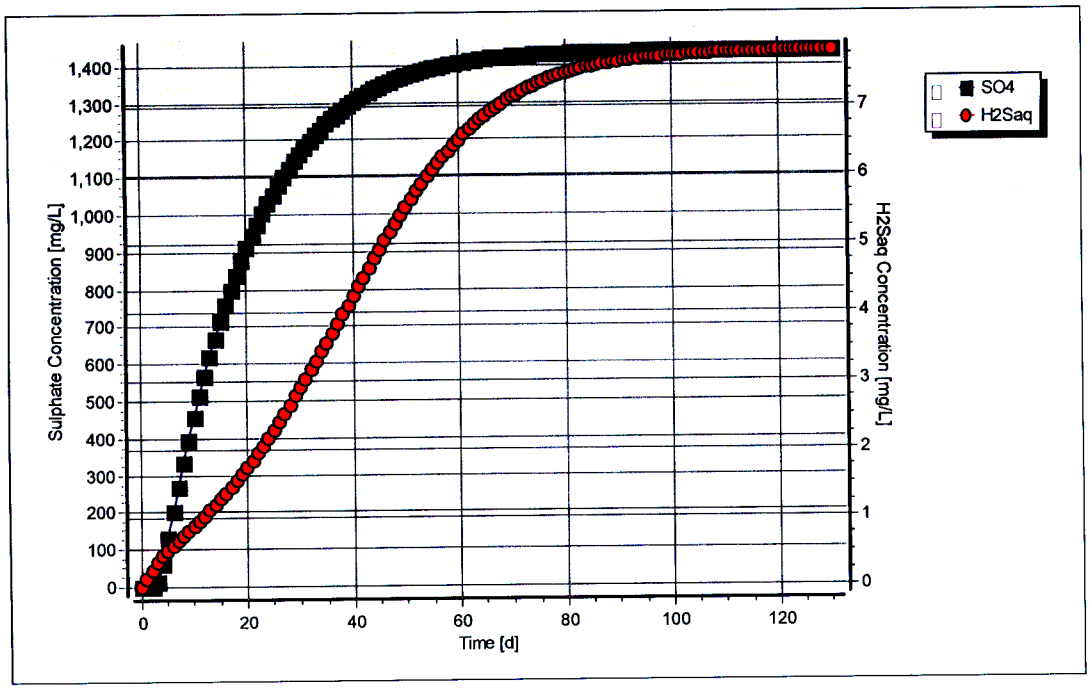


**Figure C-105:** Simulated sulphate and aqueous hydrogen sulphide concentration profiles for steady state number 42

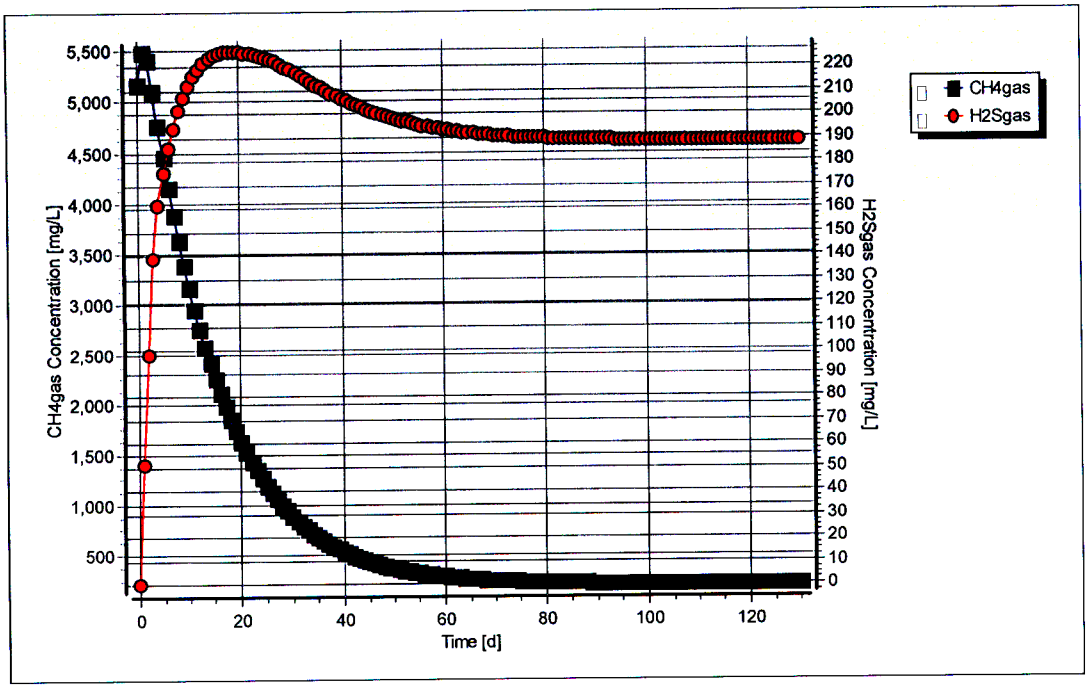


**Figure C-106:** Simulated methane and hydrogen sulphide gas concentration profiles for steady state number 42

## Steady State Number 46

**Table C-63:** Operating conditions for steady state number 46

| | |
|---|---|
| **Feed Batch Number** | F15 |
| **Reactor Volume (ℓ)** | 20 |
| **Retention Time (d)** | 10 |
| **pH** | steady state |
| **Biological Groups Present** | acidogenic, acetogenic, methanogenic and sulphidogenic |

**Table C-64:** Results summary for steady state number 46

| | **Measured** | **Model** | **Relative error (%)** |
|---|---|---|---|
| **Feed Total COD (mg COD/ℓ)** | 989 | 989 | - |
| **Feed Soluble COD (mg COD/ℓ)** | 102 | 102 | - |
| **Feed TKN (mg N/ℓ)** | 19 | 19 | - |
| **Feed FSA (mg N/ℓ)** | 7 | 7 | - |
| **Effluent Total COD (mg COD/ℓ)** | 897 ± 25 | 477.42 | -87.88 |
| **Effluent Soluble COD (mg COD/ℓ)** | 466 ± 18 | 71.89 | -548.20 |
| **Reactor pH** | 7.92 ± 0.04 | 5.98 | -32.49 |
| **Effluent VFA (mg HAc/ℓ)** | 3 ± 6 | 0.14 | -2046.72 |
| **Effluent Alkalinity (mg/ℓ as $CaCO_3$)** | 1025 ± 26 | 414.56 | -147.25 |
| **Sulphate Addition (mg SO4/ℓ)** | 1000 | 1000 | - |
| **Effluent Sulphate (mg SO4/ℓ)** | 51 ± 9 | 734 | 79.98 |
| **% Sulphate Conversion** | 94.90 | 26.59 | - |
| **Methane Production (ℓ/d)** | 0 | 0.32 | 100 |
| **Gas Composition (% $CH_4$)** | 0 | 37.74 | 100 |
| **Effluent FSA (mg N/ℓ)** | - | 13.06 | - |
| **Effluent TKN (mg N/ℓ)** | - | 23.76 | - |

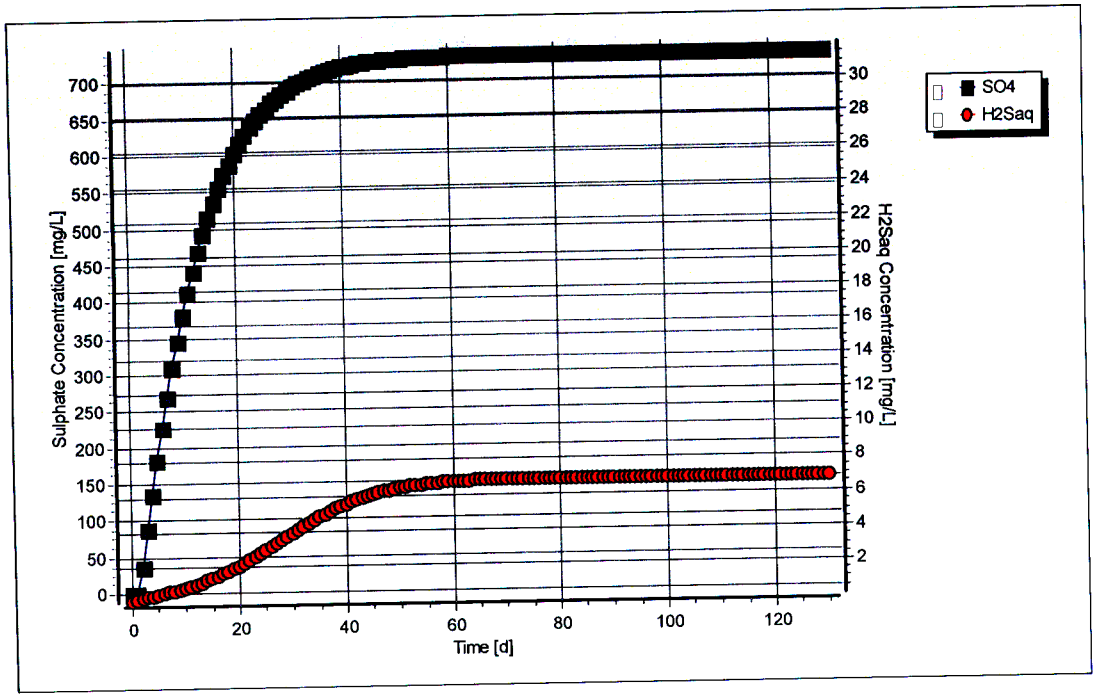


**Figure C-110:** Simulated sulphate and aqueous hydrogen sulphide concentration profiles for steady state number 46

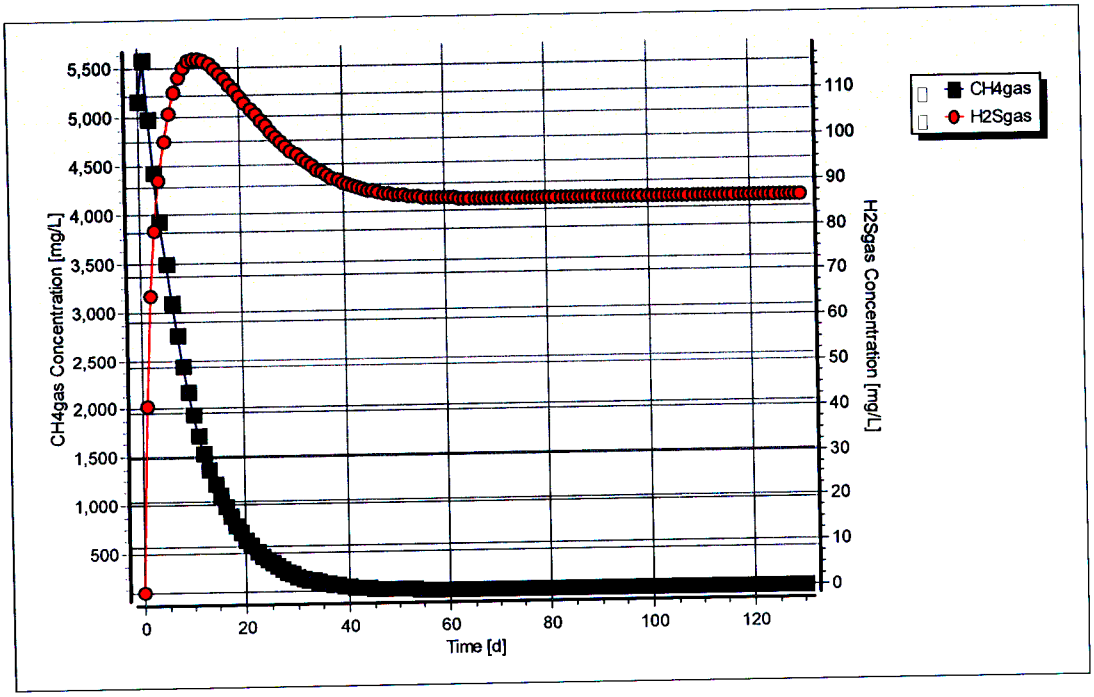


**Figure C-111:** Simulated methane and hydrogen sulphide gas concentration profiles for steady state number 46

## Steady State Number 47

**Table C-65:** Operating conditions for steady state number 47

| | |
|---|---|
| **Feed Batch Number** | F15 |
| **Reactor Volume (ℓ)** | 16 |
| **Retention Time (d)** | 8 |
| **pH** | controlled to ~ 8.3 |
| **Biological Groups Present** | acidogenic, acetogenic, methanogenic and sulphidogenic |

**Table C-66:** Results summary for steady state number 47

| | **Measured** | **Model** | **Relative error (%)** |
|---|---|---|---|
| **Feed Total COD (mg COD/ℓ)** | 1900 | 1900 | - |
| **Feed Soluble COD (mg COD/ℓ)** | 203 | 203 | - |
| **Feed TKN (mg N/ℓ)** | 46 | 46 | - |
| **Feed FSA (mg N/ℓ)** | 4 | 4 | - |
| **Effluent Total COD (mg COD/ℓ)** | 2020 ± 43 | 1206.19 | -67.47 |
| **Effluent Soluble COD (mg COD/ℓ)** | 926 ± 47 | 392.69 | -135.81 |
| **Reactor pH** | 8.27 ± 0.04 | 8.27 | - |
| **Effluent VFA (mg HAc/ℓ)** | 34 ± 14 | 0.17 | -19809.77 |
| **Effluent Alkalinity (mg/ℓ as $CaCO_3$)** | 1950 ± 50 | 2104.80 | 7.35 |
| **Sulphate Addition (mg SO4/ℓ)** | 2000 | 2000 | - |
| **Effluent Sulphate (mg SO4/ℓ)** | 47 ± 52 | 1487 | 96.84 |
| **% Sulphate Conversion** | 97.65 | 25.64 | - |
| **Methane Production (ℓ/d)** | 0 | 0.63 | 100 |
| **Gas Composition (% $CH_4$)** | 0 | 90.33 | 100 |
| **Effluent FSA (mg N/ℓ)** | - | 14.76 | - |
| **Effluent TKN (mg N/ℓ)** | - | 35.67 | - |

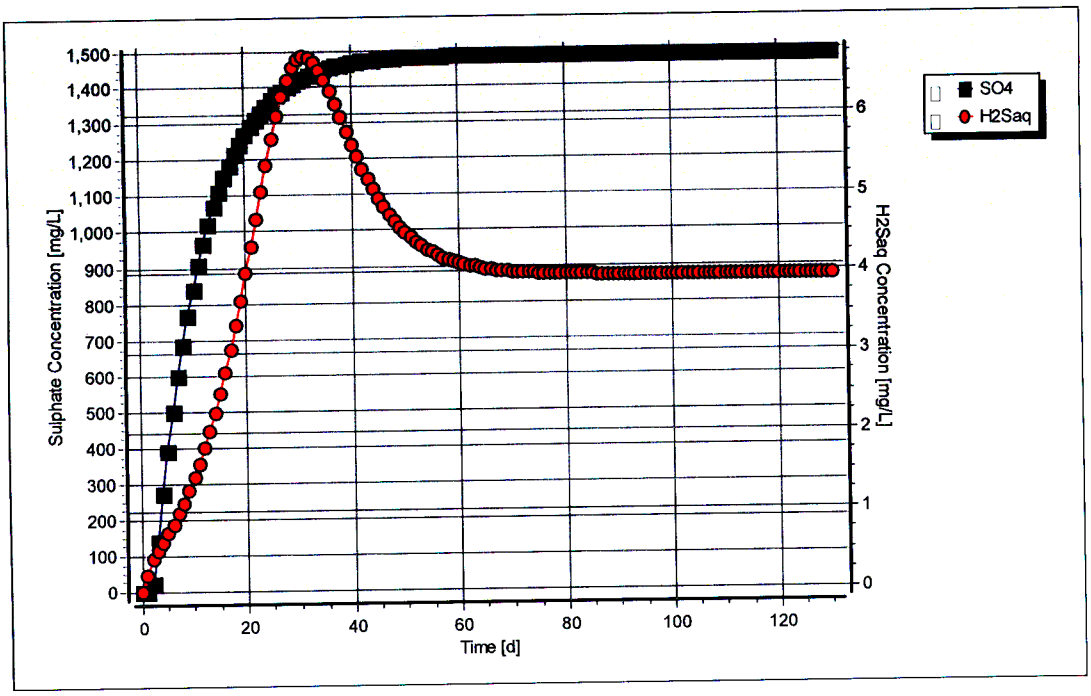


**Figure C-115:** Simulated sulphate and aqueous hydrogen sulphide concentration profiles for steady state number 47

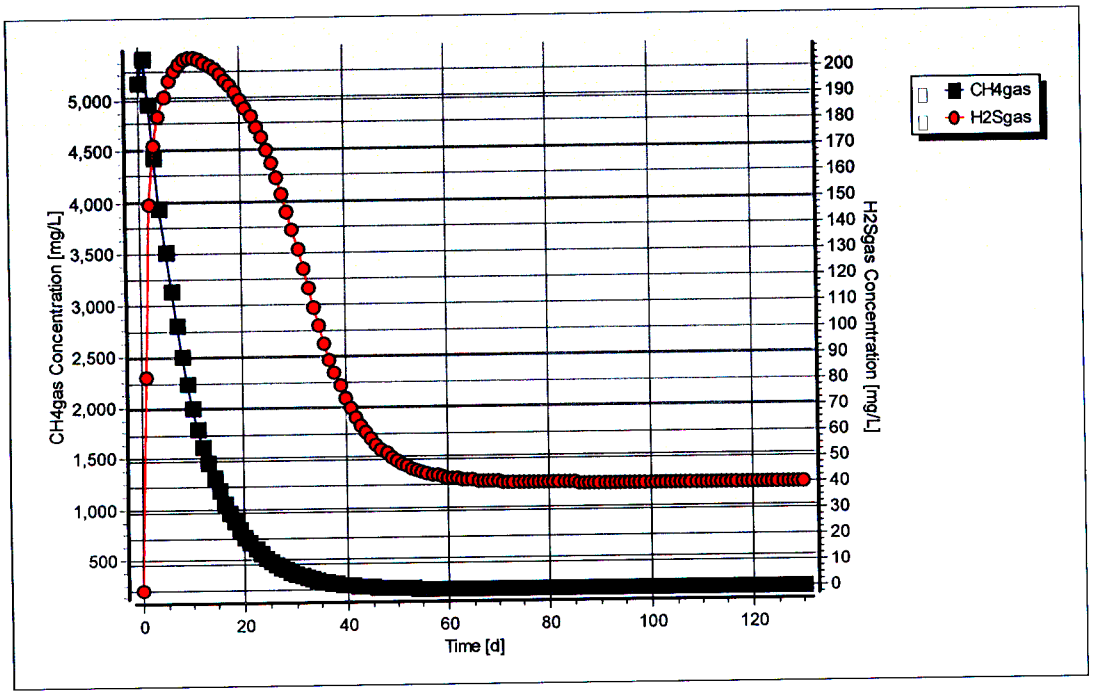


**Figure C-116:** Simulated methane and hydrogen sulphide gas concentration profiles for steady state number 47

# APPENDIX D

## SIMULATION RESULTS OF PILOT PLANT MODELLING

**Table D-1:** PSS feed stream specifications

| | |
|---|---|
| **Temperature (°C)** | 23 °C |
| **pH** | 7 |
| **Alkalinity (mg/ℓ as $CaCO_3$)** | 300 |
| **COD (mg/ℓ)** | ~ 30 000 |
| **Flowrate (ℓ/d)** | 13 200 |

**Table D-2:** Mine water feed stream specifications

| | |
|---|---|
| **Temperature (°C)** | 23 °C |
| **pH** | 7.5 |
| **Alkalinity (mg/ℓ as $CaCO_3$)** | 350 |
| **Sulphate (mg $SO_4$/ℓ)** | 1300 |
| **Flowrate (ℓ/d)** | 230 000 |

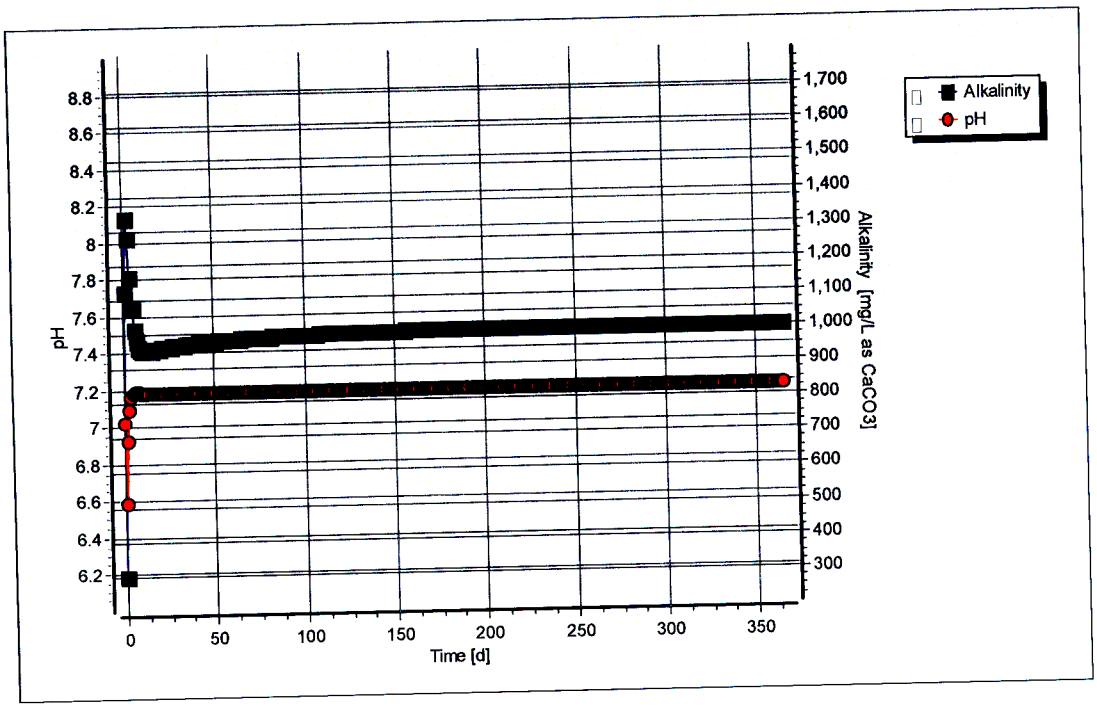


**Figure D-1:** Simulated pH and alkalinity profiles for pilot plant

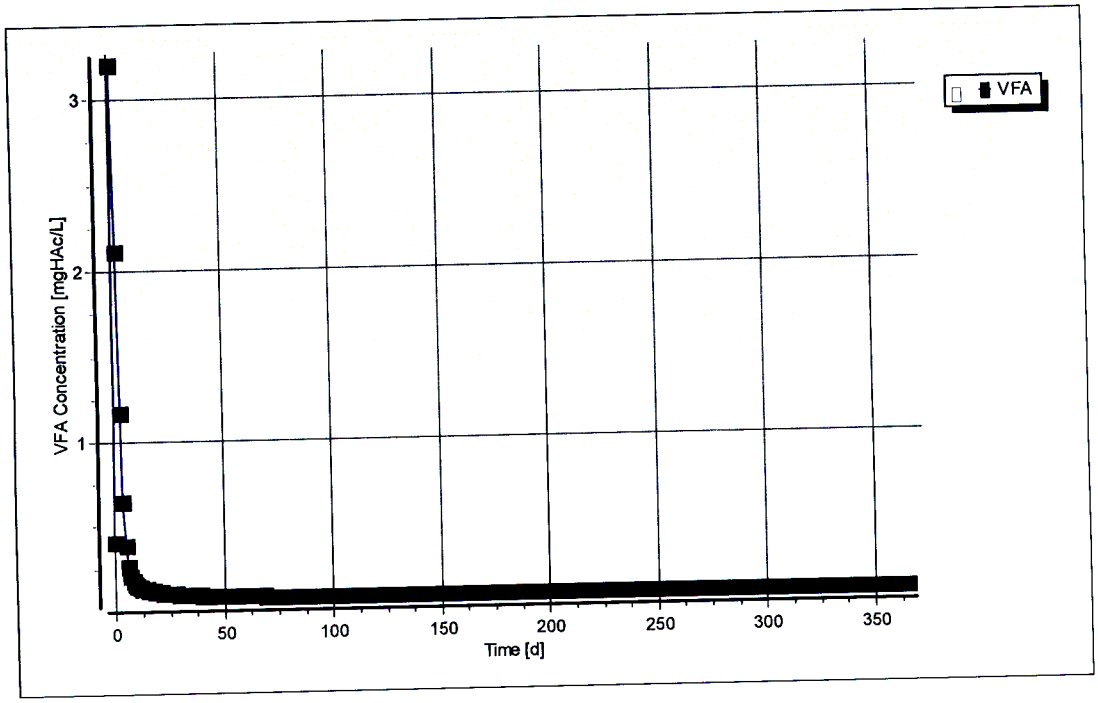


**Figure D-2:** Simulated VFA concentration profile for pilot plant

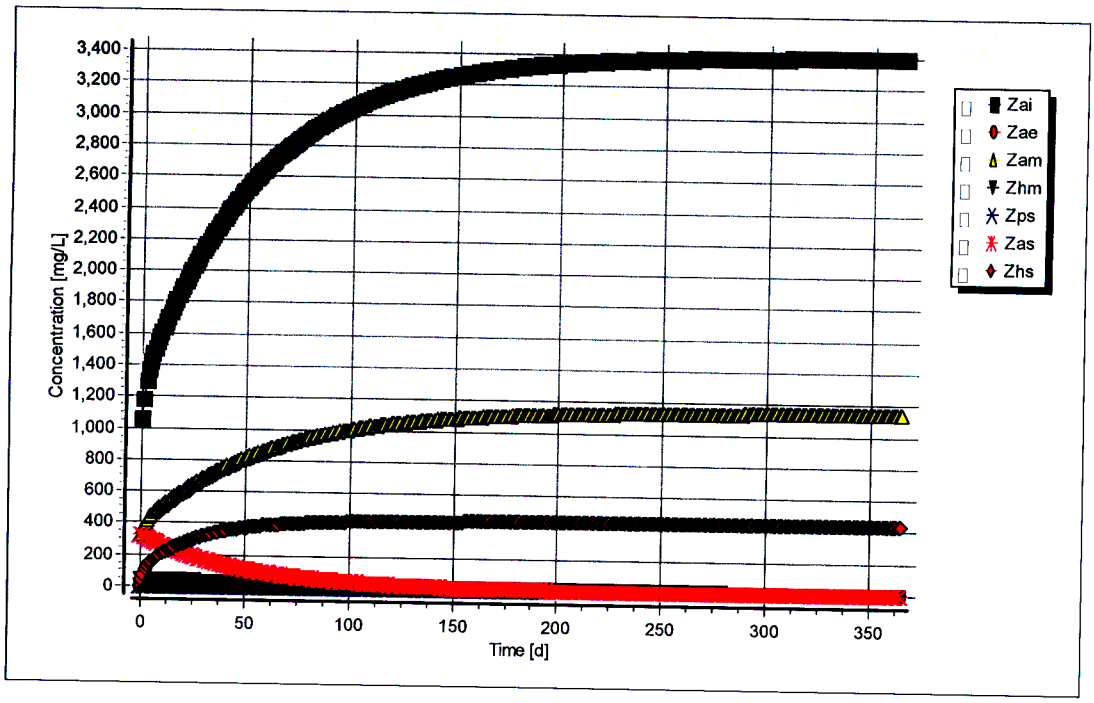


**Figure D-5:** Simulated biomass concentration profiles for pilot plant